Antifungal Metabolites Produced by *Bacillus amyloliquefaciens* Biocontrol Strain SD-32

（生物農薬 *Bacillus amyloliquefaciens* SD-32 株の生産する抗菌性代謝産物）

Keijitsu Tanaka

田中　計実

2016

CONTENTS

List of Abbreviations Used

AcOH	acetic acid
CD	circular dichroism
CH_3CN	acetonitrile
DMSO	dimethyl sulfoxide
ESI-MS	electrospray ionization-mass spectrometry
EtOAc	ethyl acetate
FAB-MS	fast atom bombardment-mass spectrometry
FDAA	*N*-(5-fluoro-2,4-dinitrophenyl)-$_L$-alaninamide
HCl	hydrochloric acid
^{1}H-^{1}H COSY	^{1}H-^{1}H correlation spectroscopy
HMBC	heteronuclear multiple bond connectivity
HR-ESI-MS	high resolution-electrospray ionization-mass spectrometry
HR-FAB-MS	high resolution-fast atom bombardment-mass spectrometry
HSQC	heteronuclear single quantumn coherence
HPLC	high-performance liquid chromatography
IC_{50}	median inhibitory concentration
LC-MS	liquid chromatography-mass spectrometry
MALDI-TOF-MS	matrix assisted laser desorption ionization-time of flight-mass spectrometry
MeOH	methanol
$LiBH_4$	lithium borohydride
MTPA	α-methoxy-α-(trifluoromethyl)phenylacetic acid
NBS	*N*-bromosuccinimide
NMR	nuclear magnetic resonance
NOE	nuclear overhauser effect
NOESY	nuclear overhauser effect correlated spectroscopy
OPA	*o*-phthalaldehyde
PCR	polymerase chain reaction

PDA	potato dextrose agar
SD	standard deviation
SPE	solid-phase extraction
TFA	trifluoroacetic acid
THF	tetrahydrofuran
TMS-diazomethane	trimethylsilyl-diazomethane

List of Tables and Figures

Chapter 1
General Introduction

The yield of cultivated crop plants is threatened by destruction by plant pathogens, especially when such crop plants are grown in large-scale monocultures. Because these crop plants are all genetically identical, if one is susceptible to a pathogen, all will be. Thus plant diseases caused by plant pathogens are a serious agricultural problem worldwide.[1] Indeed, plant pathogens are estimated to cause a 16% loss in the production of major crop plants around the world.[1] In order to meet the increasing food demands of the expanding human population, agricultural production must be increased; accordingly, the practice of crop protection plays a key role. Crop protection practices have been based on abundant increases in the use of synthetic pesticides, which are sometimes highly toxic to humans and non-target organisms and in some cases show a prolonged persistence in the environment.

Botrytis cinerea Pers. Fr. causes gray mold disease in more than 200 mostly dicotyledonous plant species and leads to serious losses in yield and quality in many crops, particularly vegetables and fruits.[2] *B. cinerea* is difficult to control because of its variety of modes of attack, diverse inoculum sources, and survival strategy as both mycelia and conidia.[2] Although chemical control has been used as a standard practice for many years, *B. cinerea* possesses an ability to adapt quickly to chemical fungicides and to develop tolerant or resistant strains.[3] For example, two benzimidazole-type compounds, benomyl and carbendazim, have been widely used against gray mold disease in the past but have been abandoned because of the development of widespread resistance to the compounds.[4] This adaptive capacity of *B. cinerea* underscores the need for the continuous development of new chemical fungicides.

In addition, due to the many concerns over chemical fungicides (their toxicity to humans and persistence in the environment, the rapid emergence of fungicide resistance, and the high cost of discovering, developing, and registering these chemicals), biological control agents (BCAs) have also been attracting considerable attention.[5] In fact, many BCA formulations are already available for practical use.[6] Among them, *Bacillus*-species-based BCAs are considered to have promise due to their safety, ubiquity in nature, and exhibition of high

thermal tolerance through the formation of resistant spores. Biological control by *Bacillus* sp. involves a number of mechanisms, such as competition for space and nutrition, antagonism, and induction of systemic resistance.

Bacillus species biological control strains (mainly *B. subtilis*, *B. amyloliquefaciens*, and *B. cereus*) are known to produce a wide variety of bioactive metabolites such as cyclic lipopeptides (iturins)[7,8] and cyclic lipodepsipeptides (surfactins and fengycins or plipastatins),[7,8] polyketides (bacillaenes, difficidin, oxidifficidin, and macrolactins),[9,10] peptides (plantazolicins),[11] and aminopolyols (zwittermicin A and kanosamine).[12,13] Among these bioactive compounds, cyclic lipopeptides (iturins) and cyclic lipodepsipeptides (surfactins, and fengycins or plipastatins) have received much attention as key compounds in BCAs because they play an important role in colonization on the plant, show potent activities against a wide variety of microorganisms, and induce systemic resistance of plants.[7,8,14,15]

Iturins are cyclic lipopeptides produced by several strains of *Bacillus* species and show antibiotic action against fungi, including plant pathogenic fungi. Iturin A,[16-18] bacillomycins D,[19] F,[20] and Lc,[21] bacillopeptins,[22] and mycosubtilin[23] are the main variants of the iturin family. Bacillomycin D homologues are cyclic lipopeptides containing seven α-amino acids and a β-amino fatty acid. The β-amino fatty acids vary from C_{14} to C_{16} in their carbon numbers, and possess *normal*-, *iso*-, or *anteiso*-terminal structures. Of these, the bacillomycin D homologues containing the *normal*-C_{14}, *iso*-C_{15}, and *anteiso*-C_{15} β-amino fatty acids are the predominant ones in bacillomycin D (Table 1-1).[19,24-30]

Surfactins are cyclic lipodepsipeptides produced by several strains of *Bacillus* species and are well known to act as potent surface-active compounds. Generally, they contain seven α-amino acids and a β-hydroxy fatty acid. Standard surfactin possesses a heptapeptide moiety, $_{L}$-Glu^{1}-$_{L}$-Leu^{2}-$_{D}$-Leu^{3}-$_{L}$-Val^{4}-$_{L}$-Asp^{5}-$_{D}$-Leu^{6}-$_{L}$-Leu^{7}, linked by an ester bond to a (*R*)-β-hydroxy fatty acid.[31-33] In addition to standard surfactin, [Ala^{4}]surfactin,[34,35] [Leu^{4}]surfactin,[36] [Ile^{4}]surfactin,[36] [Val^{7}]surfactin,[37-40] [Ile^{7}]surfactin,[37,41-44] and halobacillin[45,46] (or lichenysins)[47,48] are the main variants (Table 1-2).

Table 1-1. Structures of Lipopeptides from *Bacillus* species

	α-amino acids							β-amino acid
	1	2	3	4	5	6	7	
Iturin A	Asn	Tyr[b]	Asn	Gln	Pro	Asn	Ser	*n*-C_{14}, *ai*-C_{15}, *iso*-C_{15}, *n*-C_{15}, *iso*-C_{16}, *n*-C_{16}, *ai*-C_{17}
Bacillomycin D	Asn	Tyr	Asn	Pro	Glu	Ser	Thr	*n*-C_{14}, *ai*-C_{15}, *iso*-C_{15}, *iso*-C_{16}, *n*-C_{16}
Bacillomycin F	Asn	Tyr	Asn	Gln	Pro	Asn	Thr	*ai*-C_{15}, *iso*-C_{15}, *iso*-C_{16}, *n*-C_{16}, *ai*-C_{17}, *iso*-C_{17}
Bacillomycin Lc[a]	Asn	Tyr	Asn	Ser	Glu	Ser	Thr	*n*-C_{14}, *ai*-C_{15}, *iso*-C_{15}, *iso*-C_{16}, *n*-C_{16}
Mycosubtilin	Asn	Tyr	Asn	Gln	Pro	Ser	Asn	*iso*-C_{16}, *n*-C_{16}, *ai*-C_{17}, *iso*-C_{17}

[a]or bacillopeptins; [b]underline indicates $_D$-form.

Table 1-2. Structures of Lipodepsipeptides from *Bacillus* species

	α-amino acids							β-OH-fatty acid
	1	2	3	4	5	6	7	
Surfactin	Glu	Leu	Leu[b]	Val	Asp	Leu	Leu	*ai*-C_{13}, *iso*-C_{13}, *n*-C_{13}, *iso*-C_{14}, *n*-C_{14}, *ai*-C_{15}, *iso*-C_{15}, *n*-C_{15}, *iso*-C_{16}, *ai*-C_{17}
[Ala[4]]Surfactin	Glu	Leu	Leu	Ala	Asp	Leu	Leu	*iso*-C_{14}, *n*-C_{14}, *ai*-C_{15}, *iso*-C_{15}, *n*-C_{15}
[Leu[4]]Surfactin	Glu	Leu	Leu	Leu	Asp	Leu	Leu	-
[Ile[4]]Surfactin	Glu	Leu	Leu	Ile	Asp	Leu	Leu	-
[Val[7]]Surfactin	Glu	Leu	Leu	Val	Asp	Leu	Val	*ai*-C_{13}, *iso*-C_{14}, *n*-C_{14}, *ai*-C_{15}
[Ile[7]]Surfactin	Glu	Leu	Leu	Val	Asp	Leu	Ile	*iso*-C_{14}, *n*-C_{14}, *ai*-C_{15}, *iso*-C_{15}
Halobacillin[a]	Gln	Leu	Leu	Val	Asp	Leu	Ile	-

[a]or lichenysins; [b]underline indicates $_D$-form.

To develop new and effective BCAs against gray mold disease, a screening search was performed, and *Bacillus amyloliquefaciens* SD-32 was isolated from a soil sample obtained in Japan (Figure 1-1). In order to gain insight into the mechanisms responsible for the biological control attained by *B. amyloliquefaciens* strain SD-32, the factors that are produced by the bacterium and contribute to the control of gray mold disease were identified, and their roles in the biological control system were clarified in this study.

This thesis is composed of four chapters. Chapter 2 deals with the isolation of antifungal compounds, an elucidation of their structures, and an assessment of their activities against several plant pathogens, including *B. cinerea*. In chapter 3, the isolation of synergistic factors that enhance the activities of the antifungal compounds, the elucidation of their structures, and an evaluation of their effects in combination with the antifungal compounds are described. In addition, the mechanism of the synergism is discussed.

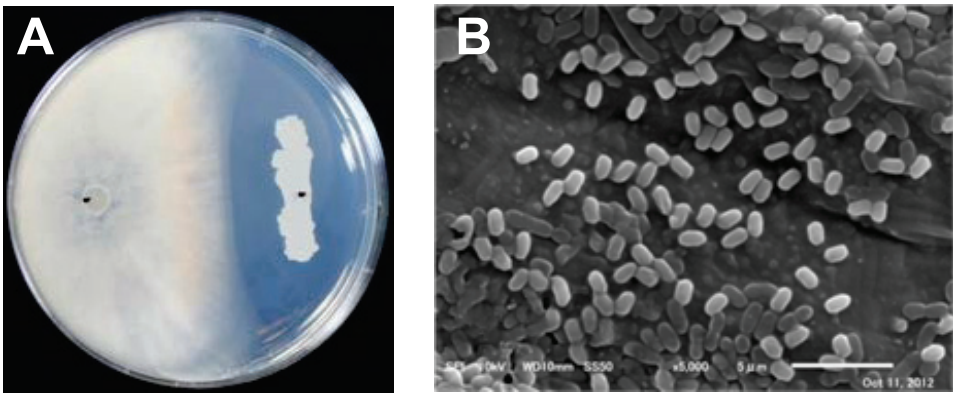

Botrytis cinerea *Bacillus amyloliquefaciens* SD-32

Figure 1-1. (A) Dual culture of *Bacillus amyloliquefaciens* SD-32 with *Botrytis cinerea* on a PDA plate. (B) *B. amyloliquefaciens* SD-32 on a cucumber leaf. The scale bar indicates 5 μm.

References

(1) Oerke, E. C. Crop losses to pests. *J. Agric. Sci.* **2006**, *144*, 31-43.

(2) Williamson, B.; Tudzynski, B.; Tudzynski, P.; van Kan, J. A. L. *Botrytis cinerea*: the cause of grey mould disease. *Mol. Plant Pathol*. **2007**, *8*, 561-580.

(3) Rosslenbroich, H. J.; Stuebler, D. *Botrytis cinerea* - history of chemical control and novel fungicides for its management. *Crop Prot.* **2000**, *19*, 557-561.

(4) Leroch, M.; Plesken, C.; Weber, R. W. S.; Kauff, F.; Scalliet, G.; Hahn, M. Gray mold populations in German strawberry fields are resistant to multiple fungicides and dominated by a novel clade closely related to *Botrytis cinerea*. *Appl*. *Environ*. *Microbiol*. **2013**, *79*, 159-167.

(5) Glare, T.; Caradus, J.; Gelernter, W.; Jackson, T.; Keyhani, N.; Köhl, J.; Marrone, P; Morin, L.; Stewart, A. Have biopesticides come of age? *Trends Biotechnol.* **2012**, *30*, 250-258.

(6) Fravel, D. R. Commercialization and implementation of biocontrol. *Annu. Rev. Phytopathol*. **2005**, *43*, 337-359.

(7) Stein, T. *Bacillus subtilis* antibiotics: structures, syntheses and specific functions. *Mol. Microbiol*. **2005**, *56*, 845-857.

(8) Ongena, M.; Jacques, P. *Bacillus* lipopeptides: versatile weapons for plant disease biocontrol. *Trends Microbiol*. **2008**, *16*, 115-125.

(9) Chen, X. H.; Vater, J.; Piel, J.; Franke, P.; Scholz, R.; Schneider, K.; Koumoutsi, A.; Hitzeroth, G.; Grammel, N.; Strittmatter, A. W.; Gottschalk, G.; Süssmuth, R. D.; Borriss, R. Structural and functional characterization of three polyketide synthase gene clusters in *Bacillus amyloliquefaciens* FZB42. *J. Bacteriol.* **2006**, *188*, 4024-4036.

(10) Schneider, K.; Chen, X. H.; Vater, J.; Franke, P.; Nicholson, G.; Borriss, R.; Süssmuth, R. D. Macrolactin is the polyketide biosynthesis product of the pks2 cluster of *Bacillus amyloliquefaciens* FZB42. *J. Nat. Prod.* **2007**, *70*, 1417-1423.

(11) Kalyon, B.; Helaly, S. E.; Scholz, R.; Nachtigall, J.; Vater, J.; Borriss, R.; Süssmuth, R. D. Plantazolicin A and B: Structure elucidation of ribosomally synthesized thiazole/oxazole peptides from *Bacillus amyloliquefaciens* FZB42. *Org. Lett.* **2011**, *13*, 2996-2999.

(12) Silo-Suh, L.; Lethbridge, B.; Raffel, S. J.; He, H.; Clardy, J.; Handelsman, J. Biological activities of two fungistatic antibiotics produced by *Bacillus cereus* UW85. *Appl. Environ.*

Microbiol. **1994**, *60*, 2023-2030.

(13) Milner, J. L.; Silo-Suh, L.; Lee, J. C.; He, H.; Clardy, J.; Handelsman, J. Production of kanosamine by *Bacillus cereus* UW85. *Appl. Environ. Microbiol.* **1996**, *62*, 3061-3065.

(14) Raaijmakers, J. M.; de Bruijin, I.; Nybroe, O.; Ongena, M. Natural functions of lipopeptides from *Bacillus* and *Pseudomonas*: more than surfactants and antibiotics. *FEMS Microbiol. Rev.* **2010**, *34*, 1037-1062.

(15) Chowdhury, S. P.; Hartmann, A.; Gao, X.; Borriss, R. Biocontrol mechanism by root-associated *Bacillus amyloliquefaciens* FZB42 – a review. *Frontiers in Microbiol.* **2015**, *6*, 1-11.

(16) Peypoux, F.; Guinard, M.; Michel, G.; Delcambe, L.; Das, B. C.; Lederer, E. Structure of iturin A, a peptidolipid actibiotic from *Bacillus subtilis*. *Biochemstry* **1978**, *17*, 3992-3996.

(17) Isogai, A.; Takayama, S.; Murakoshi, S.; Suzuki, A. Structures of β-amino acids in antibiotics iturin A. *Tetrahedron Lett.* **1982**, *23*, 3065-3068.

(18) Hiradate, S.; Yoshida, S.; Sugie, H.; Yada, H.; Fujii, Y. Mulberry anthracnose antagonists (iturins) produced by *Bacillus amyloliquefaciens* RC-2. *Phytochemistry* **2002**, *61*, 693-698.

(19) Peypoux, F.; Pommier, M. T.; Das, B. C.; Besson, F.; Delcambe, L.; Michel, G. Structures of bacillomycin D and bacillomycin L peptidolipid antibiotics from *Bacillus subtilis*. *J. Antibiot.* **1984**, *37*, 1600-1604.

(20) Peypoux, F.; Marion, D.; Maget-Dana, R.; Ptak, M.; Das, B. C.; Michel, G. Structure of bacillomycin F, a new peptidolipid antibiotic of the iturin group. *Eur. J. Biochem*. **1985**, *153*, 335-340.

(21) Eshita, S. M.; Roberto, N. H.; Beale, J. M.; Mamiya, B. M.; Workman, R. F. Bacillomycin Lc, a new antibiotic of the iturin group: Isolation, structures, and antifungal activities of the congeners. *J. Antibiot*. **1995**, *48*, 1240-1247.

(22) Kajimura, Y.; Sugiyama, M.; Kaneda, M. Bacillopeptins, new cyclic lipopeptide antibiotics from *Bacillus subtilis* FR-2. *J. Antibiot*. **1995**, *48*, 1095-1103.

(23) Peypoux, F; Pommier, M. T.; Marion, D.; Ptak, M.; Das, B. C.; Michel, G. Revised structure of mycosubtilin, a peptidolipid antibiotic from *Bacillus subtilis*. *J. Antibiot*. **1986**, *39*, 636-641.

(24) Moyne, A. L.; Shelby, R.; Cleveland, T. E.; Tuzun, S. Bacillomycin D: an iturin with antifungal activity against *Aspergillus flavus*. *J. Appl. Microbiol.* **2001**, *90*, 622-629.

(25) Oleinikova, G. K.; Kuznetsova, T. A.; Huth, F.; Laatsch, H.; Isakov, V. V.; Shevchenko, L. S.; Elyakov, G. B. Cyclic lipopeptides with fungicidal activity from the sea isolate of the bacterium *Bacillus subtilis*. *Russ. Chem. Bull., Int. Ed.* **2001**, *50*, 2231-2235.

(26) Oleinikova, G. K.; Dmitrenok, A. S.; Voinov, V. G.; Chaikina, E. L.; Shevchenko, L. S.; Kuznetsova, T. A. Bacillomycin D from the marine isolate of the bacterium *Bacillus subtilis* KMM 1922. *Chem. Nat. Compd.* **2005**, *41*, 240-242.

(27) Zhao, Z.; Wang, Q.; Wang, K.; Brian, K.; Liu, C.; Gu, Y. Study of the antifungal activity of *Bacillus vallismortis* ZZ185 *in vitro* and identification of its antifungal components. *Bioresour. Technol.* **2010**, *101*, 292-297.

(28) Yuan, J.; Li, B.; Zhang, N.; Waseem, R.; Shen, Q.; Huang, Q. Production of bacillomycin- and macrolactin-type antibiotics by *Bacillus amyloliquefaciens* NJN-6 for suppressing soilborne plant pathogens. *J. Agric. Food Chem.* **2012**, *60*, 2976-2981.

(29) Kumar, A.; Saini, S.; Wray, V.; Nimtz, M.; Prakash, A.; Johri, B. N. Characterization of an antifungal compound produced by *Bacillus* sp. A_5F that inhibits *Sclerotinia sclerotiorum*. *J. Basic Microbiol.* **2012**, *52*, 670-678.

(30) Cao, Y.; Xu, Z.; Ling, N.; Yuan, Y.; Yang, X.; Chen, L.; Shen, B.; Shen, Q. Isolation and identification of lipopeptides produced by *B. subtilis* SQR 9 for suppressing Fusarium wilt of cucumber. *Sci. Hortic.* **2012**, *135*, 32-39.

(31) Arima, K.; Kakinuma, A.; Tamura, G. Surfactin, a crystalline peptidelipid surfactant produced by *Bacillus subtilis*: isolation, characterization and its inhibition of fibrin clot formation. *Biochem. Biophys. Res. Commun.* **1968**, *31*, 488-494.

(32) Kakinuma, A.; Hori, M.; Isono, M.; Tamura, G.; Arima, K. Determination of amino acid sequence in surfactin, a crystalline peptidelipid surfactant produced by *Bacillus subtilis*. *Agric. Biol. Chem.* **1969**, *33*, 971-972.

(33) Nagai, S.; Okimura, K.; Kaizawa, N.; Ohki, K.; Kanatomo, S. Study on surfactin, a cyclic depsipeptide. II. Synthesis of surfactin B_2 produced by *Bacillus natto* KMD 2311. *Chem. Pharm. Bull.* **1996**, *44*, 5-10.

(34) Peypoux, F.; Bonmatin, J. M.; Labbé, H.; Grangemard, I.; Das, B. C.; Ptak, M.; Wallach,

J.; Michel, G. [Ala4]Surfactin, a novel isoform from *Bacillus subtilis* studied by mass and NMR spectroscopies. *Eur. J. Biochem.* **1994**, *224*, 89-96.

(35) Romano, A.; Vitullo, D.; Pietro, A. D.; Lima, G.; Lanzotti, V. Antifungal lipopeptides from *Bacillus amyloliquefaciens* strain BO7. *J. Nat. Prod.* **2011**, *74*, 145-151.

(36) Bonmatin, J. M.; Labbé, H.; Grangemard, I.; Peypoux, F.; Maget-Dana, R.; Ptak, M.; Michel, G. Production, isolation and characterization of [Leu^4]- and [Ile^4]surfactins from *Bacillus subtilis*. *Lett. Pept. Sci.* **1995**, *2*, 41-47.

(37) Baumgart, F.; Kluge, B.; Ullrich, C.; Vater, J.; Ziessow, D. Identification of amino acid substitutions in the lipopeptide surfactin using 2D NMR spectroscopy. *Biochem. Biophys. Res. Commun.***1991**, *177*, 998-1005.

(38) Peypoux, F.; Bonmatin, J. M.; Labbé, H.; Das, B. C.; Ptak, M.; Michel, G. Isolation and characterization of a new variant of surfactin, the [Val7]surfactin. *Eur. J. Biochem.* **1991**, *202*, 101-106.

(39) Peypoux, F.; Michel, G. Controlled biosynthesis of Val^7- and Leu^7-surfactins. *Appl. Microbiol. Biotechnol.* **1992**, *36*, 515-517.

(40) Hue, N.; Serani, L.; Laprévote, O. Structural investigation of cyclic peptidolipids from *Bacillus subtilis* by high-energy tandem mass spectrometry. *Rapid Commun. Mass Spectrom.* **2001**, *15*, 203-209.

(41) Jenny, K.; Käppeli, O.; Fiechter, A. Biosurfactants from *Bacillus licheniformis*: structural analysis and characterization. *Appl. Microbiol. Biotechnol.* **1991**, *36*, 5-13.

(42) Itokawa, H.; Miyashita, T.; Morita, H.; Takeya, K.; Hirano, T.; Homma, M.; Oka, K. Structural and conformational studies of [Ile^7] and [Leu^7]surfactins from *Bacillus subtilis natto*. *Chem. Pharm. Bull.* **1994**, *42*, 604-607.

(43) Kowall, M.; Vater, J.; Kluge, B.; Stein, T.; Franke, P.; Ziessow, D. Separation and characterization of surfactin isoforms produced by *Bacillus subtilis* OKB 105. *J. Colloid Interface Sci.* **1998**, *204*, 1-8.

(44) Tang, J. S.; Gao, H.; Hong, K.; Yu, Y.; Jiang, M. M.; Lin, H. P.; Ye, W. C.; Yao, X. S. Complete assignments of ^1H and ^{13}C NMR spectral data of nine surfactin isomers. *Magn. Reson. Chem.* **2007**, *45*, 792-796.

(45) Trischman, J. A.; Jensen, P. R.; Fenical, W. Halobacillin: a cytotoxic cyclic acylpeptide of

the iturin class produced by a marine *Bacillus*. *Tetrahedron Lett*. **1994**, *35*, 5571-5574.

(46) Hasumi, K.; Takizawa, K.; Takahashi, F.; Park, J. K.; Endo, A. Inhibition of acyl-CoA: cholesterol acyltransferase by isohalobacillin, a complex of novel cyclic acylpeptides produced by *Bacillus* sp. A1238. *J. Antibiot.* **1995**, *48*, 1419-1424.

(47) Yakimov, M. M.; Abraham, W. R.; Meyer, H.; Giuliano, L.; Golyshin, P. N. Structural characterization of lichenysin A components by fast atom bombardment tandem mass spectrometry. *Biochim. Biophys. Acta, Mol. Cell Biol. Lipids* **1999**, *1438*, 273-280.

(48) Grangemard, I.; Bonmatin, J. M.; Bernillon, J.; Das, B. C.; Peypoux, F. Lichenysins G, a novel family of lipopeptide biosurfactants from *Bacillus licheniformis* IM 1307: production, isolation and structural evaluation by NMR and mass spectrometry. *J. Antibiot.* **1999**, *52*, 363-373.

Chapter 2

Isolation of Bacillomycin D Homologues from *Bacillus amyloliquefaciens* SD-32 and Their Antifungal Activities against Plant Pathogens

2.1. Introducction

Botrytis cinerea Pers. Fr. is a pathogen of gray mold diseases in many fruit, vegetable, and ornamental crops and causes serious losses worldwide.[1] Although chemical fungicides have been used for many years to control the pathogen, the ability of *B. cinerea* to adapt quickly to new chemicals by developing its resistance always creates the need for developing new fungicides.[2] With increasing concern regarding fungicide resistance of pathogens, environmental impact, and food safety of the chemical fungicides, biological control has attracted considerable attention.

In this context, a screening search was performed to develop effective biological control agents against gray mold disease and *Bacillus amyloliquefaciens* SD-32 showing strong antagonistic activity against *B. cinerea* was isolated from a soil sample obtained in Japan. To clarify the mechanisms of the biological control by *B. amyloliquefaciens* strain SD-32, the factors, which contribute to control gray mold disease, produced by the bacterium were identified and their roles in the biological control system were evaluated. The identification and evaluation of the factors in SD-32 responsible for controlling gray mold disease could contribute to a better understanding of the molecular basis of this biological control system.

Using an in vitro antifungal activity-guided purification, four antifungal compounds, **1-4** (Figure 2-1), were isolated from its fermentation broth. In this chapter, I describe the isolation of these compounds, the elucidation of their structures, and their activities against some plant pathogens including *B. cinerea*.

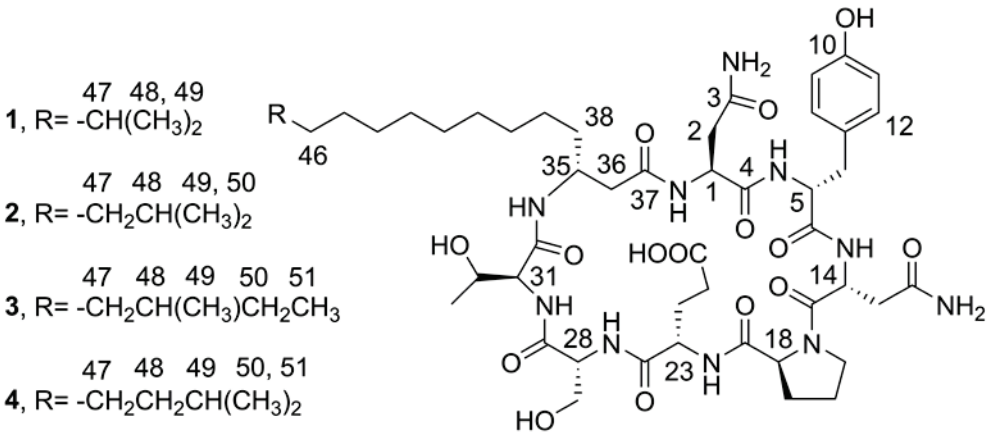

Figure 2-1. Structures of compounds **1**-**4.**

2.2. Materials and Methods

General Experimental Procedures. The solvents and reagents used in this study were purchased from Sigma-Aldrich, St. Louis, MO, USA, unless otherwise noted. NMR spectra were measured with Bruker Avance II 800US2, Bruker Avance II 600, and Bruker DRX500 systems (Bruker Daltonics, Billerica, MA, USA). The spectra for compounds **1-4** were acquired in pyridine-d_5 (δ_H 7.19; δ_C 123.5) at room temperature. HR-ESI-MS spectra were obtained with a Waters Micromass LCT Premier XE (Waters, Milford, MA, USA), and HR-FAB-MS spectra were obtained with a JEOL JMS-700 spectrometer (JEOL, Tokyo, Japan). Preparative HPLC and HPLC analyses were performed with a Waters Alliance system.

Microorganisms. Soil samples collected in Ibaraki prefecture, Japan, were suspended in sterilized water and vortexed. The supernatants were serially diluted with sterilized water and spread on nutrient agar plates (15 x 90 mm). The plates were incubated at 30 ˚C for 48 h in darkness, and 500 colonies were transferred to other nutrient agar plates. Bacteria thus isolated were tested for their antifungal activity against a phytopathogenic fungus, *Botrytis cinerea* Persoon MAFF 744071. PCR amplification of the 16S rRNA gene of strain SD-32 with universal forward (5'-AGAGTTTGATCCTGGCTCAG-3') and reverse (5'-GGCTACCTTGTTACGACTT-3') primers was carried out. The 16S sequence for SD-32 was deposited in GenBank (accession no. AB853319).

Isolation of Compounds 1-4. Strain SD-32 was grown at 30 ˚C with 150 rpm shaking for 64 h in 500 mL flasks containing liquid medium (50 mL/flask, total 800 mL) composed of maltose (80 g/L), soybean powder (80 g/L; J-OIL MILLS, Tokyo, Japan), yeast extract (10 g/L; Becton, Dickinson and Co., Franklin Lakes, NJ, USA), $MgSO_4 \cdot 7H_2O$ (2 g/L), $CaCl_2$ (2 g/L), K_2HPO_4 (1 g/L), $FeSO_4 \cdot 7H_2O$ (0.1 g/L), $MnSO_4 \cdot 5H_2O$ (0.1 g/L), and H_2O adjusted pH 7.0 by Na_2CO_3. Antifungal metabolites were extracted from the culture filtrate (750 mL) with 1 L of EtOAc three times after adjustment of the pH to 4.0 with HCl. The EtOAc solution was dehydrated over anhydrous Na_2SO_4 and concentrated to dryness to afford an extract (3.8 g). The extract was dissolved in H_2O, and the pH of the solution was adjusted to 7.0. The solution was purified with solid-phase extraction (Oasis HLB 35 cc LP Extraction Cartridge, Waters) eluted stepwise with 50 mL each of 0, 20, 40, 60, 80, and 100% (v/v)

MeOH in H_2O. The antifungal activity of each fraction was determined by the paper-disk method using *B. cinerea* as the test organism on a potato dextrose agar (PDA, Becton, Dickinson and Co.) plate at 20 ˚C for 3 days. The active fractions eluted with 60-80% MeOH in H_2O were combined and concentrated to dryness. The concentrate was subjected to Sephadex LH-20 column chromatography with MeOH. The active fractions were pooled and evaporated to dryness to afford a residue (0.80 g). The residue was further purified by preparative HPLC (XBridge C18, 250 x 10 mm) eluted with 45% (v/v) CH_3CN-H_2O containing 0.1% TFA at a flow rate of 4.7 mL/min at 40 ˚C, and absorbance at 205 nm was measured to afford the active compounds **1** (23 mg), **2** (92 mg), **3** (120 mg), and **4 (**56 mg).

Amino Acid Analysis. Compound **3** (1 mg) was hydrolyzed with 6 N HCl at 110 ˚C for 18 h, and the hydrolysate was dried with N_2. The amino acids were analyzed using the Shimadzu Prominence Amino Acid Analysis System (Shimadzu Corp., Tokyo, Japan) by postcolumn fluorescence derivatization with *o*-phthalaldehyde (OPA) / *N*-acetylcysteine as the reaction reagent.

***N*-Bromosuccinimide Cleavage and Edman Degradation.** Compound **3** (2.5 mg) was dissolved in 0.5 mL of 70% aqueous AcOH. *N*-Bromosuccinimide[3] (2.5 mg) was added, and the solution was allowed to stand for 1 h at room temperature. Three drops of formic acid were added to the solution to terminate the reaction. The open-up fragment of compound **3** was purified by preparative HPLC (XBridge C18, 250 x 4.6 mm) eluted with 50% (v/v) CH_3CN-H_2O containing 0.1% TFA at a flow rate of 1.0 mL/min at 40 ˚C, and absorbance at 205 nm was measured. The *N*-terminal amino acid sequence of the fragment was determined by Edman degradation using the Shimadzu Protein Sequencer PPSQ-23A.

Matrix-Associated Laser Desorption Ionization Time of Flight (MALDI-TOF) MS/MS Analysis. MALDI-TOF MS/MS data were obtained with a Shimadzu AXIMA Resonance using a 337.1 nm nitrogen laser for desorption and ionization. 2,5-Dihydroxybenzoic acid (10 mg/mL) in 50% (v/v) CH_3CN-H_2O containing 0.1% TFA was used as the matrix solution. Positive-ion detection and reflectron mode were used.

Absolute Configuration of α-Amino Acid. Compound **3** (1 mg) was hydrolyzed with 0.5 ml of 6 N HCl at 110 ˚C for 18 h and dried with N_2. To the hydrolysate was added 100 μL of H_2O, 200 μL of 1% FDAA (Marfey's reagent)[4] in acetone, and 40 μL of 1 M $NaHCO_3$. The

mixture was kept at 40 ˚C for 1 h, and 20 μL of 2 M HCl was added to terminate the reaction. The reaction mixture was analyzed by HPLC equipped with a reverse-phase column (XBridge C18, 250 x 4.6 mm) eluted with a linear gradient of 10% to 50% (v/v) CH_3CN-H_2O containing 0.1% TFA in 45 min at a flow rate of 1.0 mL/min, 40 ˚C, and absorbance at 340 nm was measured. Derivatives of standard $_L$- and $_D$-amino acids were co-injected. To determine the absolute configuration of Asn1 and Asn2, two tripeptides, NH_2-$_L$-Asp-$_D$-Tyr-$_D$-Asp and NH_2-$_D$-Asp-$_D$-Tyr-$_L$-Asp, were used as standard peptides (Sigma-Aldrich). Compound **3** (3 mg) was hydrolyzed in 0.5 mL of 3 N HCl at 105 ˚C for 1 h and dried with N_2. To the hydrolysate was added 100 μL of H_2O, and the hydrolysate solution was analyzed by HPLC equipped with a phenyl column (XBridge Phenyl, 250 x 4.6 mm), eluted with 5% (v/v) CH_3CN-H_2O containing 0.1% TFA at a flow rate of 1.0 mL/min, 40 ˚C, and absorbance at 280 nm was measured. Two standard tripeptides, NH_2-$_L$-Asp-$_D$-Tyr-$_D$-Asp and NH_2-$_D$-Asp-$_D$-Tyr-$_L$-Asp, were eluted at 8.2 and 7.3 min, respectively.

Absolute Configuration of β-Amino Fatty Acid. A β-amino fatty acid of compound **3** was produced by the hydrolysis (1 mL of 6 N HCl, 110 ˚C, 24 h) of compound **3** (10 mg) and extraction with chloroform. Dinitrophenylation of the β-amino fatty acid was carried out according to Sanger's procedure.[5] The Dnp derivative thus obtained was treated with *p*-methoxyaniline, 1-ethyl-3-(3-dimethylaminopropyl)carbodiimide, and 1-hydroxybenzotriazole in methylene chloride. The reaction products were purified by preparative HPLC using a column (XBridge C18, 250 x 4.6 mm) eluted with 90% (v/v) CH_3CN-H_2O containing 0.1% TFA at a flow rate of 1.0 mL/min at 40 ˚C, and absorbance at 340 nm was measured to yield the dinitrophenyl-*p*-methoxyaniline derivative (< 1.0 mg). The structure was confirmed by mass ($[M+H]^+$, 557.4) and ^{1}H-NMR ($CDCl_3$) spectra. The amount of the derivative was determined to be 0.41 mg by a calculation based on ε value at A_{347} in the literature.[6] The CD spectrum of the derivative was compared to that in the literature.[6] CD (*c* 8.4 x 10^{-5} M, MeOH) λ_{max} ($\Delta\ \varepsilon$) 262 (+4.29), 300 (+0.54), 330 (+0.77), 400 (–1.82) nm.

In Vitro Assay against Plant Pathogens. We obtained the following from the National Institute of Agrobiological Science, Tsukuba, Japan: *Botrytis cinerea* Persoon MAFF 744071, *Rhizoctonia solani* J. G. Kuehn MAFF 305219, *Fusarium oxysporum* Schlechtendahl MAFF

410171, *Pyricularia grisea* (Cooke) Saccardo MAFF 101583, *Alternaria alternata* (Fries) Keissler MAFF 731001, *Botryosphaeria berengeriana* De Notaris f. sp. *pyricola* Koganezawa et Sakuma MAFF 645002, *Didymella bryoniae* (Fuckel) Rehm MAFF 235932, and *Pythium aphanidermatum* (Edson) Fitzpatrick MAFF 239200. The following strains were obtained from Biological Resource Center (NBRC), National Institute of Technology and Evaluation, Chiba, Japan: *Colletotrichum acutatum* Simmonds NBRC 32849, *Monilinia fructicola* (Winter) Honey NBRC 30451, *Penicillium expansum* Link ex S.F. Gray NBRC 5453, and *Sclerotinia sclerotiorum* (Libert) de Bary NBRC 4876. *Fusarium graminearum* Schwabe ARC 2075-1 was supplied from NARO Agricultural Research Center, Tsukuba, Japan. The DMSO solution (60 μL) of the each compound was added to 6 mL of PDA held at 50˚C. The agar medium was poured onto a 60 mm plate. Each compound was tested at concentrations of 2.5, 5.0, 10, 20, 40, and 80 μg/mL. A PDA disk (5 mm in diameter) with mycelia of each test pathogen was placed on each plate containing a compound. The pathogens were incubated at 22 ˚C for 1.5 days (*B. cinerea*, *D. bryoniae,* and *S. sclerotiorum*), 2 days (*R. solani*, *P. aphanidermatum*, *F. graminearum*, *B. berengeriana,* and *M. fructicola*), 2.5 days (*F. oxysporum*), 3 days (*P. expansum* and *C. acutatum*), 4 days (*A. alternata*), and 5 days (*P. grisea*). The pathogens growing on PDA (6 mL) containing 60 μL of DMSO were used as controls. All experiments were performed in triplicate. IC_{50} values (median inhibitory concentrations) were calculated using the inhibition rate of mycelial growth. That rate was calculated as

$$\text{Inhibition rate of mycelial growth (\%)} = (1 - D_a/D_b) \times 100$$

where D_a is the diameter of the pathogen colony in the plate containing a test compound and D_b is the diameter of the colony in the control plate. The results were expressed as IC_{50} (mean, μM (95% confidential interval)).

Leaf-Disk Assay Using Cucumber Cotyledon and *Botrytis cinerea*. Cucumber seeds (*Cucumis stativus* L., Sagami-Hanjiro) were planted in 12 cm pots containing artificial soil and grown in the greenhouse at 16 to 23 ˚C without supplemental lighting. The cotyledons were collected from 3-week-old plants. The test compound was dissolved in an appropriate

amount of phosphate buffer (40 mM, pH 7.2), and 50 μL of the solution was applied to a paper disk (8 mm in diameter, thick type, Advantec Toyo Kaisha, Ltd., Tokyo, Japan) on the cucumber cotyledon. For the control, only phosphate buffer was applied. Then the paper disks on the leaves were inoculated with 50 μL of *B. cinerea* spore suspension (2 x 10^4/mL) containing 0.2% (w/v) yeast extract and 2 % (w/v) sucrose. Each compound was tested at final concentrations of 10, 20, 30, 40, 60, and 80 μM. The leaves were kept in a humidity chamber (relative humidity >95%) at 20 ˚C for 4 days in darkness. The experiment was repeated four times. The inhibition rate of *B. cinerea* infection was calculated as

$$\text{Inhibition rate of infection (\%)} = (1 - D_c/D_d) \times 100$$

where D_c is the diameter of the infection zone in the leaf with a test compound and D_d is the diameter of the infection zone in the control leaf. The results were expressed as inhibition rate (mean % ± SD).

2.3. Results and Discussion

Isolation of Compounds 1-4 from *Bacillus amyloliquefaciens* SD-32. In my screening search, SD-32, a bacterium isolated from soil, was found to have strong antifungal activity against plant pathogen *Botrytis cinerea*. The PCR product of its 16S rRNA gene was sequenced to give a 1472 bp sequence followed by a BLAST similarity search; it was identified as *Bacillus amyloliquefaciens* (99.9% similarity with *B. amyloliquefaciens* type strain). SD-32 was cultured in a medium (800 mL) composed of maltose, soybean powder, yeast extract, and some minerals at 30˚C for 64 h. Antifungal activity-guided purification of the EtOAc extract of the culture filtrate with solid-phase extraction, gel filtration, and preparative HPLC afforded compounds **1** (23 mg), **2** (92 mg), **3** (120 mg), and **4** (56 mg) as white amorphous powders. The HPLC profile at the final step of purification is shown in Figure 2-2.

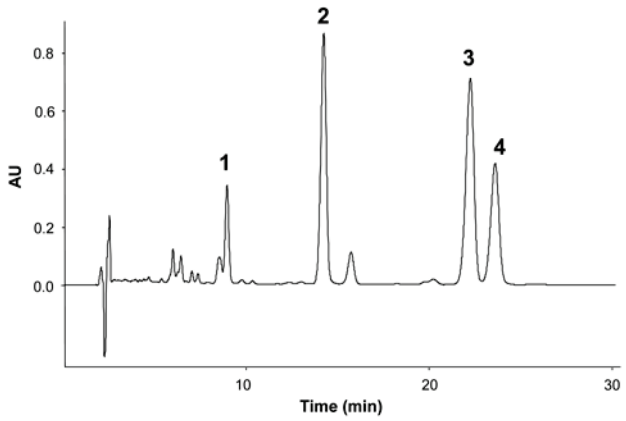

Figure 2-2. Preparative HPLC of compounds **1-4** in the active fractions after Sephadex LH-20 column chromatography.

Structures of Compounds 1-4. Since compound **3** was most abundant in the culture broth, we elucidated its structure first. Compound **3** gave an $[M+H]^+$ peak at *m*/*z* 1073.5902 (Calcd for $C_{51}H_{81}N_{10}O_{15}$, 1073.5883) in HR-ESI-MS. Six α-amino acids, Asp, Tyr, Glu, Pro, Ser, and Thr, were found in a 2:1:1:1:1:1 ratio in an amino-acid analysis of the hydrolysate. Because the ^{1}H-NMR spectrum of compound **3** in DMSO-d_6 showed peaks due to a couple of conformers, pyridine-d_5 was used as NMR solvent. The ^{1}H-NMR data for compound **3** (Table

2-1 and Figure S1) indicated the presence of 11 amide protons (δ_H 9.66-7.80) and 7 α-protons (δ_H 5.39-4.72, partially overlapped) of amino acid residues of a peptide, a *p*-substituted benzene ring (δ_H 7.47 d, 7.06 d, 2H each), a long methylene chain (δ_H 1.20-1.15), and three terminal methyl groups (δ_H 1.34 d, 0.82 t, and 0.82 d, each 3H). The ^{13}C-NMR data for compound **3** (Table 2-2 and Figure S2) exhibited 49 signals, including 11 carbonyl groups (δ_C 175.5–171.1), a *p*-substituted benzene (δ_C 157.5, 1C; 131.3, 2C; 128.6, 1C; 116.1, 2C), methylene carbons (δ_C 63.5-26.1), and three methyl carbons (δ_C 20.8, 19.3 and 11.5). Thus compound **3** was deduced to be *anteiso*-C_{17} bacillomycin D, a cyclic lipopeptide consisting of two Asn, one Tyr, one Pro, one Glu, one Ser, and one Thr residues and a β-amino acid with a $-(CH_2)_{10}CH(CH_3)CH_2CH_3$ group as a side chain from the ^{1}H-^{1}H COSY, HSQC, HMBC, and NOESY data shown in Figure 2-3 and Figures S3-S6, and also by considering the molecular formula. To confirm this, chemical and MALDI-TOF MS/MS analyses were conducted as follows. Compound **3** was cleaved at the C-terminus of the Tyr residue by *N*-bromosuccinimide[3] and the cleaved product (oxidized form of Tyr with 2 moles of Br, molecular mass 1246) was purified by preparative HPLC. The fragment was analyzed by Edman degradation and yielded the following sequence: NH_2-Asn-Pro-Glu-Ser-Thr-X (Figure 2-4A). Compound **3** was also analyzed by MALDI-TOF MS/MS to afford the sequence information as shown in Figure 2-4B. These results confirmed that the structure of compound **3** was *anteiso*-C_{17} bacillomycin D.

The absolute configurations of α-amino acids in compound **3** were determined by treatment of the hydrolysate with Marfey's reagent[4] and HPLC analysis of the derivatives. The hydrolysate was shown to contain $_L$-Asp, $_D$-Tyr, $_D$-Asp, $_L$-Pro, $_L$-Glu, $_D$-Ser, and $_L$-Thr. There is no ambiguity in the absolute configuration of the five amino acids other than Asn (in the form of the corresponding Asp). The absolute configurations of the two Asn were determined by HPLC comparison of the tripeptide in the partial hydrolysate of compound **3** with two synthesized tripeptides, NH_2-$_L$-Asp-$_D$-Tyr-$_D$-Asp and NH_2-$_D$-Asp-$_D$-Tyr-$_L$-Asp. The existence of NH_2-$_L$-Asp-$_D$-Tyr-$_D$-Asp in the hydrolysate finally allowed us to establish the amino acid sequence, NH_2-$_L$-Asn-$_D$-Tyr-$_D$-Asn-$_L$-Pro-$_L$-Glu-$_D$-Ser-$_L$-Thr of compound **3**.

To determine the absolute configuration of C3 in the β-amino fatty acid, the β-amino fatty acid was isolated from the hydrolysate of compound **3** and modified with

dinitrofluorobenzene and *p*-methoxyaniline (Figure 2-4C). The CD spectra of the dinitrophenyl-*p*-methoxyaniline derivative was similar to that of the derivative of iturinic acid,[6] indicating apparently that the β-amino fatty acid of compound **3** had an *R*-configuration, the same as iturinic acid.

The HR-MS of compounds **1**, **2**, and **4** showed their $[M+H]^+$ ion peaks at *m*/*z* 1045.5552 (HR-FAB-MS; Calcd for $C_{49}H_{77}N_{10}O_{15}$, 1045.5570), 1059.5756 (HR-ESI-MS; Calcd for $C_{50}H_{79}N_{10}O_{15}$, 1059.5726), and 1073.5876 (HR-ESI-MS; Calcd for $C_{51}H_{81}N_{10}O_{15}$, 1073.5883), respectively. A series of NMR spectral analyses (Figures S7-S16) revealed that compounds **1**, **2**, and **4** had the same amino acid sequence as compound **3**, except for the side chain structures of the β-amino fatty acids. The ^{1}H-NMR and ^{13}C-NMR spectra of compounds **1**, **2**, and **4** showed the presence of the $-(CH_2)_9CH(CH_3)_2$, $-(CH_2)_{10}CH(CH_3)_2$, and $-(CH_2)_{11}CH(CH_3)_2$ groups, respectively. Thus compounds **1**, **2**, and **4** were determined to be *iso*-C_{15}, *iso*-C_{16}, and *iso*-C_{17} bacillomycin D, respectively.

Compounds **1** and **2** are known,[7] and **3** and **4** are new. Compounds **3** and **4** have *anteiso*- and *iso*-C_{17} β-amino fatty acids, and seven α-amino acids with the same chiral sequence, LDDLLDL, as the iturin family. This is the first report to establish the absolute structure of bacillomycin D. The metabolites assumed to be *anteiso*-C_{17} and *iso*-C_{17} bacillomycin D (**3** and **4**) were previously detected in mass spectrometric analyses of extracts from *Bacillus* species by Koumoutsi et al.,[8] Ramarathnam et al.,[9] Athukorala et al.,[10] and Liu et al.,[11] although their chemical structures were not determined. The lipid moieties of compounds **3** (*anteiso*-C_{17}) and **4** (*iso*-C_{17}) were previously reported in iturin A,[12, 13] bacillomycin F,[14] and mycosubtilin,[15] and the reported contents of C_{17} homologues in iturin A, bacillomycin F, and mycosubtilin were 3, 39, and 61%, respectively. In case of bacillomycin D, Peypoux et al.[7] reported percentages of each homologue (C_{14}, C_{15}, and C_{16}) in bacillomycin D were 48, 35, and 12 %, respectively, and did not mention C_{17} homologues. Hourdou et al.[16] showed contents of each homologue (C_{14}, C_{15}, C_{16}, and C_{17}) in bacillomycin D were 48, 30, 22, and 0 %, respectively. It is noteworthy that the content of the C_{17} bacillomycin D homologues was very high (60%) in the present study.

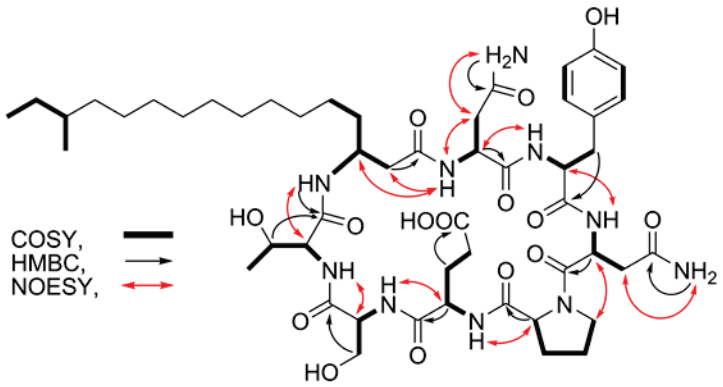

Figure 2-3. Key COSY, HMBC, and NOESY correlations detected for compound **3**.

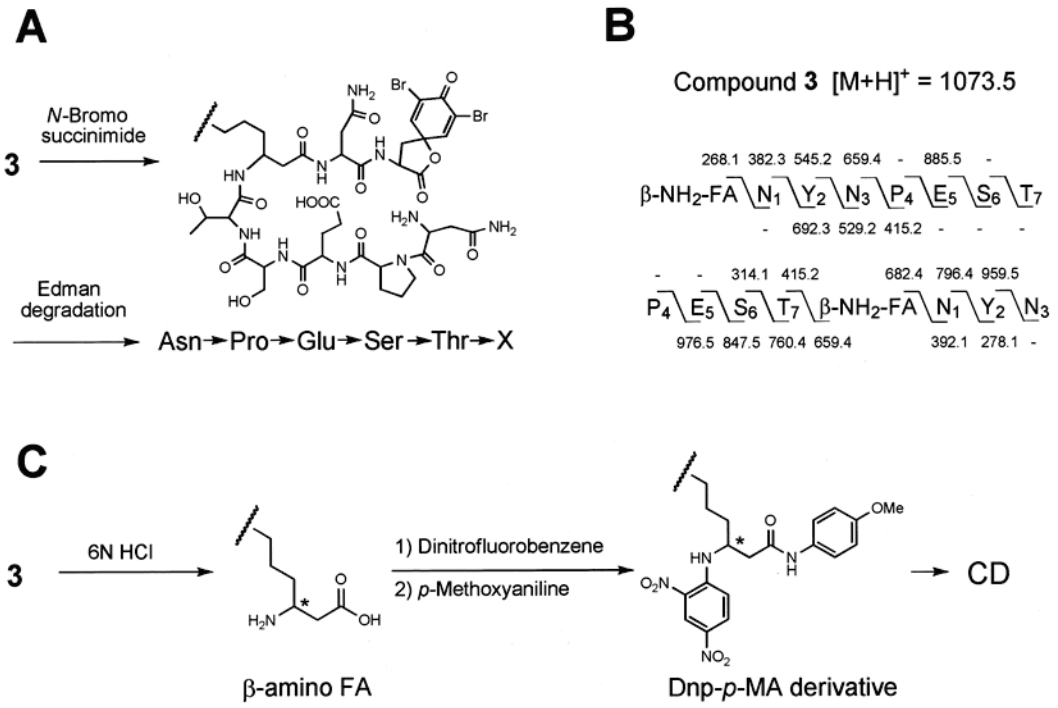

Figure 2-4. Reaction schemes for chemical analyses and MALDI-TOF MS/MS analysis: (A) *N*-bromosuccinimide cleavage of compound **3** followed by Edman degradation; (B) MALDI-TOF MS/MS analysis of compound **3**; (C) preparation of Dnp-*p*-MA derivative of β-amino fatty acid from compound **3** to determine the absolute configuration of β-amino fatty acid.

Table 2-1. ^{1}H NMR Data for Compounds 1-4 in Pyridine-d_5[a]

moiety	position	δ_H (J in Hz)			
		1	**2**	**3**	**4**
$_L$-Asn1	1	5.31m	5.27m	5.27m	5.27m
	2	3.08m, 3.03m[b]	3.08dd (15.3, 5.4), 3.02m[b]	3.08dd (15.4, 5.6), 3.02m[b]	3.07dd (15.4, 5.5), 3.01m[b]
	1-NH	9.17brs	9.04brs	9.03brs	9.02brs
	3-NH_2	8.45brs[c], 7.89brs	8.38brs[c], 7.81brs	8.37brs[c], 7.80brs	8.37brs[c], 7.80brs
$_D$-Tyr	5	5.40m	5.32m	5.32m	5.32m
	6	3.72dd (13.6, 4.6), 3.41dd (13.6, 10.0)	3.72m, 3.40m	3.72dd (13.8, 4.7), 3.40dd (13.8, 9.8)	3.72dd (13.7, 4.6), 3.39dd (13.7, 10.0)
	8, 12	7.47d (8.1)	7.47d (8.2)	7.47d (8.3)	7.47d (8.1)
	9, 11	7.06d (8.1)	7.06d (8.2)	7.06d (8.3)	7.06d (8.1)
	5-NH	9.68brs	9.66brs	9.66brs	9.66brs
$_D$-Asn2	14	5.55m	5.38m	5.39m	5.39m
	15	3.58dd (15.7, 8.6), 3.18dd (15.7, 4.8)	3.57dd (15.5, 9.1), 3.18dd (15.5, 4.8)	3.57dd (15.6, 9.2), 3.18dd (15.6, 5.1)	3.57dd (15.6, 9.3), 3.18dd (15.6, 5.0)
	14-NH	9.00brs	8.96brs	8.95brs	8.94brs
	16-NH_2	8.62brs, 7.97brs	8.56brs, 7.90brs	8.55brs, 7.89brs	8.55brs, 7.88brs
$_L$-Pro	18	4.73m	4.73dd (8.0, 5.3)	4.72dd (8.2, 5.4)	4.72dd (7.9, 5.6)
	19	2.10m, 2.08m	2.10m, 2.08m	2.11m, 2.08m	2.10m, 2.07m
	20	1.84m, 1.61m	1.86m, 1.65m	1.86m, 1.65m	1.86m, 1.65m
	21	4.22m, 4.00m	4.27m, 4.04m	4.26m, 4.03m	4.26m, 4.03m
$_L$-Glu	23	4.87m[d]	4.87m[d]	4.87m[d]	4.87m[d]
	24	2.78m, 2.61m[e]	2.79m, 2.62m[e]	2.79m, 2.62m[e]	2.79m, 2.62m[e]
	25	3.03m[b], 2.94m	3.03m[b], 2.95m	3.03m[b], 2.95m	3.03m[b], 2.95m
	23-NH	8.45brs[c]	8.38brs[c]	8.36brs[c]	8.36brs[c]
$_D$-Ser	28	4.92m[d]	4.89m[d]	4.89m[d]	4.89m[d]
	29	4.40m, 4.33m	4.38dd (11.4, 3.3), 4.33dd (11.4, 3.5)	4.38dd (11.3, 3.2), 4.33dd (11.3, 3.5)	4.38dd (11.4, 3.0), 4.33dd (11.4, 3.2)
	28-NH	8.84brs	8.74brs	8.74brs	8.75brs
$_L$-Thr	31	4.92m[d]	4.89m[d]	4.89m[d]	4.89m[d]
	32	4.94m[d]	4.95m	4.95m	4.95m
	33	1.34d (6.0)	1.34d (6.3)	1.34d (6.4)	1.34d (6.2)
	31-NH	8.23brs	8.16brs	8.15brs	8.14brs
$_D$-β-AA	35	4.62m	4.62m	4.61m	4.61m
	36	2.64m[e], 2.45m	2.62m[e], 2.43m	2.62m[e], 2.43m	2.63m[e], 2.43m
	38	1.57m, 1.43m[f]	1.55m, 1.45m[f]	1.56m, 1.45m	1.56m, 1.45m[f]
	39	1.30m	1.30m	1.28m	1.30m
	40	1.18-1.12[g]	1.19-1.14[g]	1.20-1.15[g]	1.21-1.15[g]
	41	1.18-1.12[g]	1.19-1.14[g]	1.20-1.15[g]	1.21-1.15[g]
	42	1.18-1.12[g]	1.19-1.14[g]	1.20-1.15[g]	1.21-1.15[g]
	43	1.18-1.12[g]	1.19-1.14[g]	1.20-1.15[g]	1.21-1.15[g]
	44	1.18-1.12[g]	1.19-1.14[g]	1.20-1.15[g]	1.21-1.15[g]
	45	1.18-1.12[g]	1.19-1.14[g]	1.20-1.15[g]	1.21-1.15[g]
	46	1.08m	1.19-1.14[g]	1.20-1.15[g]	1.21-1.15[g]
	47	1.43m[f]	1.11m	1.24m[f], 1.08m	1.21-1.15[g]
	48	0.82d (6.6)	1.43m[f]	1.24m[f]	1.11m
	49	0.82d (6.6)	0.83d (6.7)	0.82d (6.3)	1.45m[f]
	50		0.83d (6.7)	1.24m[f]	0.83d (6.6)
	51			0.82t (7.4)	0.83d (6.6)
	35-NH	8.20brs	8.12brs	8.11brs	8.11brs

[a] Compound **1**, 500MHz; **2**, 600MHz; **3** and **4**, 800MHz. [b, c, d, e, f, g] Overlapped in each column.

Table 2-2. ^{13}C NMR Chemical Shifts of Compounds 1-4 in Pyridine-d_5[a]

moiety	position	δ_C			
		1	**2**	**3**	**4**
$_L$-Asn1	1	52.8	52.9	52.9	52.9
	2	37.1	37.1	37.1	37.1
	3	172.7[b]	172.7[b]	172.7[b]	172.7[b]
	4	173.0[b]	172.9[b]	172.9[b]	172.9[b]
$_D$-Tyr	5	55.9	55.9	55.9	55.9
	6	36.4	36.5	36.5	36.4
	7	128.7	128.6	128.6	128.7
	8, 12	131.3	131.3	131.3	131.3
	9, 11	116.1	116.1	116.1	116.1
	10	157.4	157.5	157.5	157.5
	13	173.6[c]	173.7[c]	173.7[c]	173.7[c]
$_D$-Asn2	14	50.2	50.3	50.3	50.3
	15	37.8	37.8	37.8	37.8
	16	172.5[b]	172.5[b]	172.6[b]	172.6[b]
	17	172.9[b]	172.7[b]	172.7[b]	172.7[b]
$_L$-Pro	18	62.0	62.2	62.1	62.1
	19	29.6[d]	29.8[d]	29.7[d]	29.6[d]
	20	25.0	25.0	25.0	25.0
	21	48.5	48.6	48.6	48.5
	22	172.5[b]	172.4[b]	172.4[b]	172.4[b]
$_L$-Glu	23	55.3	55.4	55.4	55.4
	24	27.7	27.7	27.7	27.7
	25	31.7	31.7	31.7	31.7
	26	175.6	175.5	175.5	175.5
	27	173.6[c]	173.8[c]	173.8[c]	173.7[c]
$_D$-Ser	28	59.4	59.3	59.3	59.3
	29	63.4	63.6	63.5	63.5
	30	171.7	171.7	171.7	171.7
$_L$-Thr	31	57.8	57.9	57.9	57.9
	32	66.4	66.2	66.2	66.2
	33	20.7	20.8	20.8	20.8
	34	171.1	171.1	171.1	171.1
$_D$-β-AA	35	47.5	47.4	47.4	47.4
	36	41.9	42.0	42.0	42.0
	37	173.2[b]	173.2[b]	173.2[b]	173.2[b]
	38	35.7	35.7	35.7	35.7
	39	26.1	26.1	26.1	26.1
	40	29.6[d]	29.6[d]	29.6[d]	29.6[d]
	41	29.7[d]	29.9[d]	29.7[d]	29.7[d]
	42	29.8[d]	29.9[d]	29.9[d]	29.9[d]
	43	29.9[d]	29.9[d]	29.9[d]	29.9[d]
	44	29.9[d]	30.0[d]	30.0[d]	30.0[d]
	45	30.2[d]	30.2[d]	30.0[d]	30.0[d]
	46	39.2	30.5[d]	30.3[d]	30.0[d]
	47	28.1	39.2	36.8	30.2[d]
	48	22.7	28.2	34.6	39.2
	49	22.7	22.7	19.3	28.1
	50		22.7	27.4	22.7
	51			11.5	22.7

[a] Compound **1**, 125 MHz; **2**, 150 MHz; **3** and **4**, 200 MHz.

[b, c, d] Assignments may be interchanged in each column.

Activities of Compounds 1-4 against Plant Pathogens. The activities of compounds **1-4** were evaluated against 13 plant pathogens in PDA medium, and the results are shown in Table 2-3. The table reveals that the activities of compounds **3** and **4** (*anteiso*- and *iso*-C_{17}) were almost the same against all fungi tested and were stronger than those of compounds **1** and **2**; compound **1** was the weakest. Compounds **1-4** inhibited the growth of all fungi tested, and *B. berengeriana, B. cinerea*, *P. grisea*, *D. bryoniae, S. sclerotiorum,* and *M. fructicola* were the most sensitive to the compounds. By contrast, the oomycete *P. aphanidermatum* was not inhibited at all by any of the compounds. The activity of iturin family lipopeptides is attributed to their membrane-disruptive property through a direct lipopeptide-sterols interaction.[17] The oomycetes do not synthesize sterols,[18] and thus are assumed to be insensitive to bacillomycin D homologues.

The structure-antifungal activity relationships of iturin A,[19] bacillomycin Lc,[20] and bacillopeptins[21] have been studied. The activity of iturin A is directly related to the lipophilic side chain of its β-amino fatty acid; the activity increased with the number of carbon atoms in the β-amino fatty acid ($C_{16} > C_{15} > C_{14}$). The same results were obtained for bacillomycin Lc and bacillopeptins. Recently, Tabbene et al.[22] investigated bacillomycin D-like compounds and showed that their anti-*Candida* activity increased in the order of the side chain length: $C_{16} > C_{15} > C_{14}$. This result for bacillomycin D showed that the order of activity against plant pathogens was $C_{17} > C_{16} > C_{15}$; the activity of bacillomycin D increased with side chain length until C_{17}. Recently, it was reported that mycosubtilin interacts preferentially with ergosterol compared to the other classes of lipids and that the presence of ergosterol makes it easier to insert the lipopeptide into the membrane.[23] The β-amino fatty acid with 17 carbon atoms in bacillomycin D is assumed to be the best-fitting molecule for hydrophobic interactions with the sterols in the membrane.

Finally, leaf-disk assay using cucumber cotyledon and *B. cinerea* was conducted to clarify the potential effect of bacillomycin D against gray mold disease. The result is shown in Table 2-4 and Figure 2-5. Compounds **1-4** at concentrations of 80, 40, 30, and 30 μM, respectively, inhibited completely the *B. cinerea* infection in the cucumber leaf.

The present study demonstrates that strain SD-32 is unique because it produced a higher

contents of the C_{17} bacillomycin D homologues than other strains reported previously. The result of in vitro antifungal assay showed that the activities of C_{17} bacillomycin D homologues are much stronger than the known C_{15} and C_{16} homologues, and also from the result of the cucumber leaf-disk assay it was pointed out that the C_{17} bacillomycin D homologues can control gray mold disease. These indicate that this unique strain, SD-32, must be a potential promising resource for the biological control of plant disease.

Table 2-3. Activities of Compounds 1-4 against Plant Pathogens

	IC_{50} (mean, μM (95% confidential interval))			
plant pathogen	**1**	**2**	**3**	**4**
Botryosphaeria berengeriana MAFF 645002	-[a]	5.0 (4.4-5.4)	3.7 (3.4-4.2)	4.0 (3.8-4.5)
Botrytis cinerea MAFF 744071	28.2 (26.3-30.2)	8.6 (7.8-9.3)	4.2 (3.9-4.6)	4.1 (3.4-4.7)
Pyricularia grisea MAFF 101583	-	6.6 (5.9-7.3)	4.3 (3.9-4.8)	4.5 (4.1-5.0)
Didymella bryoniae MAFF 235932	-	7.6 (6.8-8.6)	4.7 (4.1-5.2)	4.6 (4.0-5.2)
Sclerotinia sclerotiorum NBRC 4876	-	6.9 (6.1-7.6)	4.9 (4.3-5.4)	4.6 (4.0-5.1)
Monilinia fructicola NBRC 30451	-	7.3 (6.5-8.2)	5.0 (4.3-5.8)	4.8 (4.3-5.6)
Rhizoctonia solani MAFF 305219	59.0 (51.9-69.6)	12.8 (11.9-14.0)	6.5 (5.8-7.3)	7.9 (7.1-8.9)
Colletotrichum acuatum NBRC 32849	30.5 (25.7-36.7)	14.6 (12.3-17.7)	10.6 (9.0-13.0)	10.4 (8.8-12.8)
Penicillum expansum NBRC 5453	29.0 (23.8-35.7)	13.0 (10.5-17.5)	10.9 (8.6-14.9)	10.9 (8.9-14.1)
Fusarium oxysporum MAFF 410171	43.9 (38.6-51.0)	18.9 (15.5-25.5)	14.1 (11.8-17.9)	12.2 (10.6-14.4)
Fusarium gramunearum ARC 2075-1	-	17.4 (15.2-20.1)	11.2 (9.5-13.0)	12.8 (11.0-14.9)
Alternaria alternata MAFF 731001	-	20.0 (15.9-28.4)	14.6 (12.1-18.6)	15.3 (13.3-18.1)
Pythium aphanidermatum MAFF 239200	>40	>40	>40	>40

[a]Not tested.

Table 2-4. Leaf-Disk Assay Using Cucumber Cotyledon and *Botrytis cinerea*

	inhibition rate (%) ± SD (n = 4)					
compd	10 μM	20 μM	30 μM	40 μM	60 μM	80 μM
1	3.8 ± 9.0	15.9 ± 12.5	7.5 ± 26.6	-14.2 ± 11.0	19.5 ± 19.6	100
2	18.3 ± 12.3	29.1 ± 25.8	77.2 ± 22.9	100	100	100
3	3.8 ± 15.2	19.5 ± 21.3	100	100	100	100
4	21.9 ± 28.9	20.7 ± 5.4	100	100	100	100

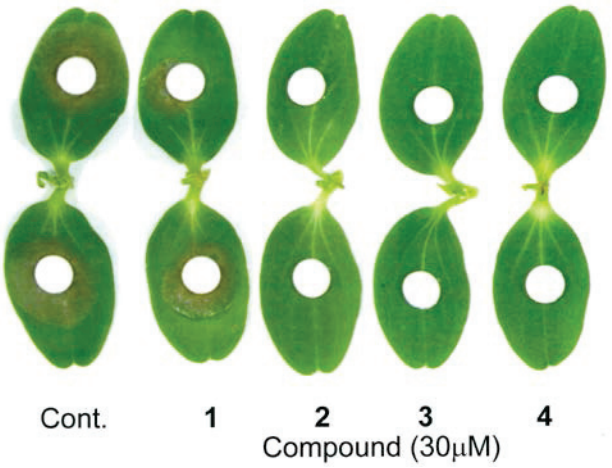

Figure 2-5. Leaf-disk assay using cucumber cotyledon and *Botrytis cinerea*.

References

(1) Williamson, B.; Tudzynski, B.; Tudzynski, P.; van Kan, J. A. L. *Botrytis cinerea*: the cause of grey mould disease. *Mol. Plant Pathol*. **2007**, *8*, 561-580.

(2) Rosslenbroich, H. J.; Stuebler, D. *Botrytis cinerea* - history of chemical control and novel fungicide for its management. *Crop Prot.* **2000**, *19*, 557-561.

(3) Ramachandran, L. K.; Witkop, B. *N*-Bromosuccinimide cleavage of peptides. *Methods Enzymol.* **1967**, *11*, 283-299.

(4) Marfey, P. Determination of $_{D}$-amino acids. II. Use of a bifunctional reagent, 1, 5-difluoro-2, 4-dinitrobenzene. *Carlsberg Res. Commun*. **1984**, *49*, 591-596.

(5) Sanger, F. The free amino groups of insulin. *Biochem. J.* **1945**, *39*, 507-515.

(6) Nagai, U.; Besson, F.; Peypoux, F. Absolute configuration of an iturinic acid as determined by CD spectrum of its DNP-p-methoxyanilide. *Tetrahedron Lett.* **1979**, *25*, 2359-2360.

(7) Peypoux, F.; Pommier, M. T.; Das, B. C.; Besson, F.; Delcambe, L.; Michel, G. Structures of bacillomycin D and bacillomycin L peptidolipid antibiotics from *Bacillus subtilis*. *J. Antibiot.* **1984**, *37*, 1600-1604.

(8) Koumoutsi, A.; Chen, X. H.; Henne, A.; Liesegang, H.; Hitzeroth, G.; Franke, P.; Vater, J.; Borriss, R. Structural and functional characterization of gene clusters directing nonribosomal synthesis of bioactive cyclic lipopeptides in *Bacillus amyloliquefaciens* strain FZB42. *J. Bacteriol.* **2004**, *186*, 1084-1096.

(9) Ramarathnam, R.; Bo, S.; Chen, Y.; Fernando, W. G. D.; Xuewen, G.; Kievit, T. Molecular and biochemical detection of fengycin- and bacillomycin D-producing *Bacillus* spp., antagonistic to fungal pathogens of canola and wheat. *Can. J. Microbiol*. **2007**, *53*, 901-911.

(10) Athukorala, S. N. P.; Fernando, W. G. D.; Rashid, K. Y. Identification of antifungal antibiotics of Bacillus species isolated from different microhabitats using polymerase chain reaction and MALDI-TOF mass spectrometry. *Can. J. Microbiol*. **2009**, *55*, 1021-1032.

(11) Liu, J.; Zhou, T.; He, D.; Li, X. Z.; Wu, H,; Liu, W.; Gao, X. Functions of lipopeptides bacillomycin D and fengycin in antagonism of *Bacillus amyloliquefaciens* C06 towards *Monilinia fructicola*. *J. Mol. Microbiol. Biotechnol.* **2011**, *20*, 43-52.

(12) Isogai, A.; Takayama, S.; Murakoshi, S.; Suzuki, A. Structures of β-amino acids in antibiotics iturin A. *Tetrahedron Lett.* **1982**, *23*, 3065-3068.

(13) Hiradate, S.; Yoshida, S.; Sugie, H.; Yada, H.; Fujii, Y. Mulberry anthracnose antagonists (iturins) produced by *Bacillus amyloliquefaciens* RC-2. *Phytochemistry*. **2002**, *61*, 693-698.

(14) Peypoux, F.; Marion, D.; Maget-Dana, R.; Ptak, M.; Das, B. C.; Michel, G. Structure of bacillomycin F, a new peptidolipid antibiotic of the iturin group. *Eur. J. Biochem*. **1985**, *153*, 335-340.

(15) Peypoux, F; Pommier, M. T.; Marion, D.; Ptak, M.; Das, B. C.; Michel, G. Revised structure of mycosubtilin, a peptidolipid antibiotic from *Bacillus subtilis*. *J. Antibiot*. **1986**, *39*, 636-641.

(16) Hourdou, M. L.; Besson, F.; Tenoux, I.; Michel, G. Fatty acid and β-amino acid syntheses in strains of *Bacillus subtilis* producing iturinic antibiotics. *Lipids* **1989**, *24*, 940-944.

(17) Bonmatin, J. M.; Laprevote, O.; Peypoux, F. Diversity among microbial cyclic lipopeptides: iturins and surfactins. Activity-structure relationships to design new bioactive agents. *Comb. Chem. High Throughput Screen*. **2003**, *6*, 541-556.

(18) Latijnhouwers, M.; Wit, P. J. G. M.; Govers, F. Oomycetes and fungi: similar weaponry to attack plants. *Trends Microbiol*. **2003**, *11*, 462-469.

(19) Bland, J. M.; Lax, A. R.; Klich, M. A. HPLC separation and antifungal activity of the naturally occurring iturin-A homologs. *Peptides 1992*: *Proceedings of the Twenty-Second European Peptide Symposium*; Schneider, C. H., Eberle, A. N., Eds.;ESCOM: Leiden, The Netherlands, 1993; pp 332-333.

(20) Eshita, S. M.; Roberto, N. H.; Beale, J. M.; Mamiya, B. M.; Workman, R. F. Bacillomycin Lc, a new antibiotic of the iturin group: Isolation, structures, and antifungal activities of the congeners. *J. Antibiot*. **1995**, *48*, 1240-1247.

(21) Kajimura, Y.; Sugiyama, M.; Kaneda, M. Bacillopeptins, new cyclic lipopeptide antibiotics from *Bacillus subtilis* FR-2. *J. Antibiot*. **1995**, *48*, 1095-1103.

(22) Tabbene, O.; Kalai, L.; Slimene, I. B.; Karkouch, I.; Elkahoui, S.; Gharbi, A.; Cosette, P.; Mangoni, M. L.; Jouenne, T.; Limam, F. Anti-*Candida* effect of bacillomycin D-like

lipopeptides from *Bacillus subtilis* B38. *FEMS Microbiol. Lett.* **2011**, *316*, 108-114.

(23) Nasir, M. N.; Besson, F. Interactions of the antifungal mycosubtilin with ergosterol-containing interfacial monolayers. *Biochim*. *Biophys*. *Acta* **2012**, *1818*, 1302-1308.

Chapter 3

Isolation of [Ile^7]Surfactin Homologues from *B. amyloliquefaciens* SD-32 and Their Synergistic Effects in Combination with Bacillomycin D in Suppression of Gray Mold Disease

3.1. Introduction

In chapter 2, I described *Bacillus amyloliquefaciens* SD-32 obtained from a soil sample in Japan as a promising and effective agent against gray mold disease, and two new compounds, *anteiso*- and *iso*-C_{17} bacillomycin D in its fermentation broth. The strain SD-32 is quite different from other strains previously reported with respect to its production of C_{17} bacillomycin D homologues as major metabolites. The activities of C_{17} bacillomycin D homologues against *B. cinerea* were stronger than those of the known C_{15} and C_{16} homologues both in vitro and in vivo. These data indicate that the strain is a potentially promising resource for the biological control of gray mold disease, and indeed, the culture supernatant of this strain possesses a strong suppressive effect on gray mold disease in vivo. However, bacillomycin D homologues did not account for all of the activity in the culture supernatant of this strain, suggesting that other factors effective against gray mold disease were also present. The identification of all factors in SD-32 that are effective in controlling gray mold disease could contribute to a better understanding of the molecular basis of this biological control system.

In the course of purifying the fractions exhibiting synergistic activity with bacillomycin D in control of gray mold disease, five cyclic lipodepsipeptides (**5-9**) were found in the culture supernatant of this strain (Figure 3-1). The synergistic effects of compounds **5-9** with bacillomycin D in the suppression of gray mold disease were evaluated using an in vivo cucumber leaf-disk assay.

In this chapter, the factors that possess synergistic effects with bacillomycin D and contribute to control gray mold disease are described.

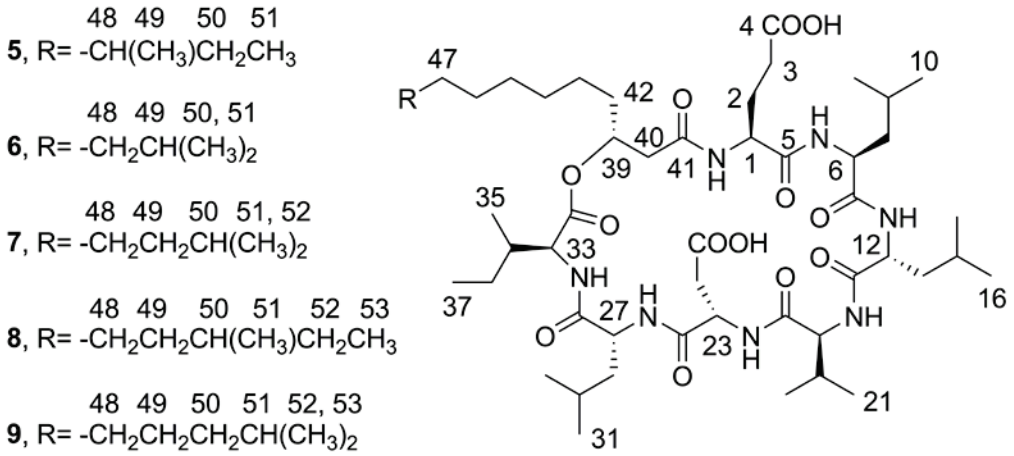

Figure 3-1. Structures of compounds **5-9**.

3.2. Materials and Methods

General Experimental Procedures. The solvents and reagents used in this study were purchased from Sigma-Aldrich (St. Louis, MO, USA) unless otherwise noted. NMR spectra were measured with Bruker Avance II 600 and Bruker Ascend 400 systems (Bruker Daltonics, Billerica, MA, USA). The spectra for compounds **5-9** were acquired in DMSO-d_6 (δ_H 2.49; δ_C 39.5) at room temperature. HR-FAB-MS was obtained with a JEOL JMS-700 spectrometer (JEOL, Tokyo, Japan). Preparative HPLC and HPLC analyses were performed with a Waters Alliance system (Waters, Milford, MA, USA).

Microorganisms. Isolation and identification of the *Bacillus amyloliquefaciens* strain SD-32 were described in the previous chapter.

Partial Purification of Factors Effective against Gray Mold Disease. Strain SD-32 was grown at 30 ˚C with shaking at 150 rpm for 64 h in a 500 mL flask containing 50 mL of liquid medium, composed of maltose (80 g/L), soybean powder (80 g/L; J-OIL MILLS, Tokyo, Japan), yeast extract (10 g/L; Becton, Dickinson and Co., Franklin Lakes, NJ, USA), $MgSO_4 \cdot 7H_2O$ (2 g/L), $CaCl_2$ (2 g/L), K_2HPO_4 (1 g/L), $FeSO_4 \cdot 7H_2O$ (0.1 g/L), $MnSO_4 \cdot 5H_2O$ (0.1 g/L), and H_2O adjusted pH 7.0 by Na_2CO_3. The culture supernatant (44 mL) was extracted with 50 mL of EtOAc three times after adjusting the pH (pH 4.0) with HCl. The EtOAc solution was dried over anhydrous Na_2SO_4 and concentrated in vacuo. The dry extract was dissolved in H_2O, and the pH of the solution was adjusted to 7.0. The solution was purified with solid-phase extraction (C18-SPE, Oasis HLB 6g/35 cc LP Extraction Cartridge; Waters) eluted stepwise with 50 mL each of 0, 20, 40, 60, 80, and 100% (v/v) CH_3CN-H_2O containing 0.1% TFA. Each fraction was evaporated in vacuo. The residues of each fraction were dissolved in 40 mL of phosphate buffer (40 mM, pH 7.2) and the each solution was evaluated in an in vivo cucumber leaf-disk assay.

HPLC Analyses of Culture Supernatant and C18-SPE Fractions. The amount of bacillomycin D in culture supernatant was determined by HPLC (XBridge C18, 250 x 4.6 mm; Waters), eluted with linear gradient 20 to 100% (v/v) CH_3CN-H_2O containing 0.1% TFA for 20 min at a flow rate of 1.0 mL/min at 40 ˚C, and detected by absorbance at 205 nm. The purified *anteiso*-C_{17} bacillomycin D was used as standard bacillomycin D. The C18-SPE fractions were analyzed under the same condition.

Isolation of Compounds 5-9. Strain SD-32 was grown at 30 ˚C with shaking at 150 rpm for 64 h in 500 mL flasks containing medium, which was the same as the case of partial purification (50 mL/flask, 1.6 L in total). The metabolites were extracted from the culture supernatant (1.5 L) with 2 L of EtOAc three times after adjusting the pH (pH 4.0) with HCl. The EtOAc solution was dried over anhydrous Na_2SO_4 and concentrated to dryness to afford a crude extract (4.6 g). This extract was dissolved in H_2O, and the pH of the solution was adjusted to 7.0. The solution was purified by SPE (C18-SPE, Oasis HLB 6g/35 cc LP Extraction Cartridge) eluted stepwise with 50 mL each of 0, 20, 40, 60, 70, 80, 90, and 100% (v/v) CH_3CN-H_2O containing 0.1% TFA. The fractions eluted with 70-80% CH_3CN-H_2O were combined and concentrated to dryness to afford a residue (0.35 g). The residue was further purified by preparative HPLC (XBridge C18, 250 x 10 mm), eluted with 70% (v/v) CH_3CN-H_2O containing 0.1% TFA at a flow rate of 4.7 mL/min at 40 ˚C, and detected by absorbance at 205 nm, to afford the active compounds **5 (**17 mg), **6 (**16 mg), **7** (79 mg), **8 (**15 mg), and **9** (10 mg). The purified compounds **5-9** were analyzed by HPLC (XBridge C18, 250 x 4.6 mm), eluted with 70% (v/v) CH_3CN-H_2O containing 0.1% TFA at a flow rate of 1.0 mL/min at 40 ˚C, and detected by absorbance at 205 nm.

Amino Acid Analysis. Amino acid analysis of compound **7** was conducted according to the method described in the previous chapter.

Matrix-Associated Laser Desorption Ionization Time of Flight (MALDI-TOF) MS/MS analysis. MALDI-TOF MS/MS analysis of compound **7** was performed according to the method described in the previous chapter.

Determination of Lactone Linkage. Determination of the lactone linkage position in compound **7** was conducted according to the method reported by Naruse et al.[1] Compound **7** (10 mg) was treated with $LiBH_4$ (50 mg) in dry THF (5 mL) under reflux for 6 h. The reaction mixture was diluted with H_2O and extracted with EtOAc at pH 2.0. The extract was dried with N_2 and hydrolyzed with 6 N HCl at 110˚C for 20 h. Amino acids in the hydrolysate were analyzed according to the method described in the previous chapter.

Absolute Configuration of α-Amino Acids. Absolute configurations of the α-amino acids, except for the three Leu residues, of compound **7** were determined according to Marfey's method.[2] The experimental details were described in the previous chapter.

To determine the absolute configurations of Leu^2 and Leu^3, four tripeptides, NH_2-L-Leu-L-Leu-L-Val, NH_2-D-Leu-D-Leu-L-Val, NH_2-D-Leu-L-Leu-L-Val, and NH_2-L-Leu-D-Leu-L-Val, were used as standard peptides (Sigma-Aldrich). Compound **7** (3 mg) was hydrolyzed in 0.5 mL of 12N HCl/AcOH (2:1, v/v) at 60 ˚C for 6 h, and dried with N_2. To the hydrolysate was added 150 μL of 25% (v/v) CH_3CN-H_2O, and then the solution was analyzed by LC/MS system (Prominence HPLC system, Shimadzu Corp., Tokyo, Japan; and 3200 QTRAP, AB SCIEX, Framingham, MA, USA) equipped with a reverse-phase column (Zorbax Extend C18, 150 x 2.1 mm; Agilent Technologies, Santa Clara, CA, USA), eluted with a linear gradient of 10 to 30% (v/v) CH_3CN-H_2O containing 0.1% formic acid in 30 min at a flow rate of 0.2 mL/min, 30 ˚C. Four standard tripeptides, NH_2-L-Leu-L-Leu-L-Val, NH_2-D-Leu-D-Leu-L-Val, NH_2-D-Leu-L-Leu-L-Val, and NH_2-L-Leu-D-Leu-L-Val, were eluted at 11.4, 15.5, 16.9, and 23.0 min, respectively.

To determine the absolute configuration of Leu^6, two tripeptides, NH_2-L-Asp-L-Leu-L-Ile and NH_2-L-Asp-D-Leu-L-Ile, were used as standard peptides (Sigma-Aldrich). The hydrolysate solution of compound **7** described above was analyzed by LC/MS system (Prominence HPLC system and 3200 QTRAP) equipped with a reverse-phase column (Zorbax Extend C18, 150 x 2.1 mm), eluted with a linear gradient of 5 to 95% (v/v) CH_3CN-H_2O containing 0.1% formic acid in 30 min at a flow rate of 0.2 mL/min, 30 ˚C. Two standard tripeptides, NH_2-L-Asp-L-Leu-L-Ile and NH_2-L-Asp-D-Leu-L-Ile were eluted at 10.4 and 11.9 min, respectively.

Absolute Configuration of the β-Hydroxy Fatty Acid. Mosher's method was used to determine the absolute stereochemistry of the β-hydroxy fatty acid residue.[3,4] Compound **7** (10 mg) was hydrolyzed in 1.0 mL of 6 N HCl at 110 ˚C for 15 h. The hydrolysate was diluted with 5 mL of H_2O, extracted with 5 mL of $CHCl_3$ three times, and dried by N_2. The residue was dissolved with 1 mL of CH_2Cl_2-MeOH (3:1, v/v) and then 0.1 mL of TMS-diazomethane (Tokyo Chemical Industry Co., Ltd., Tokyo, Japan) was added to the solution. The solution was allowed to stand at room temperature for 30 min and the reaction was terminated by addition of 10% acetic acid in MeOH. The solution was dried by N_2 and the residue was dissolved in 0.5 mL of dry CH_2Cl_2 and mixed with 5.0 mg of (dimethylamino)pyridine, 2.8 μL of triethylamine, and 3.8 μL of (+)-MTPA chloride (Tokyo Chemical Industry). The

solution was allowed to stand at room temperature for 4 h. 3-[(Dimethylamino)propyl]amine (1.9 μL) was added, and after standing for 10 min, the solution was poured into 10 mL of 0.6 N HCl and extracted with 10 mL of EtOAc three times. The EtOAc extract was washed twice with 10 mL of 0.1 M $NaHCO_3$ and evaporated, affording (*R*)-MTPA ester of β-hydroxy fatty acid methyl ester. (*S*)-MTPA ester of β-hydroxy fatty acid methyl ester was prepared according to the same procedure using (–)-MTPA chloride in place of (+)-MTPA chloride.

In Vivo Cucumber Leaf-Disk Assay against *B. cinerea*. Cucumber seeds (*Cucumis stativus* L., Sagami-Hanjiro) were planted in 12 cm pots containing artificial soil and grown in the greenhouse at 16 to 23 ˚C without supplemental lighting. The cotyledons were collected from 3-week-old plants. The test compound (or supernatant) was dissolved in an appropriate amount of phosphate buffer (40 mM, pH 7.2), and 50 μL of the solution was applied to a paper disk (8 mm in diameter, thick type, Advantec Toyo Kaisha, Ltd., Tokyo, Japan) on the cucumber cotyledon. For the control, only phosphate buffer was applied. Then the paper disks on the leaves were inoculated with 50 μL of *B. cinerea* spore suspension (2 x 10^4/mL) containing 0.2% (w/v) yeast extract and 2 % (w/v) sucrose. The leaves were kept in a humidity chamber (RH >95%) at 20 ˚C for 4 days in darkness. The experiment was repeated four times. Inhibition rate of *B. cinerea* infection was calculated as

$$\text{Inhibition rate of infection (\%)} = (1 - D_a/D_b) \times 100$$

where D_a is the diameter of the infection zone in the leaf with a test compound and D_b is the diameter of the infection zone in the control leaf. The results were expressed as inhibition rate (mean % ± SD). The assay was observed under a stereomicroscope SZX7 (Olympus Co., Tokyo, Japan).

In Vitro Mycelial Growth Inhibition Assay. The assay procedure and calculation methods were described in the previous chapter. The combined action of two compounds was evaluated using Abbott's formula.[5] The expected efficacy of a mixture of two compounds, expressed as E_{exp}, can be predicted by Abbott's formula:

$$E_{exp} = c + d - (cd/100)$$

c and *d* are the control levels given by the single compounds. Synergistic interaction was determined to be present in the mixture when the ratio of the experimentally observed efficacy of the mixture (E_{obs}) to the expected one (E_{exp}) was > 1.

In Vitro Conidial Germination Inhibition Assay. The compound was dissolved in an appropriate amount of phosphate buffer (40 mM, pH 7.2), and 100 μL of the solution was applied to a tissue culture plate (a 96-well flat-bottom plate with a low evaporation lid; Becton, Dickinson and Co.). For the control, only phosphate buffer was applied. The solution in each well of the tissue culture plate was supplied with 100 μL of *B. cinerea* conidia (2 x 10^4/mL) containing 0.2% (w/v) yeast extract and 2% (w/v) sucrose. Compound **7** and *anteiso*-C_{14} bacillomycin D were tested at final concentrations of 20 and 4 μM, respectively. The tissue culture plate was kept at 20 ˚C for 20 h in darkness. The germination of conidia was observed under a light microscope CK2 (Olympus Co.). The assay was done in triplicate.

3.3. Results and Discussion

Contribution of Bacillomycin D to the Suppressive Activity of the Culture Supernatant against Gray Mold Disease. Strain SD-32 produces $C_{15\text{-}17}$ bacillomycin D homologues, which are powerful antifungal lipopeptides. To clarify the actual contribution of bacillomycin D to the suppressive activity of the culture supernatant against gray mold disease, I subjected the culture supernatant to an in vivo cucumber leaf-disk assay and also measured the bacillomycin D concentration in the culture supernatant. A 20-fold dilution of the culture supernatant was sufficient to inhibit the infection of *B. cinerea* completely, and the total concentration of bacillomycin D homologues in this solution was 11 μM (Figure 3-2A). In this assay, 30 μM of bacillomycin D was needed to completely control *B. cinerea* (Figure 3-2B), suggesting that factors other than bacillomycin D contributed to the effect of the culture supernatant on gray mold disease. These data prompted us to perform the following experiments.

Contribution of Synergistic Factors to the Control of Gray Mold Disease. The culture supernatant from SD-32 culture was partially purified with EtOAc extraction followed by solid-phase extraction (C18-SPE) and the activities of each fraction were evaluated. The 60% CH_3CN fraction of C18-SPE showed a suppressive effect against gray mold disease in the in vivo assay (Figure 3-2C), and this fraction contained bacillomycin D homologues (Figure 3-2E). Fractions other than the 60% CH_3CN fraction showed no suppressive effects (Figure 3-2C); interestingly, however, the 80% CH_3CN fraction enhanced the suppressive effect of the 60% fraction 2-fold (Figure 3-2D), suggesting a synergistic effect of the 80% CH_3CN fraction with bacillomycin D homologues. The 80% CH_3CN fraction did not contain bacillomycin D, but did contain several unidentified metabolites (Figure 3-2E). These data led us to isolate and identify the synergistic factors in the 80% fraction.

Isolation of Compounds 5-9 from *Bacillus amyloliquefaciens* SD-32. SD-32 was cultured in a medium (1.6 L) composed of maltose, soybean powder, yeast extract, and some minerals at 30˚C for 64 h. Synergistic activity-guided purification of the EtOAc extract of the culture supernatant with solid-phase extraction and preparative HPLC afforded compounds **5** (17 mg), **6** (16 mg), **7** (79 mg), **8** (15 mg), and **9** (10 mg) as white amorphous powders (each purity, >90%). The elution profile at the final HPLC purification step is shown in Figure 3-2F.

The chromatograms of each purified compound are shown in Figure 3-2G.

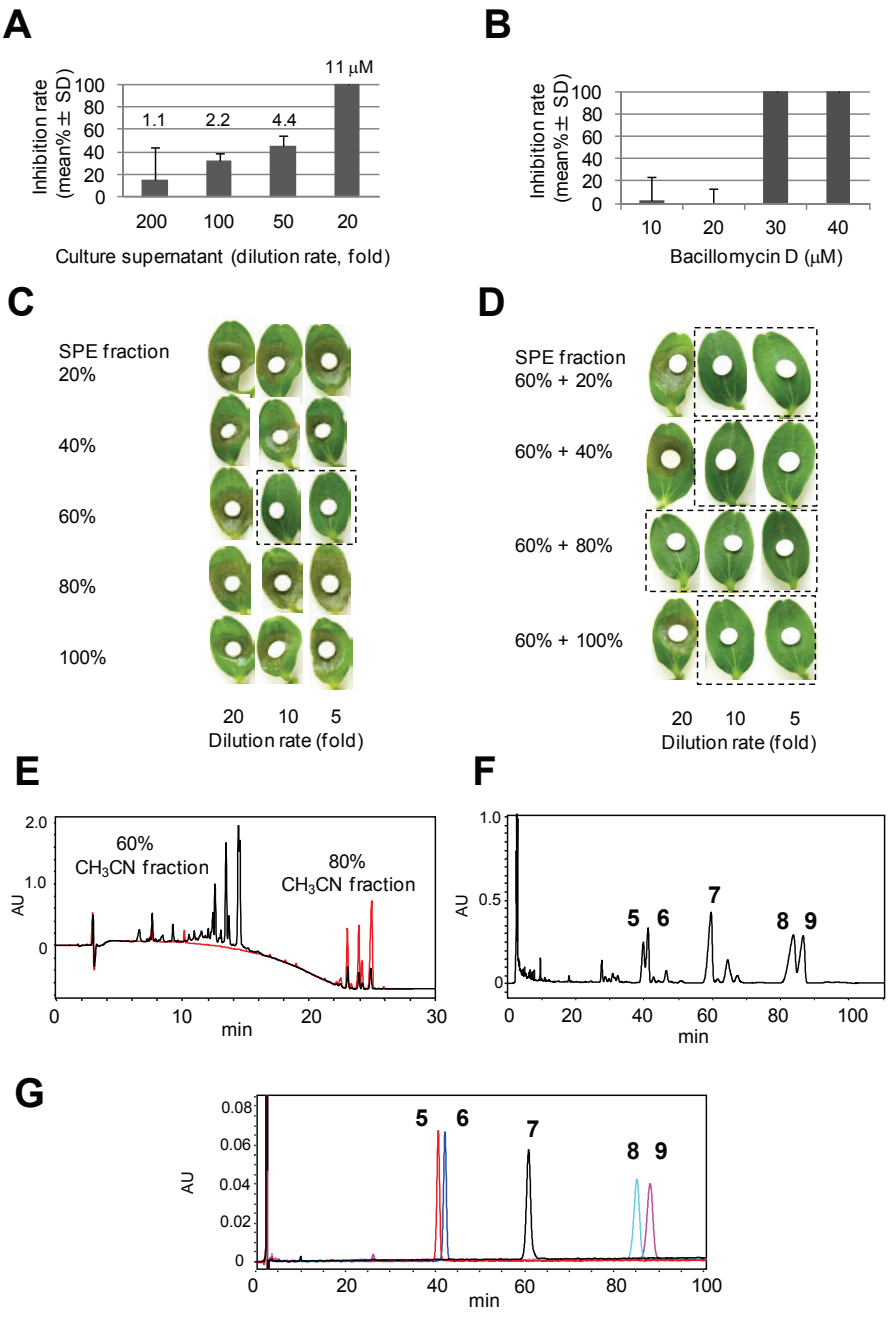

Figure 3-2. In vivo cucumber leaf-disk assay of the culture supernatant and C18-SPE (Oasis HLB) fractions and HPLC of the metabolites. (A) In vivo cucumber leaf-disk assay of the culture supernatant (n = 4). The values above each bar indicate the

bacillomycin D concentrations. (B) In vivo cucumber leaf-disk assay of the purified *anteiso*-C_{17} bacillomycin D (n = 4). (C) In vivo cucumber leaf-disk assay of the SPE fractions. Gray mold disease was completely inhibited on the leaves in the dashed box. (D) In vivo cucumber leaf-disk assay of the SPE fractions combined with a 60% CH_3CN fraction. (E) HPLC analyses of the fractions obtained from partial purification. Chromatograms of the 60 and 80% CH_3CN fractions were overlaid: black line, 60% CH_3CN fraction containing bacillomycin D; red line, 80% CH_3CN fraction containing unknown metabolites. (F) Elution profile at the final HPLC purification step of compounds **5-9**. Each peak was fractionated, pooled, and then freeze-dried. (G) HPLC analyses of purified compounds. Each chromatogram was overlaid: red line, compound **5** (0.4 mg/mL); blue line, **6** (0.4 mg/mL); black line, **7** (0.5 mg/mL); sky blue line, **8** (0.5 mg/mL); purple line, **9** (0.5 mg/mL).

Structures of Compounds 5-9. Compound **7** was the most abundant in the culture broth, and therefore its structure was elucidated first. Compound **7** gave an $[M+Na]^+$ peak at m/z 1044.6602 (calcd for $C_{52}H_{91}N_7O_{13}Na$, 1044.6573) in HR-FAB-MS. Five α-amino acids, Leu, Glu, Val, Asp, and Ile, were found in a 3:0.9:0.9:0.9:0.7 ratio in an amino acid analysis of the hydrolysate. The ^{1}H-NMR data for compound **7** (Table 3-1 and Figure S17) indicated the presence of seven amide protons (δ_H 8.34-7.68) and seven α-protons (δ_H 4.53-4.08, partially overlapped) of amino acid residues of the peptide. The ^{13}C-NMR (Table 3-2 and Figure S18) and HSQC data (Figure S20) for compound **7** exhibited 50 signals (δ_C 172.1 and 22.5; 2C each), including 9 carbonyl (δ_C 174.1-169.4; δ_C 172.1, 2C), methylene (δ_C 41.6-24.5), and 11 methyl carbon signals (δ_C 23.1-11.1; δ_C 22.5, 2C). On the basis of the ^{1}H-^{1}H COSY, HSQC, HMBC, NOESY data (Figure 3-3A and Figures S19-S22), and the molecular formula, compound **7** was deduced to be *iso*-C_{14} [Ile^7]surfactin, a cyclic depsipeptide consisting of three Leu residues, one Glu, one Val, one Asp, and one Ile residue, and a β-hydroxy fatty acid with a -$(CH_2)_8CH(CH_3)_2$ group as a side chain. To obtain the sequence information, compound **7** was analyzed by MALDI-TOF MS/MS to afford the sequence shown in Figure 3-3B, which corresponded with that of *iso*-C_{14} [Ile^7]surfactin. Then, to determine the location

of the lactone linkage, compound **7** was reduced with $LiBH_4$ in THF and the amino acid composition of the product was analyzed. The reaction product lacked the Ile residue (Figure 3-3C; the intact and reduced compound **7** afforded Leu, Val, Glu, Asp, and Ile in the ratios 3:0.9:0.9:0.9:0.7 and 3:1:0.8:0.9:0.03, respectively), indicating that the lactone linkage was between the carboxyl group of Ile and the β-hydroxy group of the fatty acid. From these results compound **7** was determined to be *iso*-C_{14} [Ile^7]surfactin (Figure 3-1).

The absolute configurations of α-amino acids in compound **7** were determined by treatment of the hydrolysate with Marfey's reagent[2] and HPLC analyses of the derivatives. The hydrolysate was shown to contain $_L$-Glu, $_L$-Val, $_L$-Asp, $_L$-Ile, $_L$-Leu, and $_D$-Leu. There is no ambiguity in the absolute configuration of the four amino acids other than Leu. The absolute configurations of the Leu^2 and Leu^3 were determined by LC/MS comparison of the tripeptide in the products from the partial hydrolysis of compound **7** with four synthesized tripeptides, NH_2-$_L$-Leu-$_L$-Leu-$_L$-Val, NH_2-$_D$-Leu-$_D$-Leu-$_L$-Val, NH_2-$_D$-Leu-$_L$-Leu-$_L$-Val, and NH_2-$_L$-Leu-$_D$-Leu-$_L$-Val. The existence of NH_2-$_L$-Leu-$_D$-Leu-$_L$-Val in the hydrolysate allowed us to determine the absolute configuration of Leu^2 and Leu^3 to be L and D, respectively. The absolute configuration of the Leu^6 was also determined by LC/MS comparison of the tripeptide in the products from the partial hydrolysis of compound **7** with two synthesized tripeptides, NH_2-$_L$-Asp-$_L$-Leu-$_L$-Ile and NH_2-$_L$-Asp-$_D$-Leu-$_L$-Ile. The existence of $_L$-Asp-$_D$-Leu-$_L$-Ile in the hydrolysate finally established the amino acid sequence, NH_2-$_L$-Glu-$_L$-Leu^2-$_D$-Leu^3-$_L$-Val-$_L$-Asp-$_D$-Leu^6-$_L$-Ile. The absolute configuration at C-3 of the fatty acid part of compound **7** was determined according to the Mosher's method[3,4] as shown in Figure 3-3D. ^{1}H NMR spectra of the (*R*)-MTPA and (*S*)-MTPA esters of β-hydroxy fatty acid methyl ester were measured, respectively, and from the $\Delta\delta_{(S-R)}$ values the absolute configuration of C-3 was determined to be *R*.

The HR-FAB-MS of compounds **5** and **6** showed their $[M+H]^+$ ion peaks at *m*/*z* 1008.6581 (calcd for $C_{51}H_{90}N_7O_{13}$, 1008.6596) and 1008.6575 (calcd for $C_{51}H_{90}N_7O_{13}$, 1008.6596), respectively. The HR-FAB-MS of compounds **8** and **9** showed their $[M+Na]^+$ ion peaks at *m*/*z* 1058.6741 (calcd for $C_{53}H_{93}N_7O_{13}Na$, 1058.6729) and 1058.6727 (calcd for $C_{53}H_{93}N_7O_{13}Na$, 1058.6729), respectively. A series of NMR spectral analyses (Figures S23-S38) revealed that compounds **5**, **6**, **8**, and **9** had the same amino acid sequence as compound **7** but differed from

compound **7** with respect to the structure of their β-hydroxy fatty acids. The ^{1}H-NMR and ^{13}C-NMR spectra of compounds **5**, **6**, **8**, and **9** showed the presence of the -$(CH_2)_6CH(CH_3)CH_2CH_3$, -$(CH_2)_7CH(CH_3)_2$, -$(CH_2)_8CH(CH_3)CH_2CH_3$, and -$(CH_2)_9CH(CH_3)_2$ groups, respectively. Thus, compounds **5**, **6**, **8**, and **9** were determined to be *anteiso*-C_{13}, *iso*-C_{13}, *anteiso*-C_{15}, and *iso*-C_{15} [Ile^{7}]surfactin, respectively (Figure 3-1).

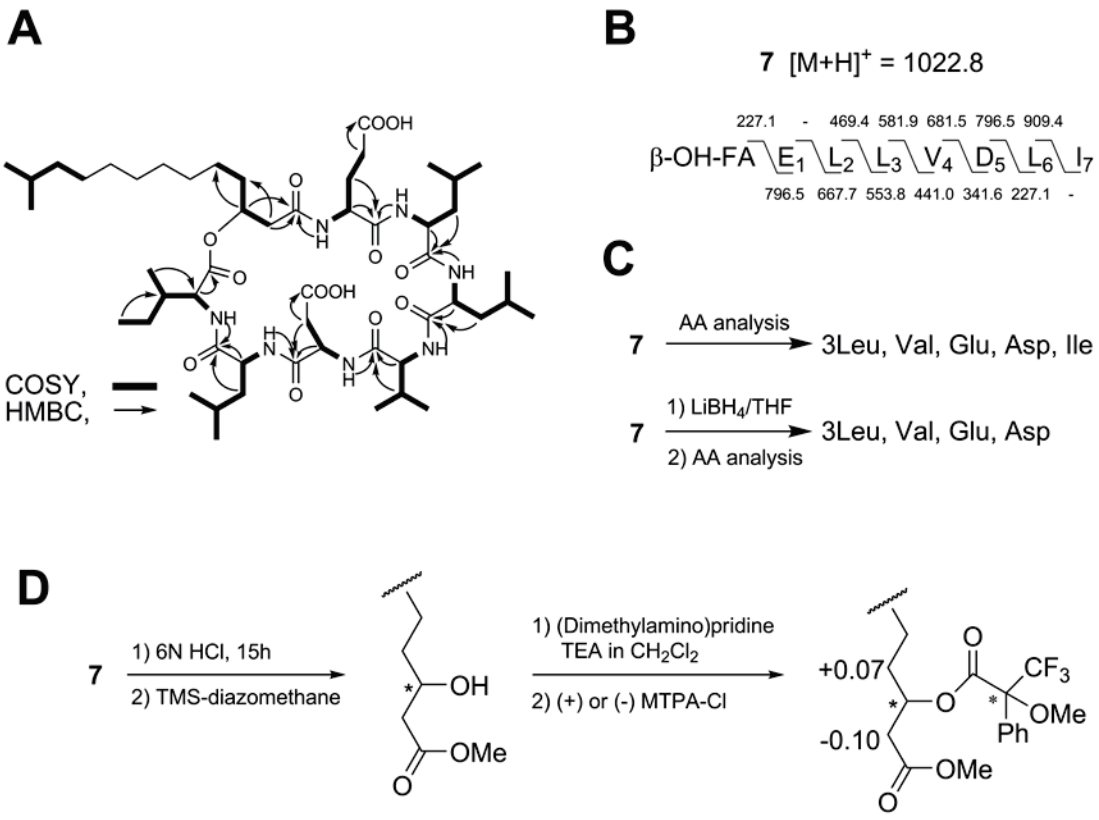

Figure 3-3. 2D-NMR, MS/MS, and chemical analyses of compound **7**: (A) key COSY and HMBC correlations detected for compound **7**; (B) MALDI-TOF MS/MS analysis of compound **7**; (C) determination of the lactone linkage position of compound **7**; (D) determination of the absolute structure of C-3 in β-hydroxy fatty acid obtained from compound **7**. $\Delta\delta_{(S-R)}$ values (in ppm) of derivatives synthesized according to a Mosher's method.

Compounds **7**, **8**, and **9** are known,[6-10] and **5** and **6** are new. Compounds **5** and **6** have *anteiso*- and *iso*-C_{13} 3-hydroxy fatty acids, and seven α-amino acids with the same chiral sequence, LLDLLDL, as the surfactin family. [Ile^7]surfactin homologues have been reported to be produced by *Bacillus subtilis*[6,8-10] and *B. licheniformis*.[7] The present study shows that *B. amyloliquefaciens* strain SD-32 is a producer of [Ile^7]surfactin homologues. Recently, Tang et al. reported the ^{13}C NMR data (in DMSO) of *anteiso*-C_{15} [Ile^7]surfactin,[10] and their data were identical to my ^{13}C NMR data for compound **8**, except for the chemical shift of αCH of Ile^7 (δ_C 56.5, present study; δ_C 50.7, reported). A metabolite from *Bacillus subtilis* OKB 105 was characterized as C_{13} [Ile^7]surfactin from NMR and MS data by Kowall et al.[9] although its chemical structure was not unambiguously determined.

Table 3-1. ^{1}H NMR Data for Compounds 5-9 in DMSO-d_6 [a]

moiety	position	δ_H (J in Hz)				
		5	**6**	**7**	**8**	**9**
L-Glu	1	4.18m[b]	4.18m[b]	4.18m[b]	4.18m[b]	4.18m[b]
	2	1.92m[c], 1.77m[d]	1.92m[c], 1.76m[d]	1.91m[c], 1.76m	1.91m[c], 1.76m[d]	1.91m[c], 1.76m[d]
	3	2.19m	2.17m	2.19m	2.19m	2.19m
	1-NH	7.84d (6.2)	7.84d (6.4)	7.84d (6.5)	7.84d (6.6)	7.83d (6.6)
L-Leu[2]	6	4.15m[b]	4.15m[b]	4.16m[b]	4.15m[b]	4.15m[b]
	7	1.53m[e]	1.53m[e]	1.53m[d]	1.53m[e]	1.53m[e]
	8	1.50m[e]	1.50m[e]	1.50m[d]	1.50m[e]	1.50m[e]
	9	0.86m	0.86m	0.86m	0.86m	0.86m
	10	0.86m	0.86m	0.86m	0.86m	0.86m
	6-NH	8.00d (5.1)	8.03d (5.3)	8.04d (5.2)	8.03d (5.6)	8.02d (5.4)
D-Leu[3]	12	4.17m[b]	4.16m[b]	4.17m[b]	4.16m[b]	4.17m[b]
	13	1.53m[e]	1.53m[e]	1.53m[d]	1.53m[e]	1.53m[e]
	14	1.50m[e]	1.53m[e]	1.50m[d]	1.50m[e]	1.50m[e]
	15	0.81m[f]	0.82d[f] (6.5)	0.83d[e] (6.5)	0.81m[f]	0.83d[f] (6.6)
	16	0.81m[f]	0.82d[f] (6.5)	0.83d[e] (6.5)	0.81m[f]	0.83d[f] (6.6)
	12-NH	8.29d (7.0)	8.32d (7.0)	8.34d (7.1)	8.32d (7.1)	8.31d (7.3)
L-Val	18	4.07m	4.07m	4.08m	4.07m	4.08m
	19	1.95m[c]	1.95m[c]	1.93m[c]	1.93m[c]	1.94m[c]
	20	0.81m[f]	0.82d[f] (6.5)	0.83d[e] (6.5)	0.81m[f]	0.83d[f] (6.6)
	21	0.75d (6.5)	0.74d (6.5)	0.75d (6.6)	0.74d (6.4)	0.75d (6.6)
	18-NH	7.73d (8.5)	7.75d (8.4)	7.76d (8.3)	7.75d (8.3)	7.75d (8.5)
L-Asp	23	4.49m[g]	4.50m[g]	4.52m[f]	4.50m[g]	4.50m[g]
	24	2.68dd (16.4, 4.3), 2.57dd (16.4, 8.7)	2.68dd (16.6, 4.3), 2.57dd (16.6, 8.7)	2.68dd (16.6, 4.6), 2.58dd (16.6, 8.9)	2.68dd (16.5, 4.2), 2.57dd (16.5, 8.7)	2.69dd (16.6, 4.7), 2.57dd (16.6, 8.6)
	23-NH	8.17d (7.1)	8.18d (7.2)	8.18d (7.1)	8.18d (7.2)	8.17d (7.2)
D-Leu[6]	27	4.51m[g]	4.51m[g]	4.53m[f]	4.51m[g]	4.52m[g]
	28	1.41m[h], 1.38m[h]	1.41m[h], 1.37m[h]	1.43m[g], 1.38m	1.43m[h], 1.38m[h]	1.44m[h], 1.39m[h]
	29	1.50m[e]	1.50m[e]	1.50m[d]	1.50m[e]	1.50m[e]
	30	0.81m[f]	0.82d[f] (6.5)	0.83d[e] (6.5)	0.81m[f]	0.83d[f] (6.6)
	31	0.81m[f]	0.82d[f] (6.5)	0.83d[e] (6.5)	0.81m[f]	0.83d[f] (6.6)
	27-NH	7.66d (8.4)	7.67d (8.5)	7.68d (8.5)	7.67d (8.3)	7.67d (8.5)
L-Ile	33	4.15m[b]	4.15m[b]	4.16m[b]	4.15m[b]	4.15m[b]
	34	1.79m[d]	1.80m[d]	1.81m	1.80m[d]	1.81m[d]
	35	0.81m[f]	0.82d[f] (6.5)	0.83d[e] (6.5)	0.81m[f]	0.83d[f] (6.6)
	36	1.31m, 1.20m[i]	1.31m, 1.20m[i]	1.32m, 1.20m[h]	1.31m, 1.20m[i]	1.32m, 1.20m[i]
	37	0.78m[f]	0.78m[f]	0.79m	0.78m[f]	0.79m[f]
	33-NH	8.23d (7.8)	8.25d (7.8)	8.27d (7.9)	8.25d (7.8)	8.24d (8.0)
(*R*)-β-OH-FA	39	4.98m	4.98m	4.98m	4.98m	4.98m
	40	2.41m	2.40m	2.40m	2.40m	2.41m
	42	1.55m[e]	1.53m[e]	1.56m[d]	1.56m[e]	1.54m[e]
	43	1.20m[i]	1.20m[i]	1.20m[h]	1.20m[i]	1.20m[i]
	44	1.20m[i]	1.20m[i]	1.20m[h]	1.20m[i]	1.20m[i]
	45	1.20m[i]	1.20m[i]	1.20m[h]	1.20m[i]	1.20m[i]
	46	1.20m[i]	1.20m[i]	1.20m[h]	1.20m[i]	1.20m[i]
	47	1.23m[i], 1.07m	1.20m[i]	1.20m[h]	1.20m[i]	1.20m[i]
	48	1.23m[i]	1.11m	1.20m[h]	1.20m[i]	1.20m[i]
	49	0.81m[f]	1.44m[h]	1.11m	1.24m[i], 1.08m	1.20m[i]
	50	1.23m[i]	0.82d[f] (6.5)	1.43m[g]	1.24m[i]	1.11m
	51	0.81m[f]	0.82d[f] (6.5)	0.83d[e] (6.5)	0.81m[f]	1.43m[h]
	52			0.83d[e] (6.5)	1.24m[i]	0.83d[f] (6.6)
	53				0.81m[f]	0.83d[f] (6.6)

[a] Compound **7**, 600 MHz; **5**, **6**, **8**, and **9**, 400 MHz. [b, c, d, e, f, g, h, i] Overlapped in each column.

Table 3-2. ^{13}C NMR Chemical Shifts of Compounds 5-9 in DMSO-d_6 [a]

moiety	position	δ_C				
		5	**6**	**7**	**8**	**9**
$_L$-Glu	1	52.1	52.1	52.1	52.1	52.1
	2	27.1	27.2	27.1	27.1	27.1
	3	29.8	29.8	29.8	29.8	29.8
	4	174	174	174.1	174	174
	5	170.6	170.6	170.6	170.6	170.6
$_L$-Leu^2	6	51.6	51.6	51.6	51.6	51.6
	7	39.5[b]	39.5[b]	39.5[b]	39.5[b]	39.5[b]
	8	24.2[c]	24.2[c]	24.2[c]	24.2[c]	24.2[c]
	9	23	23	23.1	23	23
	10	22.9	22.9	22.9	22.9	22.9
	11	171.8	171.8	171.8	171.8	171.7
$_D$-Leu^3	12	51.9	51.9	51.9	51.9	51.9
	13	39.5[b]	39.5[b]	39.5[b]	39.5[b]	39.5[b]
	14	24.2[c]	24.2[c]	24.2[c]	24.2[c]	24.2[c]
	15	22.5	22.5	22.5	22.5	22.5
	16	22.1	22.1	22.1	22.1	22.1
	17	172.1[d]	172.1[d]	172.1[d]	172.1[d]	172.1[d]
$_L$-Val	18	58.1	58.1	58.1	58.1	58.1
	19	30.5	30.5	30.5	30.5	30.5
	20	19.1	19.1	19.1	19.1	19.1
	21	18	18	18	17.9	17.9
	22	170.6	170.6	170.6	170.6	170.6
$_L$-Asp	23	49.6	49.6	49.6	49.6	49.6
	24	35.9[f]	36	36	35.9[f]	36
	25	172.1[d]	172.1[d]	172.1[d]	172.1[d]	172.1[d]
	26	169.9	169.9	169.9	169.8	169.8
$_D$-Leu^6	27	50.5	50.5	50.5	50.5	50.5
	28	41.6	41.6	41.6	41.6	41.6
	29	24.1[c]	24.1[c]	24.1[c]	24.1[c]	24.1[c]
	30	21.9	21.9	21.9	21.8	21.8
	31	21	21	21	21	21
	32	171.6	171.6	171.6	171.6	171.6
$_L$-Ile	33	56.5	56.5	56.5	56.5	56.5
	34	35.8	35.8	35.8	35.7	35.7
	35	15.5	15.5	15.5	15.4	15.4
	36	24.5[c]	24.5[c]	24.5[c]	24.5[c]	24.5[c]
	37	11	11.1	11.1	11	11
	38	171	171	171	171	171
(*R*)-β-OH-FA	39	71.6	71.6	71.6	71.6	71.5
	40	40.3	40.4	40.3	40.3	40.6
	41	169.4	169.4	169.4	169.4	169.4
	42	33.1	33.1	33.1	33.1	33.1
	43	24.4[e]	24.4[e]	24.4[e]	24.3[e]	24.3[e]
	44	29.2[e]	29.1[e]	29.3[e]	29.3[e]	29.2[e]
	45	28.9[e]	28.8[e]	28.9[e]	28.9[e]	29.0[e]
	46	28.6[e]	28.5[e]	28.8[e]	28.8[e]	28.8[e]
	47	35.9[f]	26.7	28.5[e]	28.8[e]	28.8[e]
	48	33.7	38.4	26.7	28.5[e]	28.5[e]
	49	19	27.3	38.4	35.9[f]	26.7
	50	26.3	22.5[f]	27.4	33.7	38.4
	51	11.2	22.5[f]	22.5[f]	19	27.3
	52			22.5[f]	26.4	22.4[f]
	53				11.1	22.4[f]

[a] Compound **7**, 150 MHz; **5**, **6**, **8**, and **9**, 100 MHz. [b] Overlapped with DMSO.

[c,e] Assignments may be interchanged in each column. [d,f] Overlapped in each column.

Synergistic Actions of Compounds 5-9 with Bacillomycin D in an in vivo Cucumber Leaf-Disk Assay against Gray Mold Disease. The effects of compounds **5-9** on the suppressive activity of bacillomycin D were evaluated. The results are shown in Table 3-3 and Figure 3-4A. When administered singly, bacillomycin D (10, 15, and 20 μM) did not inhibit the development of gray mold disease on cucumber leaves. Compounds **5-9** (20 and 100 μM) also exhibited no inhibition of gray mold disease in cucumber leaves when administered alone, suggesting that compounds **5-9** (20 and 100 μM) could neither inhibit the growth of *B. cinerea* directly nor induce the resistance of cucumber leaves to gray mold disease. However, the addition of compounds **5-9** (20 and 100 μM) to bacillomycin D (10, 15, and 20 μM) significantly enhanced the effect of bacillomycin D activity in the in vivo assay, indicating that compounds **5-9** have synergistic activities with bacillomycin D under this condition. The inhibition rates of compounds **5-9** (100 μM) with bacillomycin D (10 μM) were 26.8, 51.2, 78.7, 81.7, and 66.5%, indicating that the C_{14} and C_{15} [Ile^7]surfactins were more active than the C_{13} [Ile^7]surfactins. Although these data could not fully explain the suppressive activity gap between the culture supernatant and bacillomycin D in it, they clearly demonstrated that the [Ile^7]surfactin homologues enhance the suppressive activity of bacillomycin D against gray mold disease and can partially close the gap.

To examine the mechanism underlying the synergism of the [Ile^7]surfactin homologues with bacillomycin D, a mycelial growth inhibition assay and a conidial germination inhibition assay using *B. cinerea* were performed in vitro (Figures 3-4B and C). In the mycelial growth inhibition assay, no significant difference between E_{obs} and E_{exp} was observed, and thus the effect of compound **7** on the activity of bacillomycin D was additive (Figure 3-4B). In the conidial germination inhibition assay, the addition of 20 μM of compound **7** to 4 μM of bacillomycin D did not enhance the activity of bacillomycin D (Figure 3-4C). Finally, I observed stereomicroscopically the inoculated parts in the cucumber leaf-disk assay (Figure 3-4D). The synergistic activity to the disease was observed in the condition 20 μM of compound **7** with 20 μM of bacillomycin D although mycelial growth of *B. cinerea* was apparently normal in the same condition. These data suggested that the synergistic action of [Ile^7]surfactin and bacillomycin D do not interfere with the mycelial growth and conidial germination of the gray mold, but rather might inhibit infection processes such as

appressorium formation and penetration into the host.

The present study has shed light on a novel role of [Ile^7]surfactin homologues in the biological control system of strain SD-32, namely, the compounds were shown to work synergistically with bacillomycin D in controlling gray mold disease under natural conditions, and this synergism may be particularly important for inhibiting the infection process of gray mold in cucumber leaves. Surfactin family lipodepsipeptides are well-known to act as potent surface-active compounds and antibiotics against a number of bacteria and phytopathogenic fungi.[11] In addition, recent investigations have illustrated a number of other diverse activities for these compounds, including roles in the induction of plant resistance or the mechanism of biofilm formation as part of the biological control system of *Bacillus* species.[12]

It has been reported that *B. amyloliquefaciens* produces a wide variety of bioactive metabolites such as polyketides (bacillaenes, difficidin, oxidifficidin, and macrolactins),[13,14] siderophore (bacillibactin),[15] non-ribosormally synthesized lipopeptides and lipodepsipeptides (bacillomycin D, surfactins, and fengycins or plipastatins),[16] and ribosomally synthesized peptides (plantazolicins).[17] However, literatures with respect to interactions of each metabolite are limited.

Many *Bacillus* strains have been reported to produce surfactin and bacillomycin D simultaneously,[16,18-21] but the interaction of bacillomycin D and surfactin has not been studied. In contrast, several researchers have focused on the interactions of standard surfactin and iturin A.[22-24] Bacillomycin D belongs to the iturin class lipopeptides, and bacillomycin D (Asn-Tyr-Asn-Pro-Glu-Ser-Thr-β-AA) and iturin A (Asn-Tyr-Asn-Gln-Pro-Asn-Ser-β-AA) have closely related structures.[12] Hiraoka et al.[22] showed that *B. subtilis* RB14 produced both standard surfactin and iturin A, and that the standard surfactin could enhance the in vitro activity of iturin A against *Fusarium oxysporum*. They discussed the importance of the structural similarities between surfactin and iturin A in their synergism. Thimon et al.[23] reported that the antifungal activity of iturin A against *Saccharomyces cerevisiae* in vitro was enhanced in the presence of standard surfactin and that this effect was clear at a subinhibitory concentration of iturin A. Their results are in agreement with mine from the point of view of the necessary concentration although I found their synergism not in vivo but in vitro. A

mechanism for the antibiotic action of bacillomycin D and the other lipopeptides has been proposed.[24-26] Lipopeptide molecules penetrate the cytoplasmic membrane of the target cell and form oligomeric structures (lipopeptide aggregates) that are ion-conducting. Maget-Dana et al.[27] stated that the marked surfactant properties of surfactin helped iturin A to reach and disrupt the membrane of the target cells. In my experiment, however, the synergistic action of [Ile^7]surfactin and bacillomycin D was not observed with respect to in vitro mycelial growth or the conidial germination inhibition assays. These data clearly suggest that the synergistic actions of [Ile^7]surfactin and bacillomycin D were different from those of surfactin and iturin A. The difference is presumably due to structural difference between bacillomycin D and iturin A, and/or [Ile^7]surfactin and standard surfactin.

The detailed mechanism by which [Ile^7]surfactin homologues enhanced the suppressive effect of bacillomycin D in the cucumber leaf-disk assay is still unknown and remains to be studied.

Table 3-3. Leaf-Disk Assay of Compounds 5-9 in Combination with Bacillomycin D Using Cucumber Cotyledon and *B. cinerea*[a]

Bac D[b]	compd (μM)										
	none	**5**		**6**		**7**		**8**		**9**	
(μM)		20	100	20	100	20	100	20	100	20	100
0		-12.5 ± 14.7	11.6 ± 25.1	0 ±27.0	11.4 ± 6.1	3.1 ± 25.8	14.6 ± 19.9	3.1 ± 27.7	8.5 ± 15.7	6.3 ± 16.1	5.5 ± 20.8
10	-3.1 ± 35.9	21.9 ± 18.8	26.8 ± 26.3	40.6 ± 27.7	51.2 ± 17.2*	18.8 ± 21.7	78.7 ± 25.1**	21.9 ± 15.7	81.7 ± 36.6**	25.0 ± 17.7	66.5 ± 39.0**
15	0 ± 27.0	75.0 ± 35.9**	100**	59.4 ± 21.3**	100**	93.8 ± 12.5**	100**	68.8 ± 21.7**	100**	87.5 ± 17.7**	100**
20	28.1 ± 37.3	100	100**	96.9 ± 6.3**	100**	100**	100**	100**	100**	100**	100**

[a]Data are expressed as inhibition rate (mean % ± SD, n = 4).
Groups significantly different (by ANOVA followed by Dunnett's test) from the control group (bac D only) in each row are shown by * ($P < 0.05$) or ** ($P < 0.01$).

[b]*ai*-C_{17} Bacillomycin D was used.

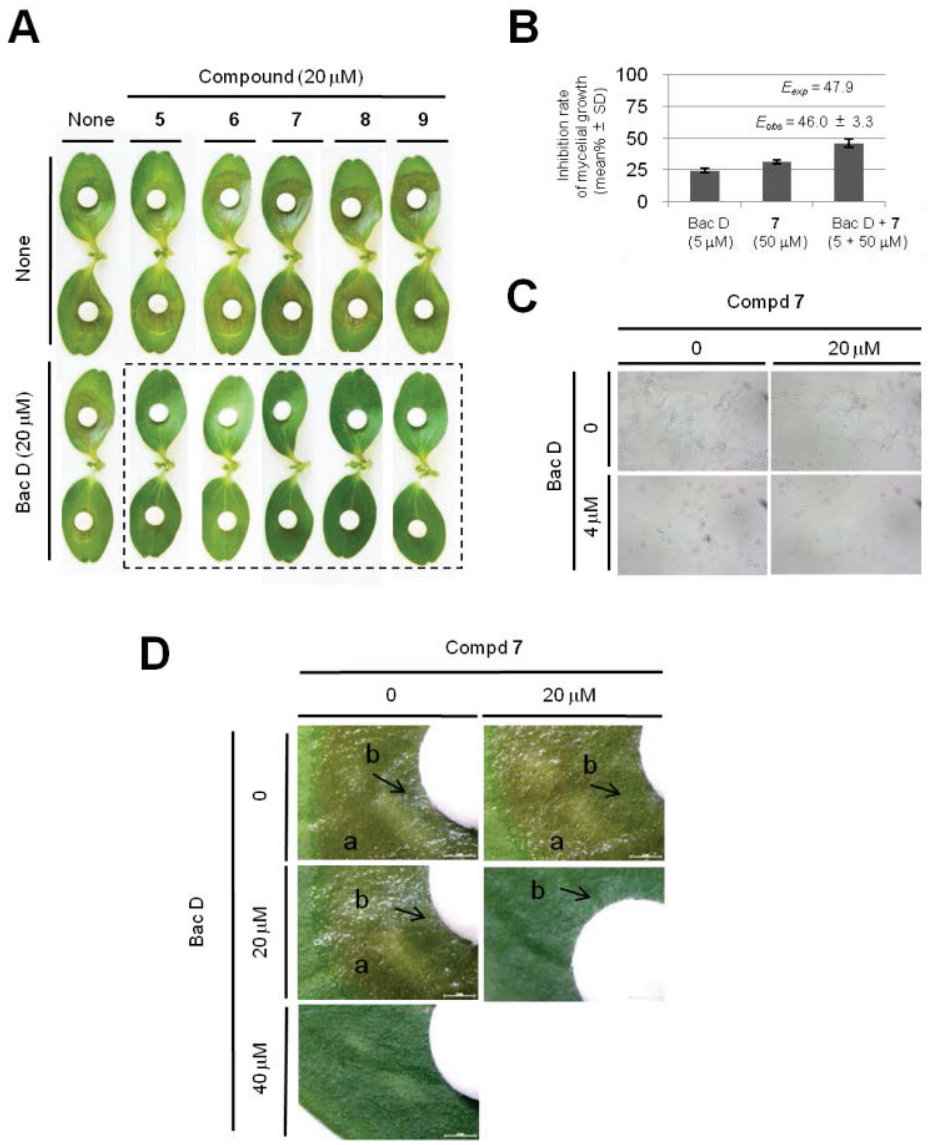

Figure 3-4. In vivo and in vitro assay of compounds **5-9** with bacillomycin D against *B. cinerea*. (A) In vivo assay of compound **5-9** with bacillomycin D using cucumber cotyledon and *B. cinerea* (n = 4). Bac D indicates *anteiso*-C_{17} bacillomycin D. Gray mold disease was completely inhibited on the leaves in the dashed box. (B) Mycelial growth inhibition assay of compound **7** with bacillomycin D in vitro (n = 3). (C) Conidial germination inhibition assay of compound **7** with bacillomycin D in vitro (n = 3). (D) Stereomicroscope observation of in vivo assay of compound **7** with *anteiso*-C_{17} bacillomycin D. Scale bar indicates 2 mm. (a), Infection zone of *B. cinerea*; (b), Mycelial growth of *B. cinerea*.

References

(1) Naruse, N.; Tenmyo, O.; Kobaru, S.; Kamei, H.; Miyaki, T.; Konishi, M.; Oki, T. Pumilacidin, a complex of new antiviral antibiotics. Production, isolation, chemical properties, structure and biological activity. *J. Antibiot.* **1990**, *43*, 267-280.

(2) Marfey, P. Determination of D-amino acids. II. Use of a bifunctional reagent, 1, 5-difluoro-2, 4-dinitrobenzene. *Carlsberg Res. Commun*. **1984**, *49*, 591-596.

(3) Dale, J. A.; Mosher, H. S. Nuclear magnetic resonance enantiomer reagents. Configurational correlations *via* nuclear magnetic resonance chemical shifts of diastereomeric mandelate, *o*-methylmandelate, and α-methoxy-α-trifluoromethyl-phenylacetate (MTPA) esters. *J. Am. Chem. Soc.* **1973**, *95*, 512-519.

(4) Ohtani, I.; Kusumi, T.; Kashman, Y.; Kakisawa, H. High-field FT NMR application of Mosher's method. The absolute configurations of marine terpenoids. *J. Am. Chem. Soc.* **1991**, *113*, 4092-4096.

(5) Gisi, U. Synergistic interaction of fungicides in mixtures. *Phytopathology* **1996**, *86*, 1273-1279.

(6) Baumgart, F.; Kluge, B.; Ullrich, C.; Vater, J.; Ziessow, D. Identification of amino acid substitutions in the lipopeptide surfactin using 2D NMR spectroscopy. *Biochem. Biophys. Res. Commun.***1991**, *177*, 998-1005.

(7) Jenny, K.; Käppeli, O.; Fiechter, A. Biosurfactants from *Bacillus licheniformis*: structural analysis and characterization. *Appl. Microbiol. Biotechnol.* **1991**, *36*, 5-13.

(8) Itokawa, H.; Miyashita, T.; Morita, H.; Takeya, K.; Hirano, T.; Homma, M.; Oka, K. Structural and conformational studies of [Ile^7] and [Leu^7]surfactins from *Bacillus subtilis natto*. *Chem. Pharm. Bull.* **1994**, *42*, 604-607.

(9) Kowall, M.; Vater, J.; Kluge, B.; Stein, T.; Franke, P.; Ziessow, D. Separation and characterization of surfactin isoforms produced by *Bacillus subtilis* OKB 105. *J. Colloid Interface Sci.* **1998**, *204*, 1-8.

(10) Tang, J. S.; Gao, H.; Hong, K.; Yu, Y.; Jiang, M. M.; Lin, H. P.; Ye, W. C.; Yao, X. S. Complete assignments of ^{1}H and ^{13}C NMR spectral data of nine surfactin isomers. *Magn. Reson. Chem.* **2007**, *45*, 792-796.

(11) Peypoux, F.; Bonmatin, J. M.; Wallach, J. Recent trends in the biochemistry of surfactin.

Appl. *Microbiol*. *Biotechnol*. **1999**, *51*, 553-563.

(12) Ongena, M.; Jacques, P. *Bacillus* lipopeptides: versatile weapons for plant disease biocontrol. *Trends Microbiol*. **2008**, *16*, 115-125.

(13) Chen, X. H.; Vater, J.; Piel, J.; Franke, P.; Scholz, R.; Schneider, K.; Koumoutsi, A.; Hitzeroth, G.; Grammel, N.; Strittmatter, A. W.; Gottschalk, G.; Süssmuth, R. D.; Borriss, R. Structural and functional characterization of three polyketide synthase gene clusters in *Bacillus amyloliquefaciens* FZB42. *J. Bacteriol.* **2006**, *188*, 4024-4036.

(14) Schneider, K.; Chen, X. H.; Vater, J.; Franke, P.; Nicholson, G.; Borriss, R.; Süssmuth, R. D. Macrolactin is the polyketide biosynthesis product of the pks2 cluster of *Bacillus amyloliquefaciens* FZB42. *J. Nat. Prod.* **2007**, *70*, 1417-1423.

(15) Chen, X. H.; Koumoutsi, A.; Scholz, R.; Eisenreich, A.; Schneider, K.; Heinemeyer, I.; Morgenstern, B.; Voss, B.; Hess, W. R.; Reva, O.; Junge, H.; Voigt, B.; Jungblut, P. R.; Vater, J.; Süssmuth, R.; Liesegang, H.; Strittmatter, A.; Gottschalk, G.; Borriss, R. Comparative analysis of the complete genome sequence of the plant growth-promoting bacterium *Bacillus amyliliquefaciens* FZB42. *Nat. Biotechnol.* **2007**, *25*, 1007-1014.

(16) Koumoutsi, A.; Chen, X. H.; Henne, A.; Liesegang, H.; Hitzeroth, G.; Franke, P.; Vater, J.; Borriss, R. Structural and fanctional characterization of gene clusters directing nonribosomal synthesis of bioactive cyclic lipopetides in *Bacillus amyloliquefaciens* strain FZB42. *J. Bacteriol*. **2004**, *186*, 1084-1096.

(17) Kalyon, B.; Helaly, S. E.; Scholz, R.; Nachtigall, J.; Vater, J.; Borriss, R.; Süssmuth, R. D. Plantazolicin A and B: Structure elucidation of ribosomally synthesized thiazole/oxazole peptides from *Bacillus amyloliquefaciens* FZB42. *Org. Lett.* **2011**, *13*, 2996-2999.

(18) Athukorala, S. N. P.; Fernando, W. G. D.; Rashid, K. Y. Identification of antifungal antibiotics of *Bacillus* species isolated from different microhabitats using polymerase chain reaction and MALDI-TOF-mass spectrometry. *Can*. *J*. *Microbiol*. **2009**, *55*, 1021-1032.

(19) Zeriouh, H.; Romero, D.; García-Gutiérrez, L.; Cazorla, F. M.; de Vicente, A.; Pérez-Garcia, A. The iturin-like lipopeptides are essential components in the biological control arsenal of *Bacillus subtilis* against bacterial disease of cucurbits. *Mol*. *Plant-Microbe Interact*. **2011**, *24*, 1540-1552.

(20) Yuan, B.; Wang, Z.; Qin, S.; Zhao, G. H.; Feng, Y. J.; Wei, L. H.; Jiang, J. H. Study of the anti-sapstain fungus activity of *Bacillus amyloliquefaciens* CGMCC 5569 associated with *Ginkgo biloba* and identification of its active components. *Bioresour. Technol*. **2012**, *114*, 536-541.

(21) Zhang, R. S.; Liu, Y. F.; Luo, C. P.; Wang, X. Y.; Liu, Y. Z.; Qiao, J. Q.; Yu, J. J.; Chen, Z. Y. *Bacillus amyloliquefaciens* Lx-11, a potential biocontrol agent against rice bacterial leaf streak. *J. Plant Pathol*. **2012**, *94*, 609-619.

(22) Hiraoka, H.; Asaka, O.; Ano, T.; Shoda, M. Characterization of *Bacillus subtilis* RB14, coproducer of peptide antibiotics iturin A and surfactin. *J. Gen. Appl. Microbiol.* **1992**, *38*, 635-640.

(23) Thimon, L.; Peypoux, F.; Maget-Dana, R.; Roux, B.; Michel, G. Interactions of bioactive lipopeptides, iturin A and surfactin from *Bacillus subtilis*. *Biotechnol. Appl. Bioc.* **1992**, *16*, 144-151.

(24) Maget-Dana, R.; Ptak, M. Iturin lipopeptides: interactions of mycosubtilin with lipids in planar membranes and mixed monolayers. *Biochim*. *Biophys*. *Acta, Biomembr.* **1990**, *1023*, 34-40.

(25) Maget-Dana, R.; Peypoux, F. Iturins, a special class of pore-forming lipopeptides: biological and physiological properties. *Toxicology* **1994**, *87*, 151-174.

(26) Bonmatin, J. M.; Laprevote, O.; Peypoux, F. Diversity among microbial cyclic lipopeptides: iturins and surfactins. Activity-structure relationships to design new bioactive agents. *Comb. Chem. High Throughput Screen* **2003**, *6*, 541-556.

(27) Maget-Dana, R.; Thimon, L.; Peypoux, F.; Ptak, M. Surfactin/iturin A interactions may explain the synergistic effect of surfactin on the biological properties of iturin A. *Biochimie* **1992**, *74*, 1047-1051.

Chapter 4
Conclusion

Two new cyclic lipopeptides (**3** and **4**) and two new cyclic lipodepsipeptides (**5** and **6**) were isolated from the culture supernatant of *B. amyloliquefaciens* biocontrol strain SD-32, together with five known metabolites, *iso*-C_{15} (**1**), *iso*-C_{16} bacillomycin D (**2**), *iso*-C_{14} (**7**), *anteiso*-C_{15} (**8**), and *iso*-C_{15} [Ile^7]surfactin (**9**). Spectroscopic and chemical analyses of the new compounds **3**-**6** revealed their structures to be *anteiso*-C_{17} bacillomycin D (**3**), *iso*-C_{17} bacillomycin D (**4**), *anteiso*-C_{13} [Ile^7]surfactin (**5**), and *iso*-C_{13} [Ile^7]surfactin (**6**), respectively.

The activities of bacillomycin D homologues (**1**-**4**) were evaluated against 13 plant pathogens in the in vitro assay: the activities of *anteiso*- and *iso*-C_{17} bacillomycin D (**3** and **4**) were almost the same of each other, and stronger than those of *iso*-C_{15} and *iso*-C_{16} bacillomycin D (**1** and **2**); the activities of *iso*-C_{15} bacillomycin D (**1**) were the weakest. Compounds **1**-**4** inhibited the growth of all fungi tested. Furthermore, compounds **1**-**4** at concentrations of 80, 40, 30, and 30 μM, respectively, completely inhibited the *Botrytis cinerea* infection in cucumber leaves. However, *Pythium aphanidermatum* was not inhibited at all by any of the compounds.

By contrast, the activities of [Ile^7]surfactin homologues (**5**-**9**) in the in vitro assay were much lower than those of bacillomycin D homologues; however, [Ile^7]surfactin homologues (**5**-**9**) clearly showed synergistic activities with bacillomycin D in the in vivo assay using cucumber cotyledon and *B. cinerea*. The synergistic effects of [Ile^7]surfactin homologues to bacillomycin D against *B. cinerea* were not observed in the in vitro mycelial growth or conidial germination inhibition assays, implying that these effects might play a role in the gray mold infection of cucumber leaves.

Based on these results, I conclude the following.

1) *B. amyloliquefaciens* biocontrol strain SD-32 produces bacillomycin D homologues and [Ile^7]surfactin homologues.

2) Bacillomycin D homologues have antifungal activity and play an important role in the biological control by *B. amyloliquefaciens* SD-32.

3) The strain SD-32 is unique because it produces a higher content of powerful C_{17} bacillomycin D homologues than other strains reported previously.

4) [Ile^7]surfactin homologues enhance the activities of bacillomycin D homologues under actual conditions.

The detailed mechanism by which [Ile^7]surfactin homologues enhanced the suppressive effect of bacillomycin D in the in vivo assay is still unknown and remains to be studied. In addition, the data shown in this study could not completely explain the suppressive activity gap between the culture supernatant on the one hand and bacillomycin D and the [Ile^7]surfactin homologues in it on the other. This indicates the presence of metabolite(s) that contribute to gray mold disease suppression other than bacillomycin D and [Ile^7]surfactin homologues. Therefore, research to identify the relevant factors other than bacillomycin D and [Ile^7]surfactin homologues is needed.

Acknowledgments

I express my gratitude and sincere appreciation to my respected advisor, Dr. Hiromitsu Nakajima, Tottori University, for his warm encouragement, valuable advice and kind support. I also express my deep appreciation to Professor Atsushi Ishihara of Tottori University for his helpful advice and support. I would like to express appreciation to Professor Makoto Ueno of Shimane University and Professor Tsuyoshi Ichiyanagi of Tottori University for their discussion and suggestion.

I am grateful to Mr. Yusuke Amaki, Dr. Motoki Tanaka, Dr. Mutsumi Fukuda, Dr. Koji Inai, Dr. Hiroshi Miyazoe, Dr. Takao Nagano, and all my laboratory members of SDS Biotech K.K. for their technical assistance.

Finally, I heartily grateful to my supervisor, Mr. Yasuhide Toshima, General Manager of Tsukuba Research and Technology Center, SDS Biotech K.K., for his warm encouragement and kind consideration.

Summary

Botrytis cinerea Pers. Fr. is a pathogen that causes gray mold disease in many crops and causes serious crop losses worldwide. Although chemical fungicides have been used for many years to control the pathogen, the ability of *B. cinerea* to adapt quickly to new chemicals by developing resistance creates the need for continuous development of new fungicides. With increasing concern over fungicide resistance and over the environmental impact and food safety of chemical fungicides, biological control has attracted considerable attention.

To develop new and effective biological control agents against gray mold disease, a screening search was performed, and *Bacillus amyloliquefaciens* SD-32 was isolated from soil in Japan as a promising and effective agent against gray mold disease. To gain insight into the mechanisms responsible for the biological control achieved by *B. amyloliquefaciens* strain SD-32, in this study, attempts were made to identify the factors produced by the bacterium that contribute to the control of gray mold disease and to clarify the role of these factors in the biological control system.

Using an in vitro antifungal-activity-guided purification, two new cyclic lipopeptides (**3** and **4**) were isolated from the culture supernatant of *B. amyloliquefaciens* strain SD-32, together with two known metabolites, *iso*-C_{15} and *iso*-C_{16} bacillomycin D (**1** and **2**). Spectroscopic and chemical analyses identified the structures of the new compounds **3** and **4** as *anteiso*-C_{17} bacillomycin D and *iso*-C_{17} bacillomycin D, respectively. The activities of compounds **1-4** were evaluated against 13 plant pathogens: compounds **1-4** inhibited the growth of all fungi tested. The activities of *anteiso*- and *iso*-C_{17} bacillomycin D (**3** and **4**) were almost the same of each other, and stronger than those of *iso*-C_{15} and *iso*-C_{16} bacillomycin D (**1** and **2**); the activities of *iso*-C_{15} bacillomycin D (**1**) were the weakest. Furthermore, compounds **1-4** at concentrations of 80, 40, 30, and 30 μM, respectively, completely inhibited *B. cinerea* infection in cucumber leaves.

The activity of the culture supernatant, however, was not ascribed exclusively to bacillomycin D homologues; therefore, metabolites other than bacillomycin D were also investigated. After purifying the fractions that exhibited synergistic activity with bacillomycin

D, two new cyclic lipodepsipeptides (**5** and **6**) were found in the culture supernatant of this strain, together with three known metabolites, *iso*-C_{14}, *anteiso*-C_{15}, and *iso*-C_{15} [Ile^7]surfactin (**7**, **8**, and **9**). Spectroscopic and chemical analyses identified the structures of the new compounds **5** and **6** as *anteiso*-C_{13} and *iso*-C_{13} [Ile^7]surfactin, respectively. Interestingly, [Ile^7]surfactin homologues significantly enhanced the suppressive effect of bacillomycin D against *B. cinerea* in an in vivo cucumber leaf-disk assay, although they showed no suppressive effect by themselves, suggesting that synergistic actions between the [Ile^7]surfactin homologues and bacillomycin D were involved in the suppression of gray mold disease by the bacterium. Furthermore, the synergistic effects were not observed in in vitro mycelial growth or conidial germination inhibition assays, implying that these effects might play a role in gray mold infection in cucumber leaves.

Based on these results, I conclude the following.

1) *B. amyloliquefaciens* biocontrol strain SD-32 produces bacillomycin D homologues and [Ile^7]surfactin homologues.

2) Bacillomycin D homologues have antifungal activity and play an important role in the biological control by *B. amyloliquefaciens* SD-32.

3) The strain SD-32 is unique because it produces a higher content of powerful C_{17} bacillomycin D homologues than other strains reported previously.

4) [Ile^7]surfactin homologues enhance the activities of bacillomycin D homologues under actual conditions.

摘要

Botrytis cinerea Pers. Fr. は多くの作物の灰色かび病の原因となる植物病原菌である。本菌を防除するため，長年にわたり化学合成農薬が使用されてきたが，化学合成農薬耐性菌の出現により，常に新しい作用特性を有する化学合成農薬の研究開発が求められ，これに大きなコストが割かれている。植物病原菌の薬剤耐性問題に加え，化学合成農薬の環境に与える影響や食料の安全性の問題等から，化学合成農薬のみに頼った植物病害防除に疑問符が付く状況の中，化学合成農薬に代わる選択枝として，生物農薬への期待が高まっている。

このような背景のもと、灰色かび病に対する効果の高い防除効果を有する菌株を探索したところ，非常に高い防除効果を示す *Bacillus amyloliquefaciens* SD-32 株を見出した。本研究では，本菌株の防除効果のメカニズムを解明するため，灰色かび病防除に関わる代謝産物を単離・精製し，その役割を明らかにすることを目的とした。

本菌の培養上清から，PDA プレート上での灰色かび病菌に対する活性を指標にして活性物質の単離を試みた。その結果，化合物 **1-4** を単離し，2D-NMR，MALDI-TOF-MS/MS，化学分析により，その構造を，それぞれ *iso*-C_{15}，*iso*-C_{16}，*anteiso*-C_{17}，*iso*-C_{17} bacillomycin D と同定した。**1** および **2** は既知化合物であったが，**3** 及び **4** は新規化合物であった。

化合物 **1-4** の各種植物病原菌に対する効果を PDA プレート上で調べたところ，化合物 **1-4** は，12 種の植物病原菌に対して生育阻害効果を示し，その効果は *anteiso*-C_{17}，*iso*-C_{17} bacillomycin D（**3**, **4**）が最も強く，次いで *iso*-C_{16} bacillomycin D（**2**），*iso*-C_{15} bacillomycin D（**1**）が最も弱かった。さらに，これらの化合物の灰色かび病に対する効果をキュウリ子葉を用いたリーフディスク試験で調べたところ，化合物 **1-4**（それぞれ 80, 40, 30, 30 μM）は，子葉上で灰色かび病の発病を完全に抑制した。

さらなる検討の過程で，本菌の培養上清の灰色かび病に対する活性は、bacillomycin D ホモログの活性だけでは説明できないことが明らかとなった。そこで，bacillomycin D に対する相乗効果を指標に活性画分の精製を行うことで，化合物 **5-9** を単離し，2D-NMR，MALDI-TOF-MS/MS，化学分析により，その構造を，それぞれ *anteiso*-C_{13}，*iso*-C_{13}，*iso*-C_{14}，

anteiso-C_{15}, *iso*-C_{15} [Ile^7]surfactin と同定した。**7-9** は既知化合物であったが，**5** および **6** は新規化合物であった。

興味深いことに，[Ile^7]surfactin ホモログは，キュウリ子葉を用いたリーフディスク試験において，それ自身は活性を持たないにもかかわらず，bacillomycin D ホモログの活性を増大させる機能を有しており，その効果は本菌の灰色かび病の抑制効果に関与していることが示唆された。さらに，in vitro における菌糸成長阻害試験・胞子発芽阻害試験において，[Ile^7]surfactin ホモログとbacillomycin Dホモログの相乗効果は認められず，キュウリ子葉を用いたリーフディスク試験で認められる相乗効果は，灰色かび病菌のキュウリに対する感染過程を阻害していることが示唆された。

List of Publications

1. Tanaka, K.; Ishihara, A.; Nakajima, H. Isolation of *anteiso*-C_{17}, *iso*-C_{17}, *iso*-C_{16}, and *iso*-C_{15} bacillomycin D from *Bacillus amyloliquefaciens* SD-32 and their antifungal activities against plant pathogens. *J. Agric. Food Chem.* **2014**, *62*, 1469-1476. (Chapter 2)

2. Tanaka, K.; Amaki, Y.; Ishihara, A.; Nakajima, H. Synergistic effects of [Ile^7]surfactin homologues with bacillomycin D in suppression of gray mold disease by *Bacillus amyloliquefaciens* biocontrol strain SD-32. *J. Agric. Food Chem.* **2015**, *63*, 5344–5353. (Chapter 3)

Appendix

Figure S29. ^{1}H NMR spectrum of *iso*-C_{13} [Ile^{7}]surfactin (**6**) in DMSO-d_6.

Figure S30. ^{13}C NMR spectrum of *iso*-C_{13} [Ile^{7}]surfactin (**6**) in DMSO-d_6.

Figure S31. COSY spectrum of *iso*-C_{13} [Ile^{7}]surfactin (**6**) in DMSO-d_6.

Figure S32. HSQC spectrum of *iso*-C_{13} [Ile^{7}]surfactin (**6**) in DMSO-d_6.

Figure S33. HMBC spectrum of *iso*-C_{13} [Ile^{7}]surfactin (**6**) in DMSO-d_6.

Figure S34. NOESY spectrum of *iso*-C_{13} [Ile^{7}]surfactin (**6**) in DMSO-d_6.

Figure S35. ^{1}H NMR spectrum of *anteiso*-C_{15} [Ile^{7}]surfactin (**8**) in DMSO-d_6.

Figure S36. ^{13}C NMR spectrum of *anteiso*-C_{15} [Ile^{7}]surfactin (**8**) in DMSO-d_6.

Figure S37. ^{1}H NMR spectrum of *iso*-C_{15} [Ile^{7}]surfactin (**9**) in DMSO-d_6.

Figure S38. ^{13}C NMR spectrum of *iso*-C_{15} [Ile^{7}]surfactin (**9**) in DMSO-d_6.

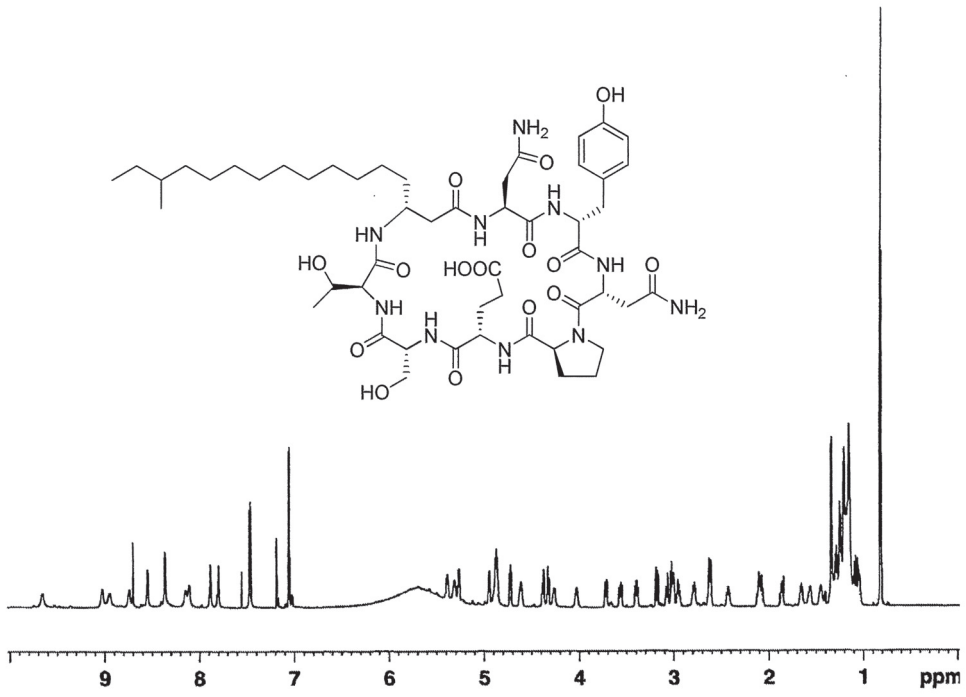

Figure S1. ^{1}H NMR spectrum of *anteiso*-C_{17} bacillomycin D (**3**) in pyridine-d_5.

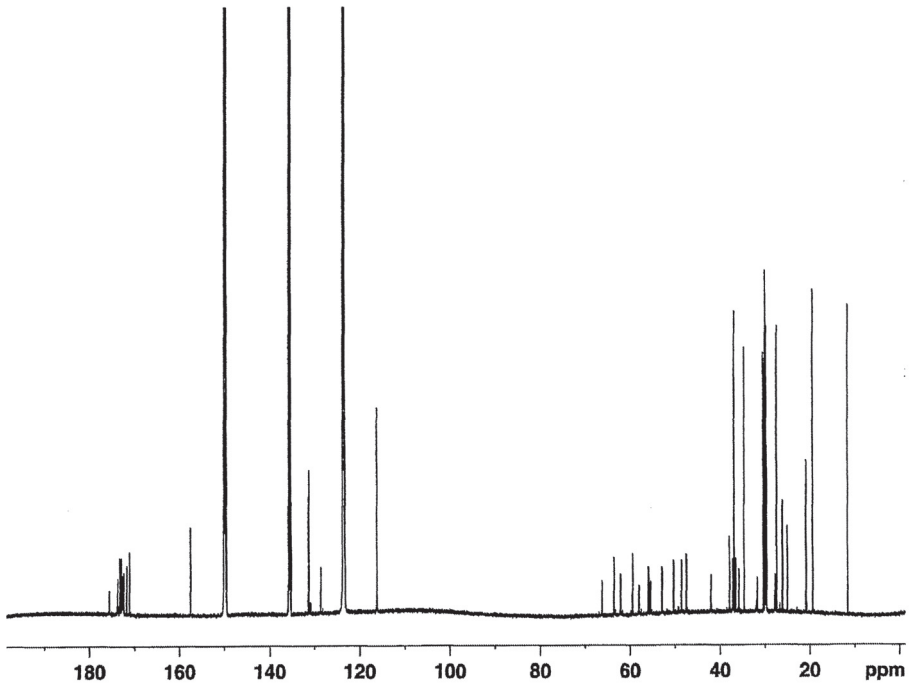

Figure S2. ^{13}C NMR spectrum of *anteiso*-C_{17} bacillomycin D (**3**) in pyridine-d_5.

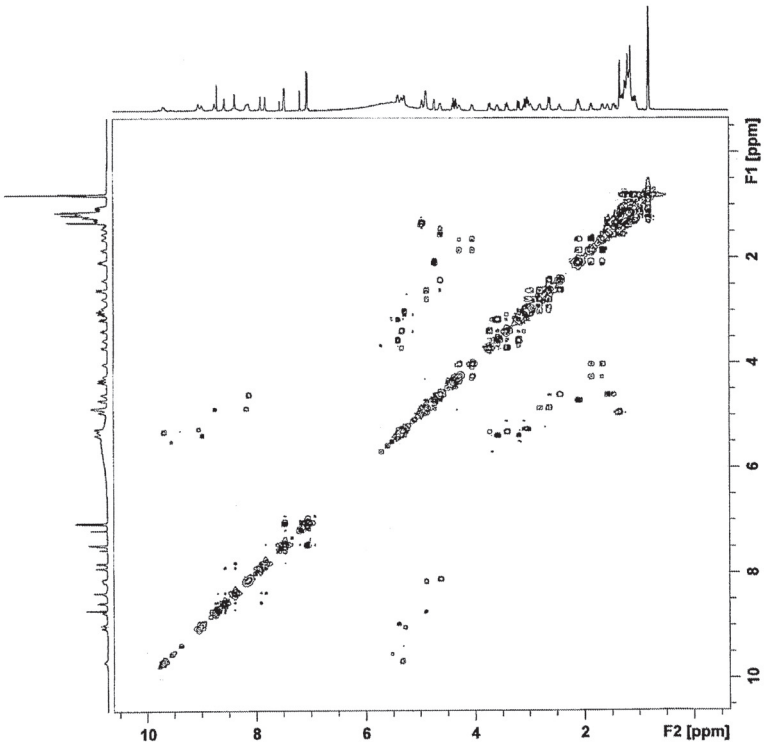

Figure S3. COSY spectrum of *anteiso*-C_{17} bacillomycin D (**3**) in pyridine-d_5.

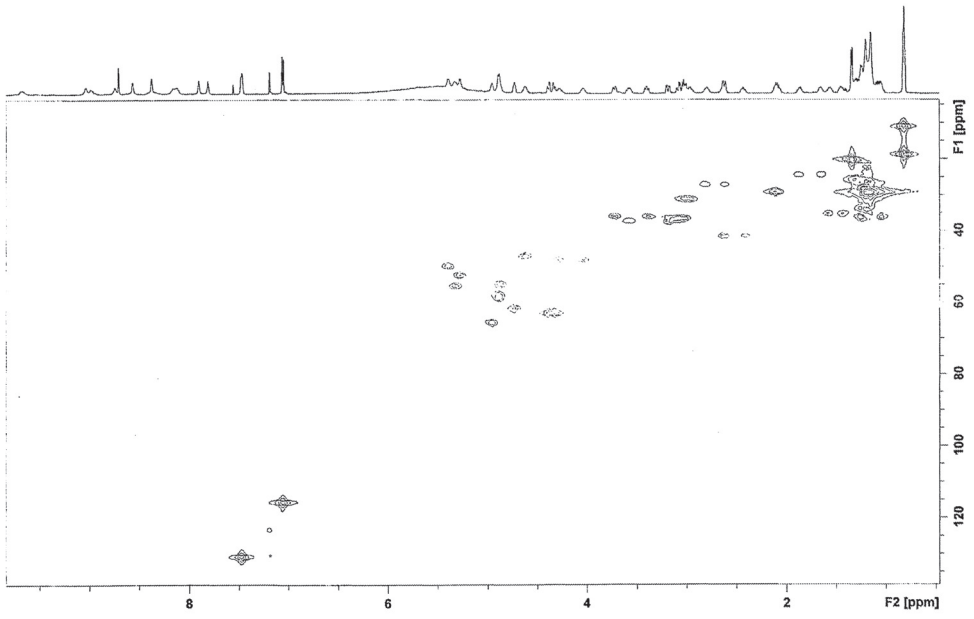

Figure S4. HSQC spectrum of *anteiso*-C_{17} bacillomycin D (**3**) in pyridine-d_5.

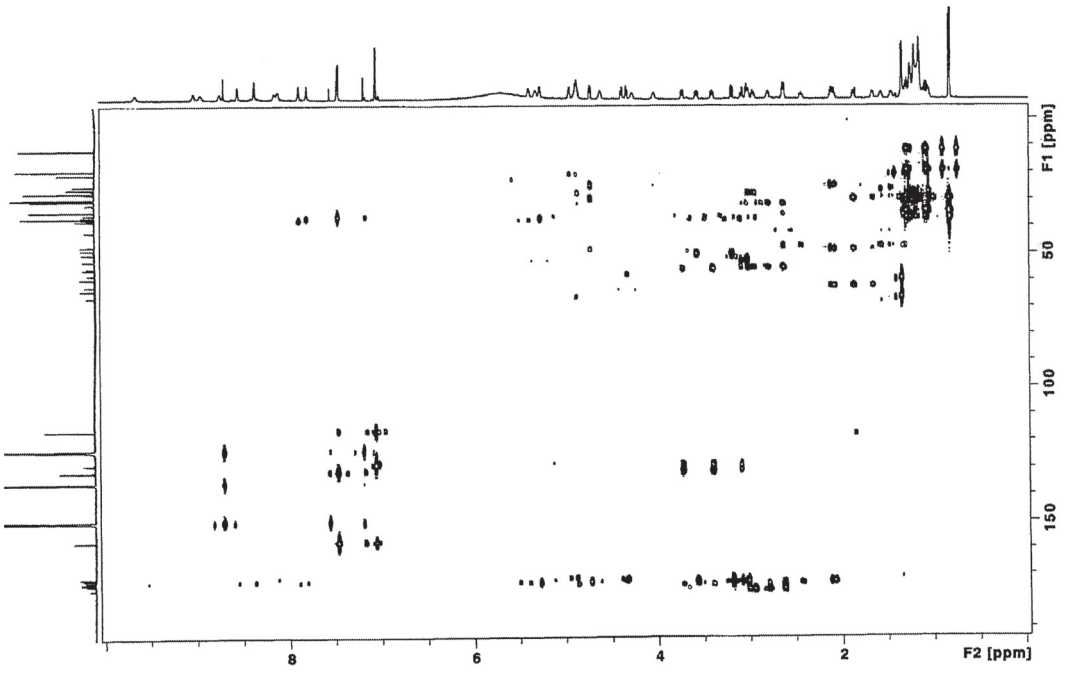

Figure S5. HMBC spectrum of *anteiso*-C_{17} bacillomycin D (**3**) in pyridine-d_5.

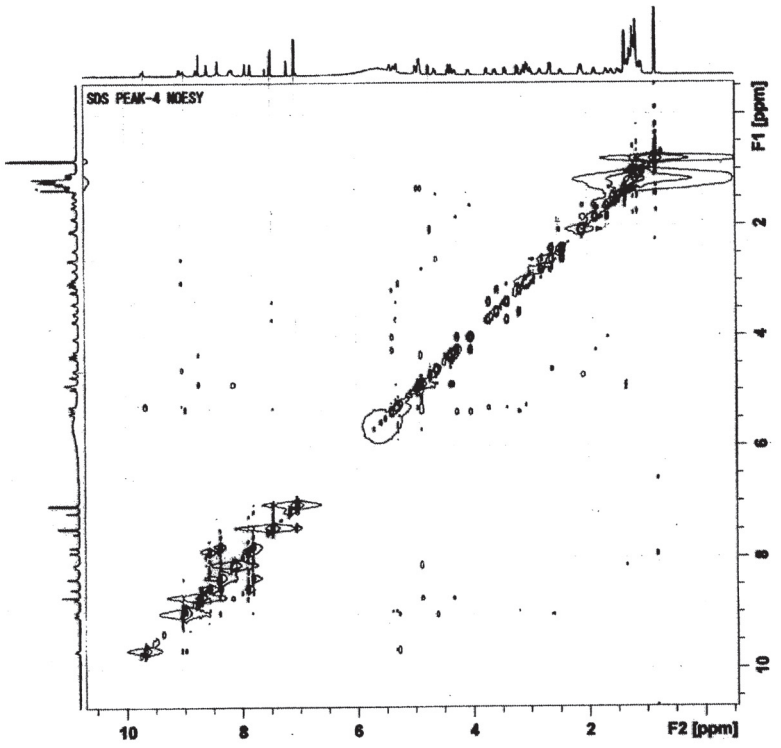

Figure S6. NOESY spectrum of *anteiso*-C_{17} bacillomycin D (**3**) in pyridine-d_5.

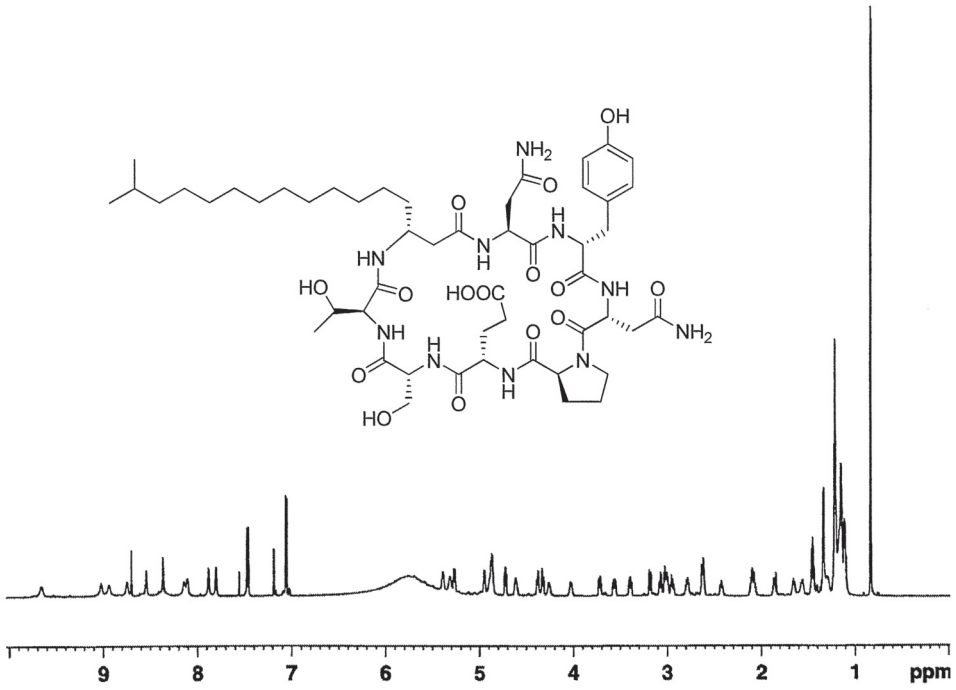

Figure S7. ^{1}H NMR spectrum of *iso*-C_{17} bacillomycin D (**4**) in pyridine-d_5.

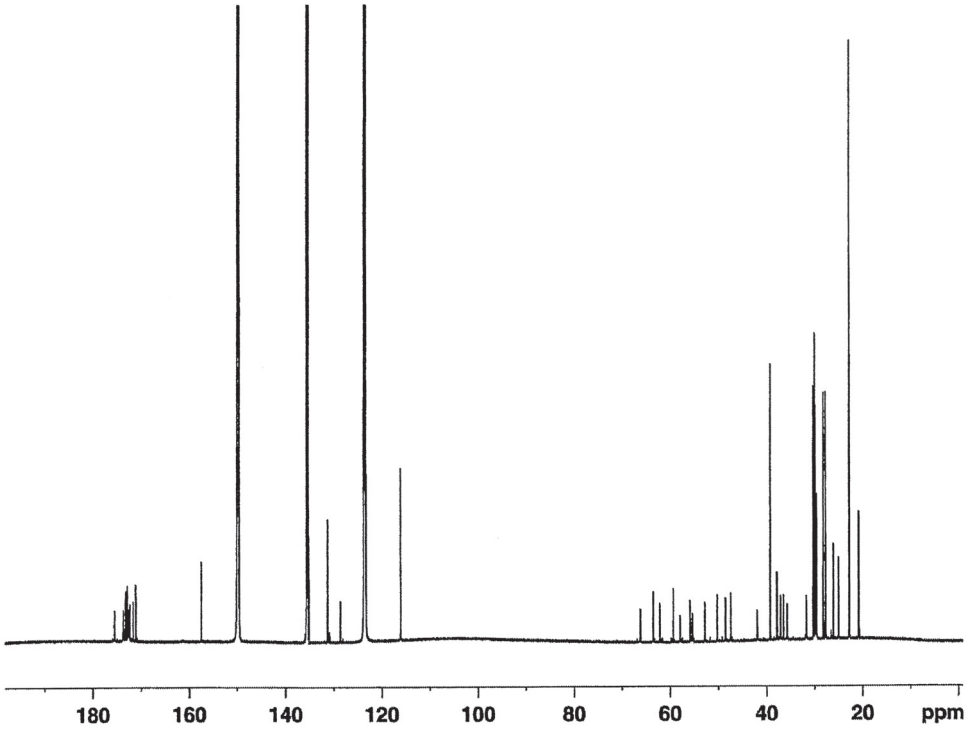

Figure S8. ^{13}C NMR spectrum of *iso*-C_{17} bacillomycin D (**4**) in pyridine-d_5.

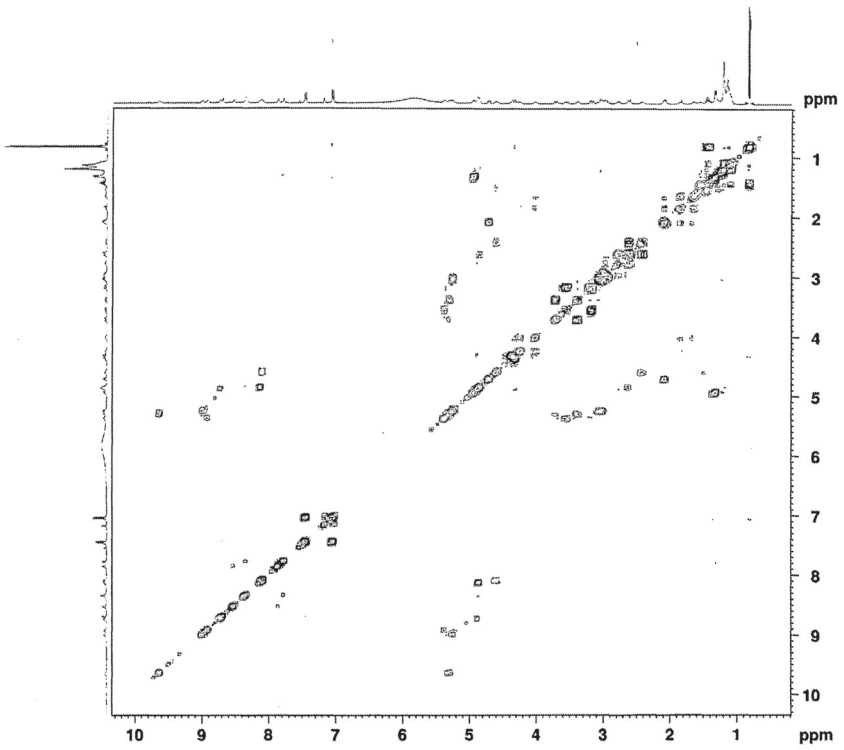

Figure S9. COSY spectrum of *iso*-C_{17} bacillomycin D (**4**) in pyridine-d_5.

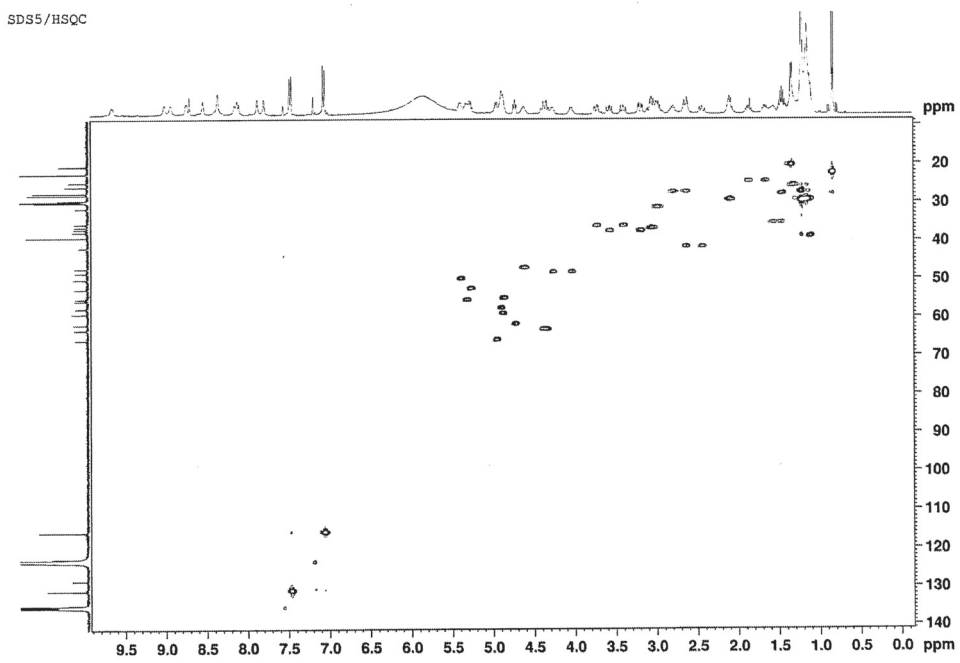

Figure S10. HSQC spectrum of *iso*-C_{17} bacillomycin D (**4**) in pyridine-d_5.

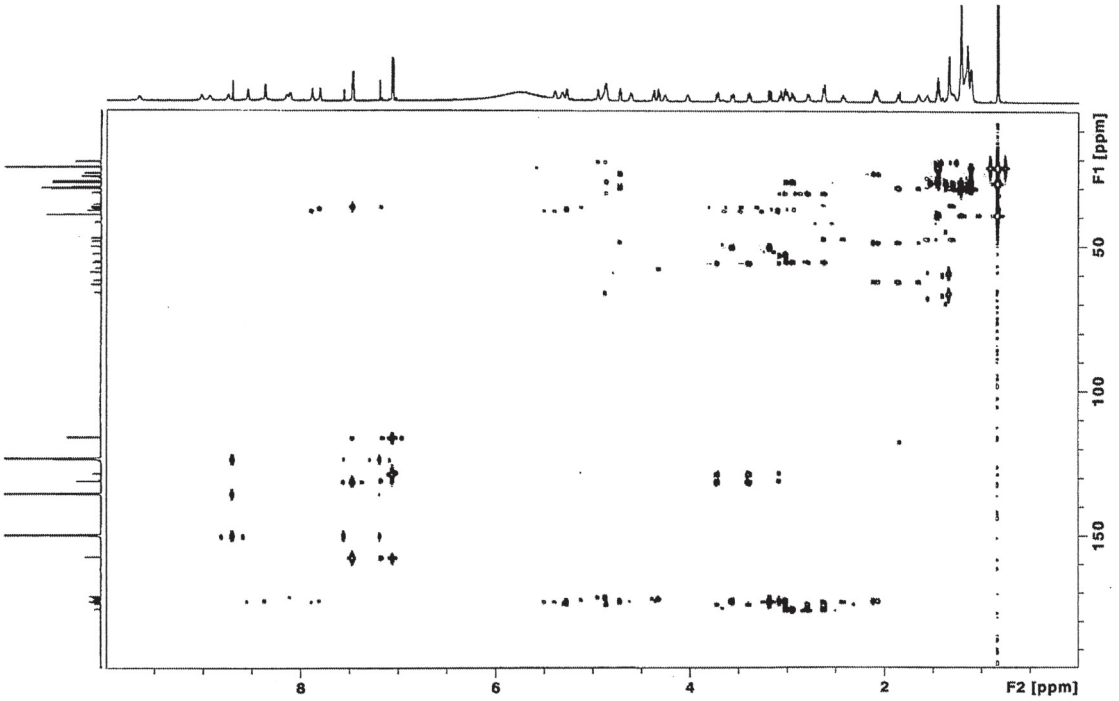

Figure S11. HMBC spectrum of *iso*-C_{17} bacillomycin D (**4**) in pyridine-d_5.

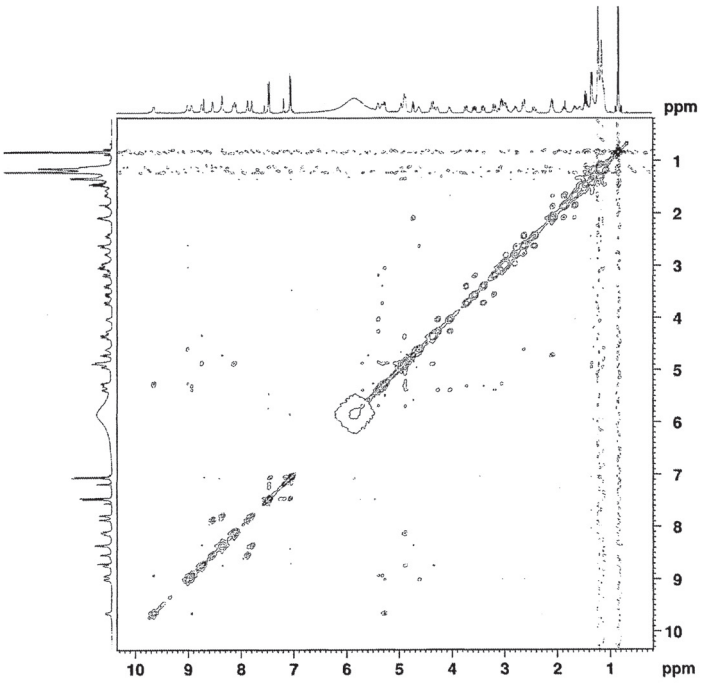

Figure S12. NOESY spectrum of *iso*-C_{17} bacillomycin D (**4**) in pyridine-d_5.

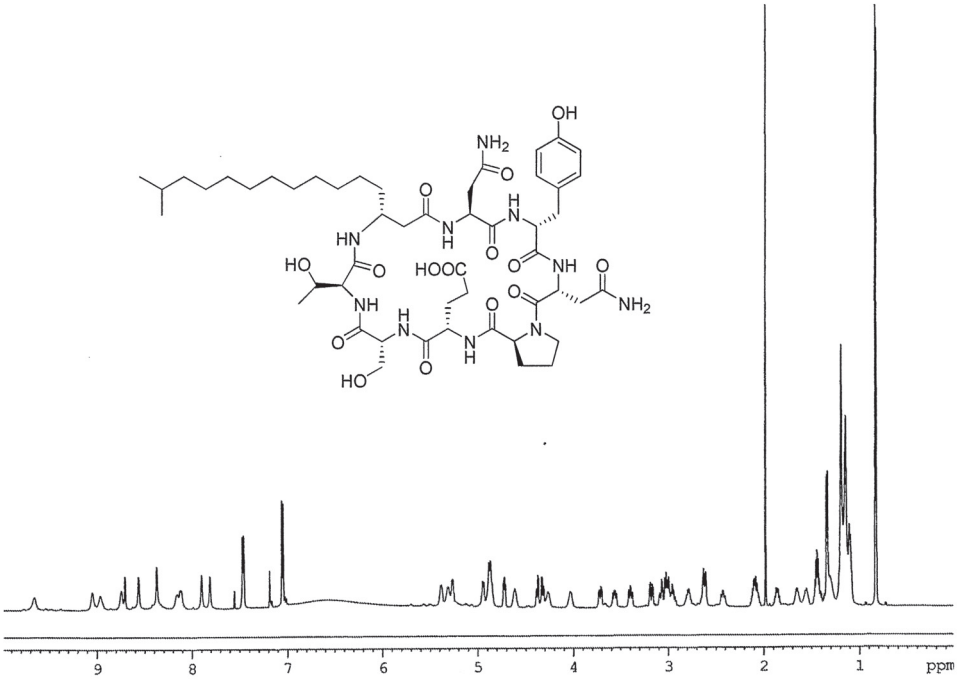

Figure S13. ^{1}H NMR spectrum of *iso*-C_{16} bacillomycin D (**2**) in pyridine-d_5.

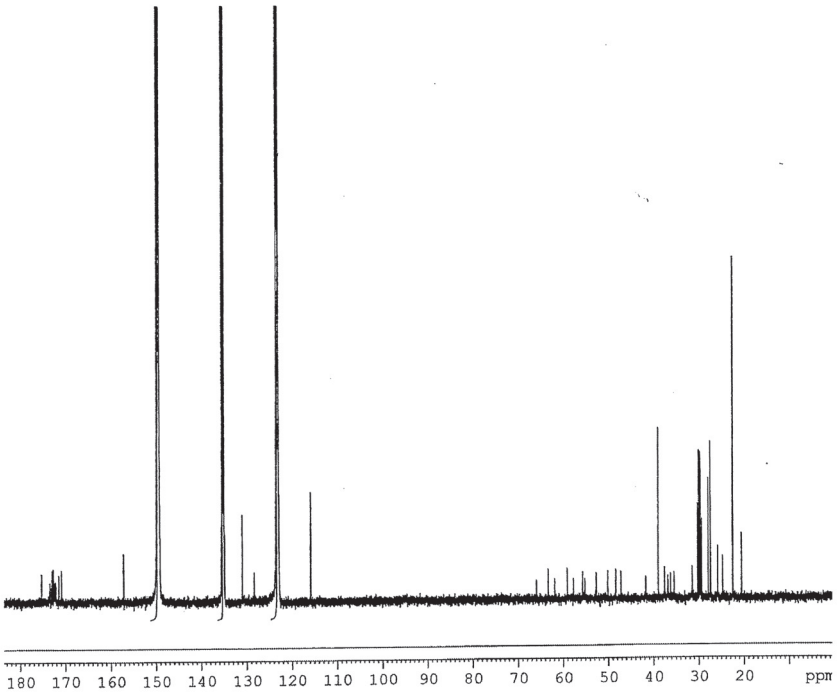

Figure S14. ^{13}C NMR spectrum of *iso*-C_{16} bacillomycin D (**2**) in pyridine-d_5.

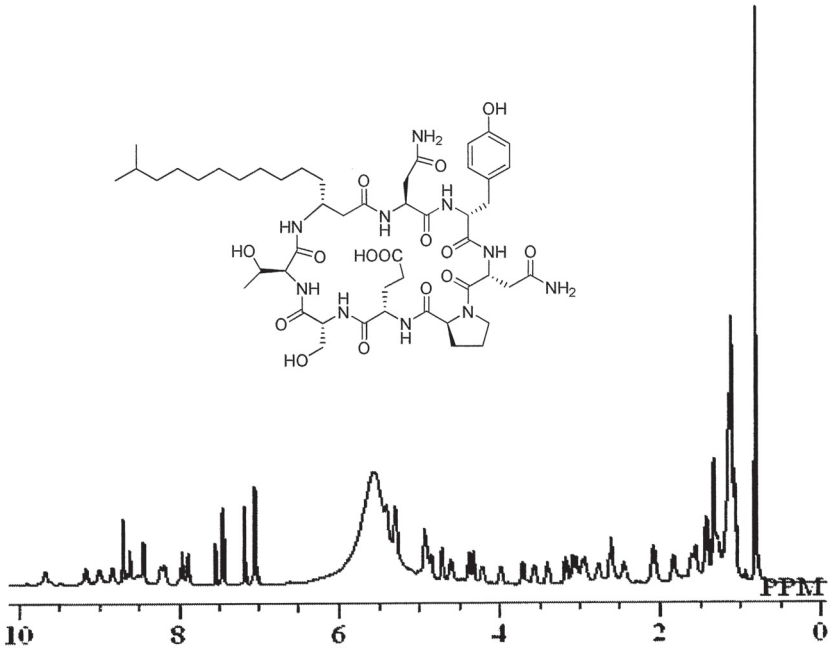

Figure S15. ^{1}H NMR spectrum of *iso*-C_{15} bacillomycin D (**1**) in pyridine-d_5.

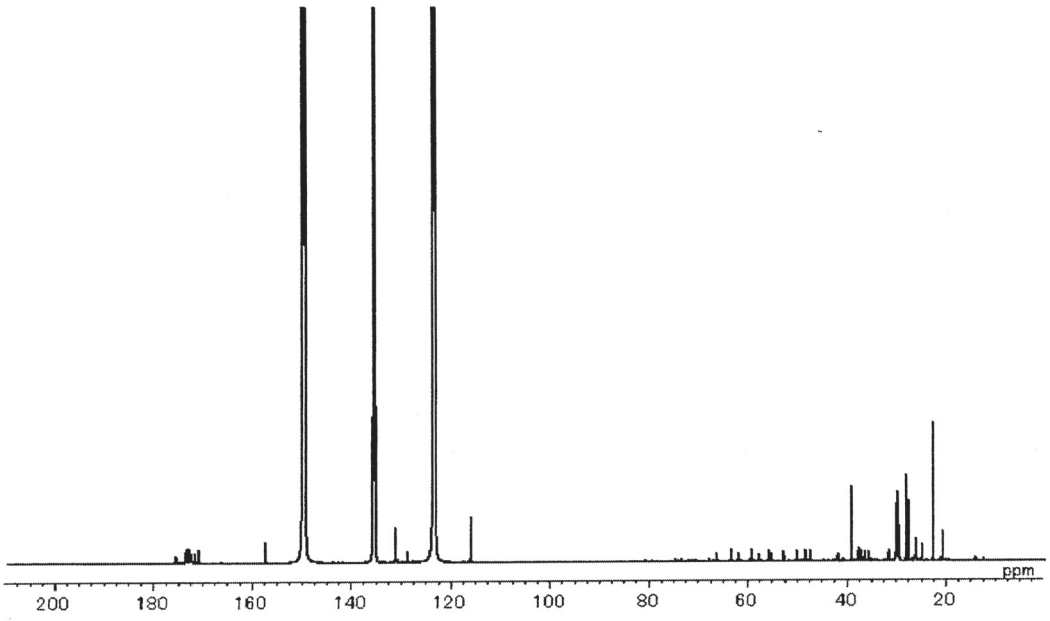

Figure S16. ^{13}C NMR spectrum of *iso*-C_{15} bacillomycin D (**1**) in pyridine-d_5.

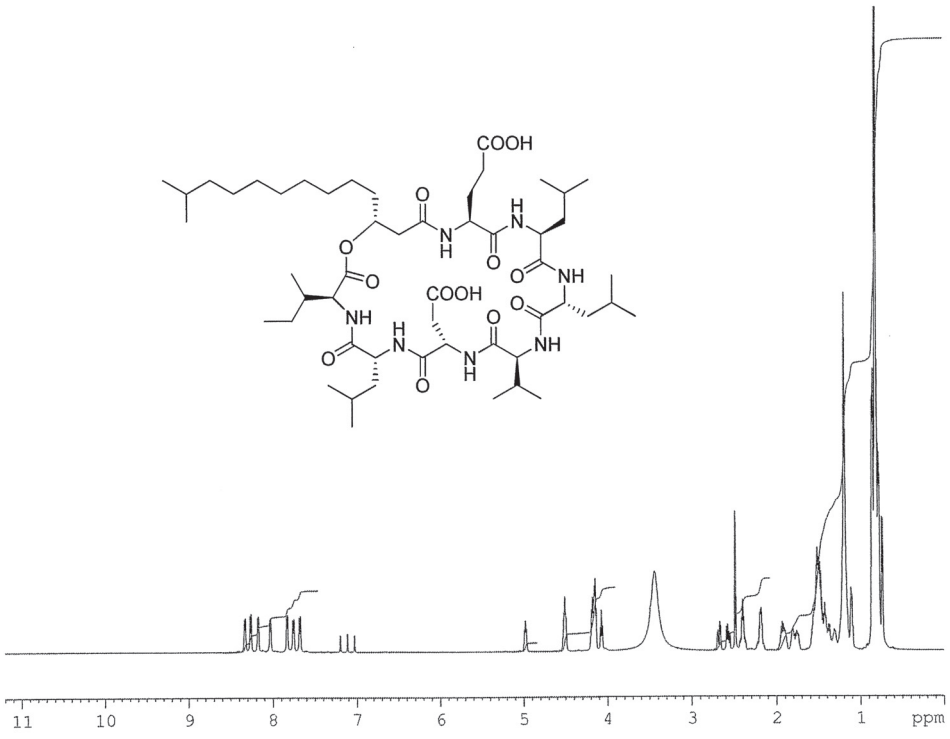

Figure S17. ^{1}H NMR spectrum of *iso*-C_{14} [Ile^{7}]surfactin (**7**) in DMSO-d_6.

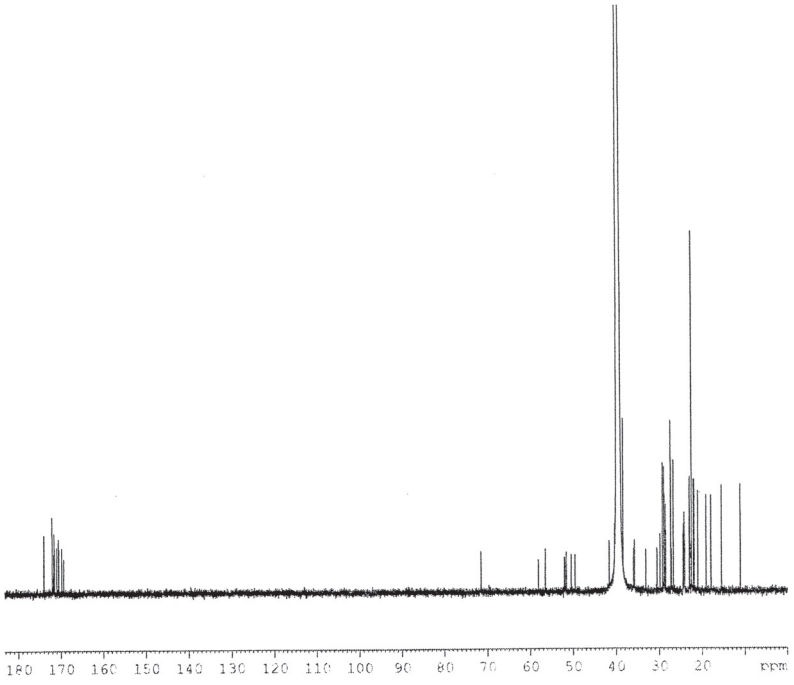

Figure S18. ^{13}C NMR spectrum of *iso*-C_{14} [Ile^{7}]surfactin (**7**) in DMSO-d_6.

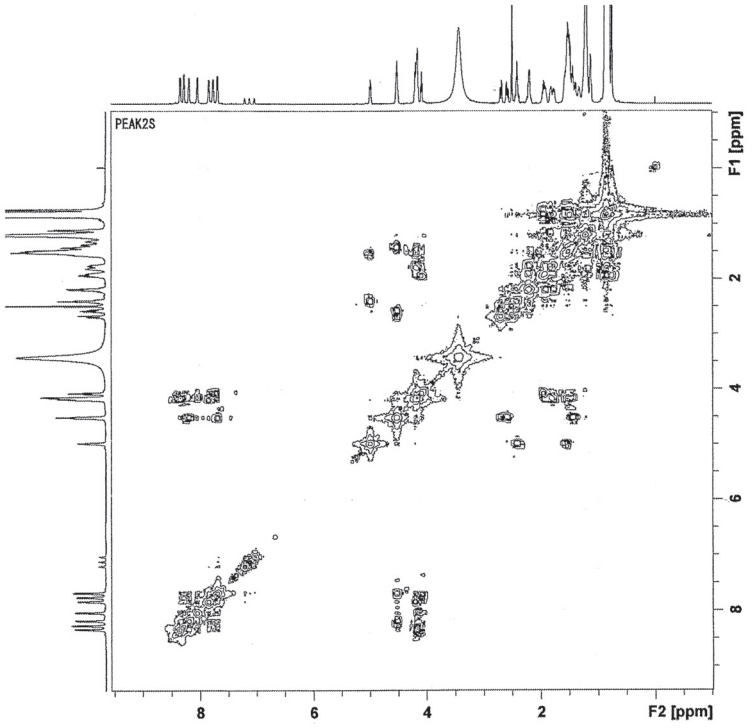

Figure S19. COSY spectrum of *iso*-C_{14} [Ile^7]surfactin (**7**) in DMSO-d_6.

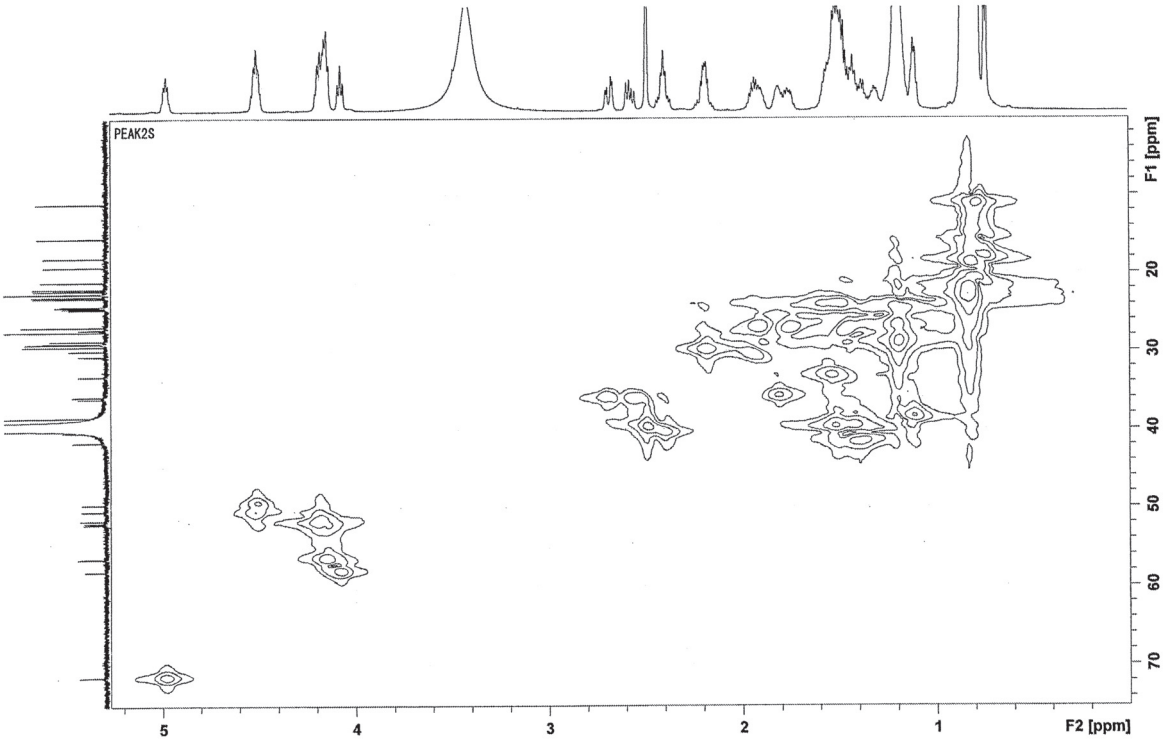

Figure S20. HSQC spectrum of *iso*-C_{14} [Ile^7]surfactin (**7**) in DMSO-d_6.

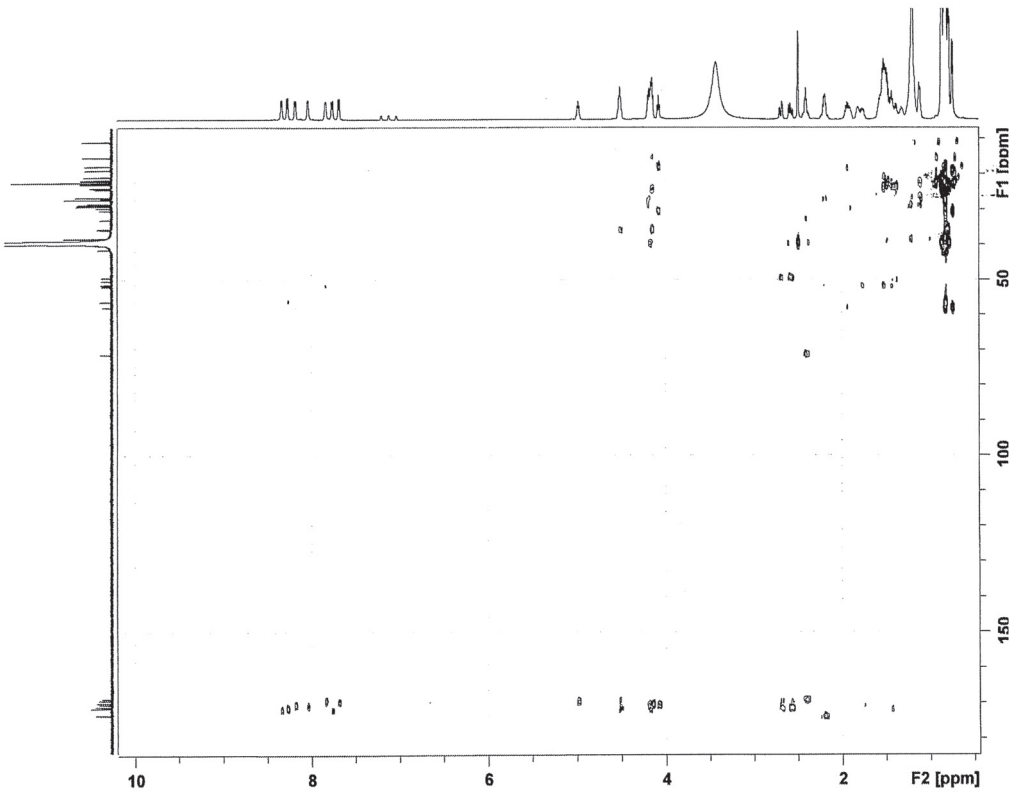

Figure S21. HMBC spectrum of *iso*-C_{14} [Ile^7]surfactin (**7**) in DMSO-d_6.

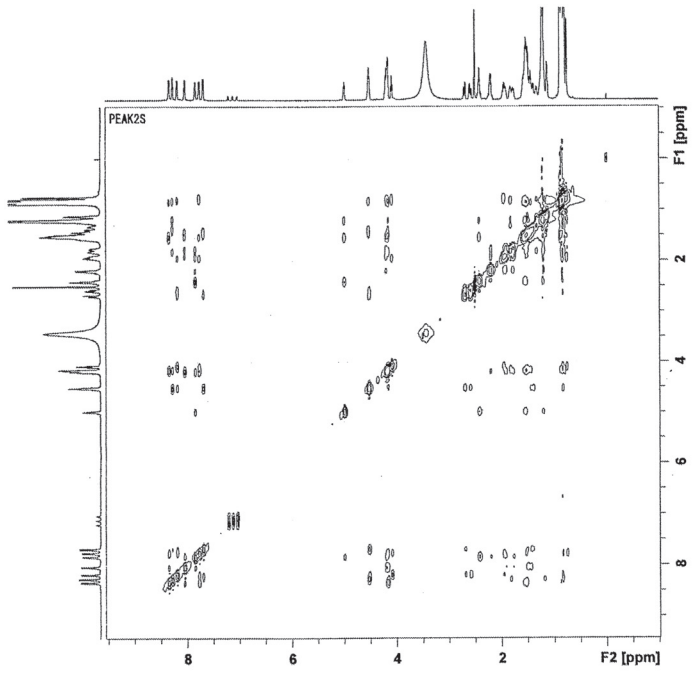

Figure S22. NOESY spectrum of *iso*-C_{14} [Ile^7]surfactin (**7**) in DMSO-d_6.

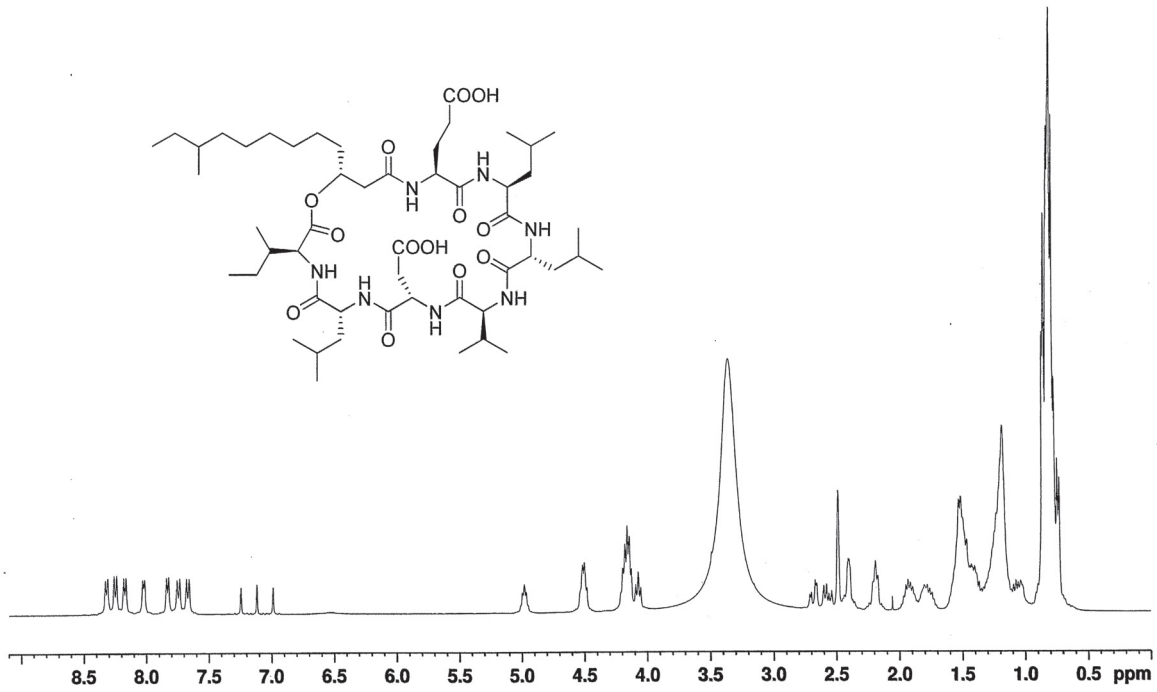

Figure S23. ^{1}H NMR spectrum of *anteiso*-C_{13} [Ile^{7}]surfactin (**5**) in DMSO-d_6.

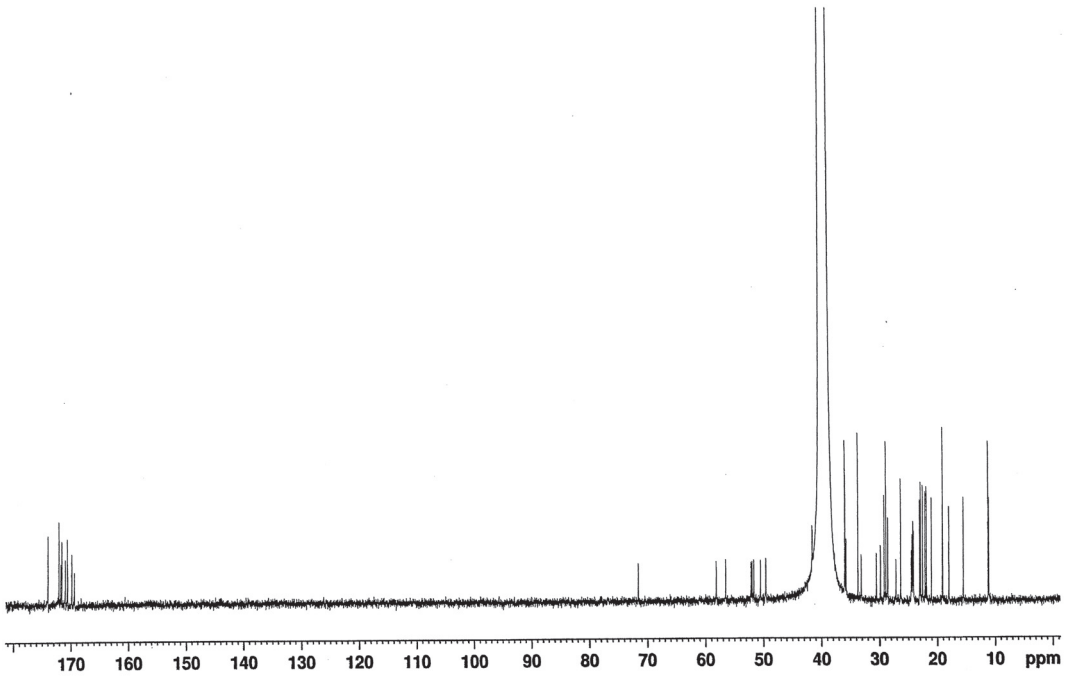

Figure S24. ^{13}C NMR spectrum of *anteiso*-C_{13} [Ile^{7}]surfactin (**5**) in DMSO-d_6.

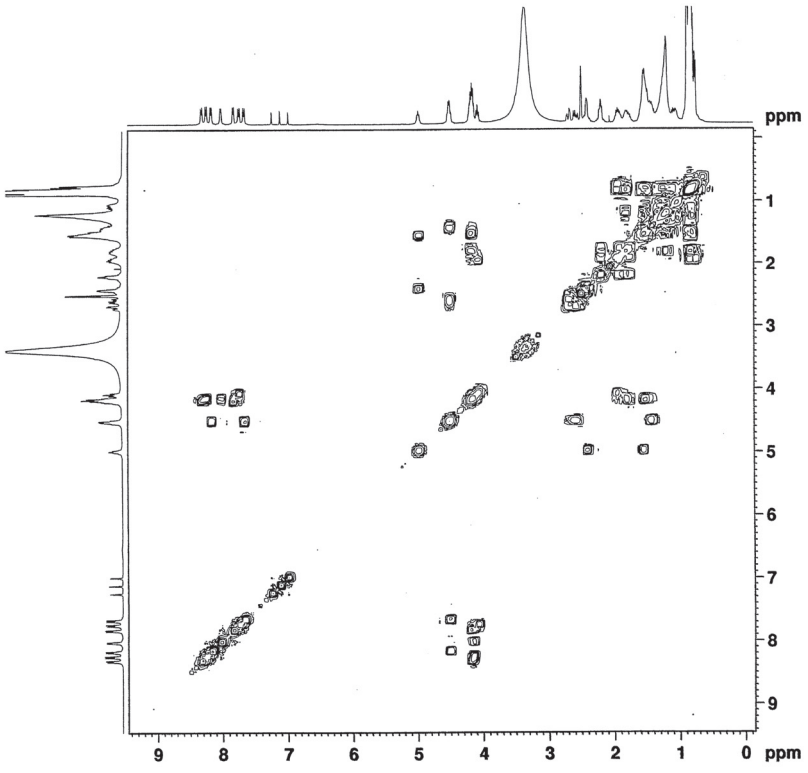

Figure S25. COSY spectrum of *anteiso*-C_{13} [Ile^7]surfactin (**5**) in DMSO-d_6.

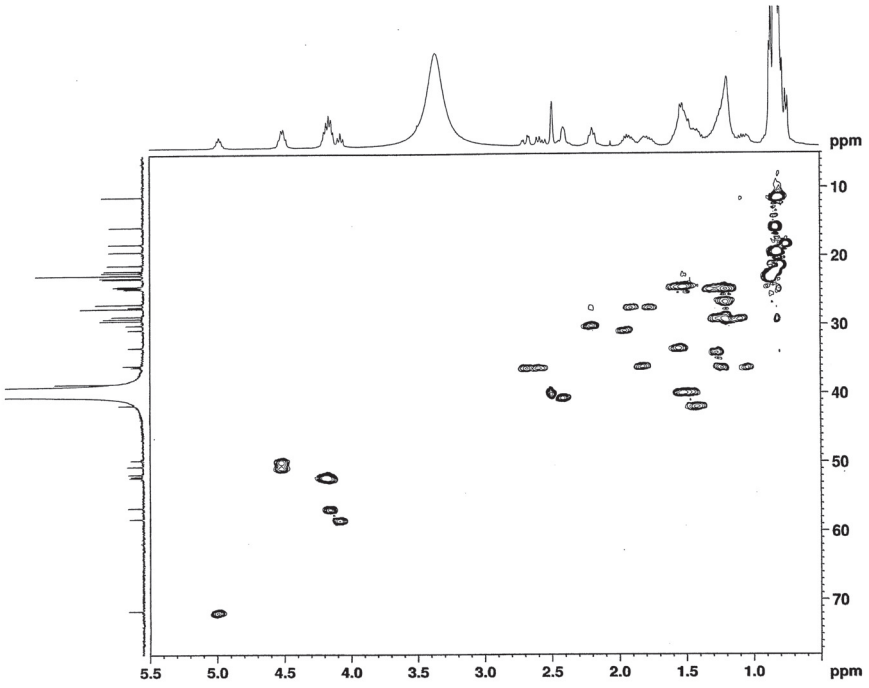

Figure S26. HSQC spectrum of *anteiso*-C_{13} [Ile^7]surfactin (**5**) in DMSO-d_6.

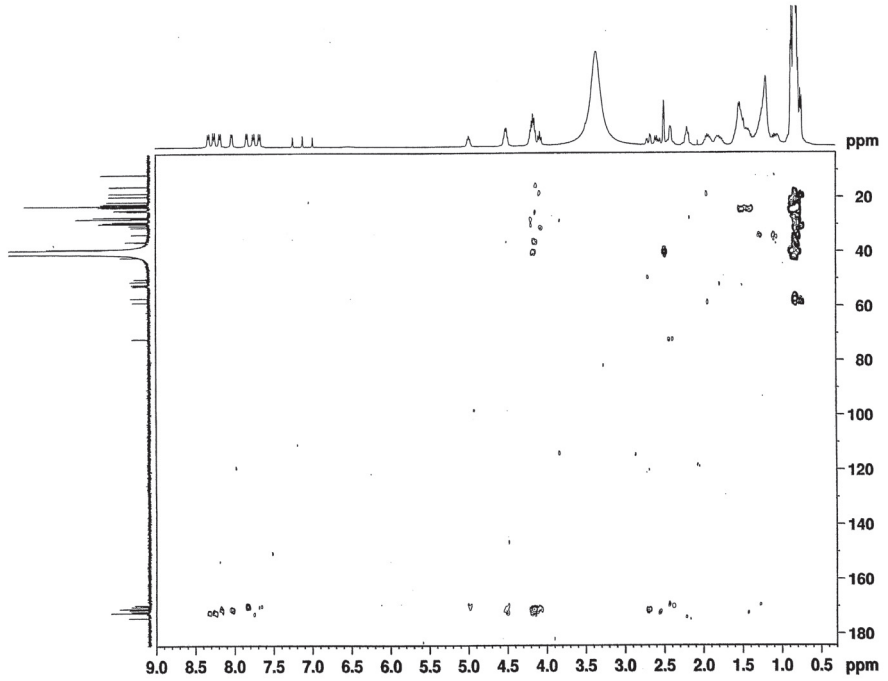

Figure S27. HMBC spectrum of *anteiso*-C_{13} [Ile^7]surfactin (**5**) in DMSO-d_6.

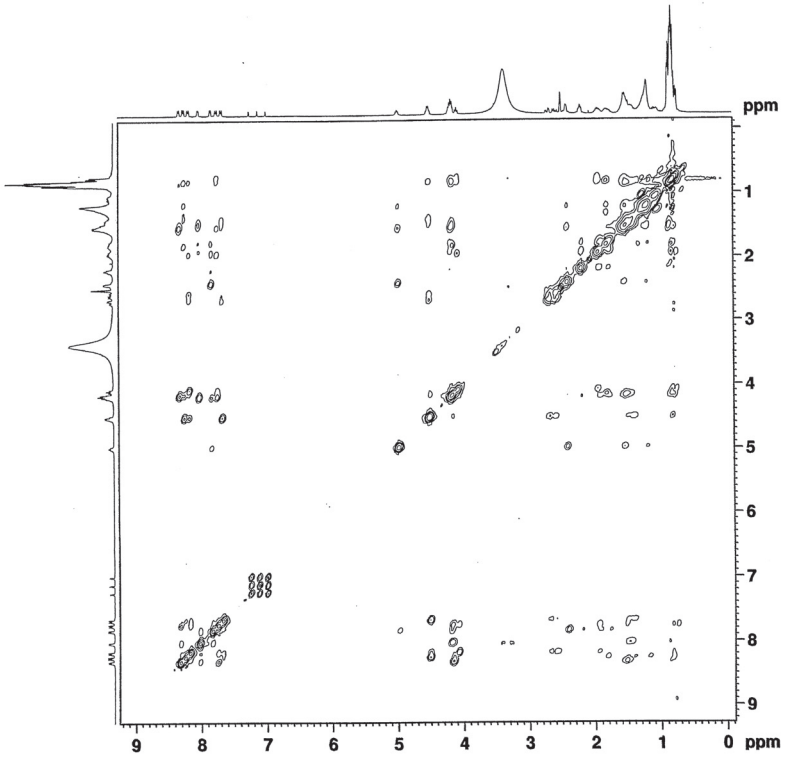

Figure S28. NOESY spectrum of *anteiso*-C_{13} [Ile^7]surfactin (**5**) in DMSO-d_6.

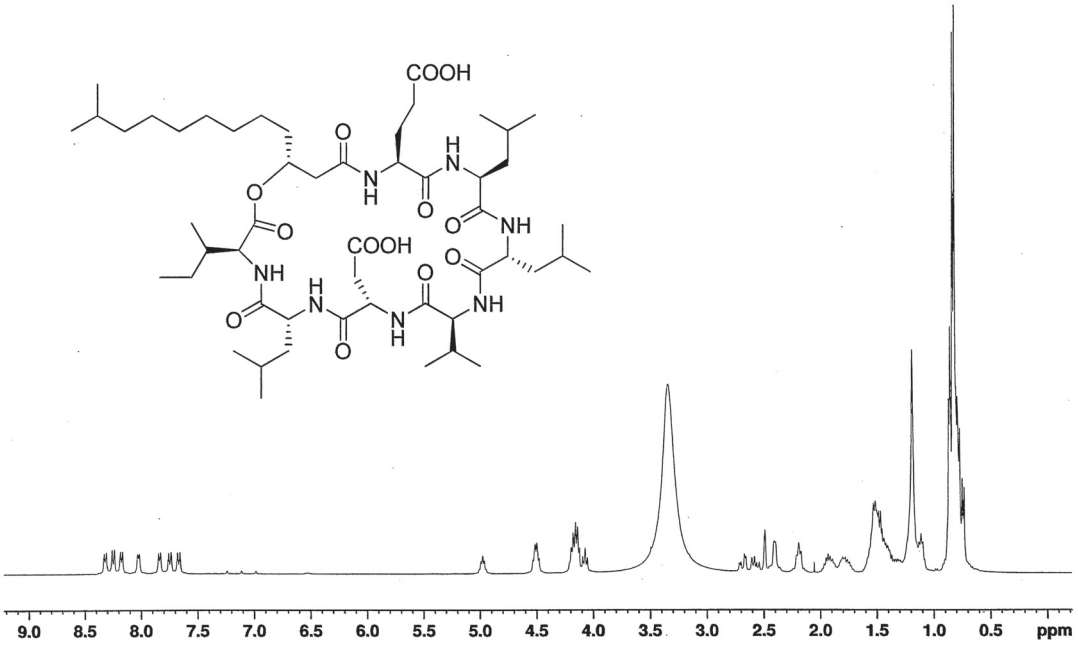

Figure S29. ^{1}H NMR spectrum of *iso*-C_{13} [Ile^{7}]surfactin (**6**) in DMSO-d_6.

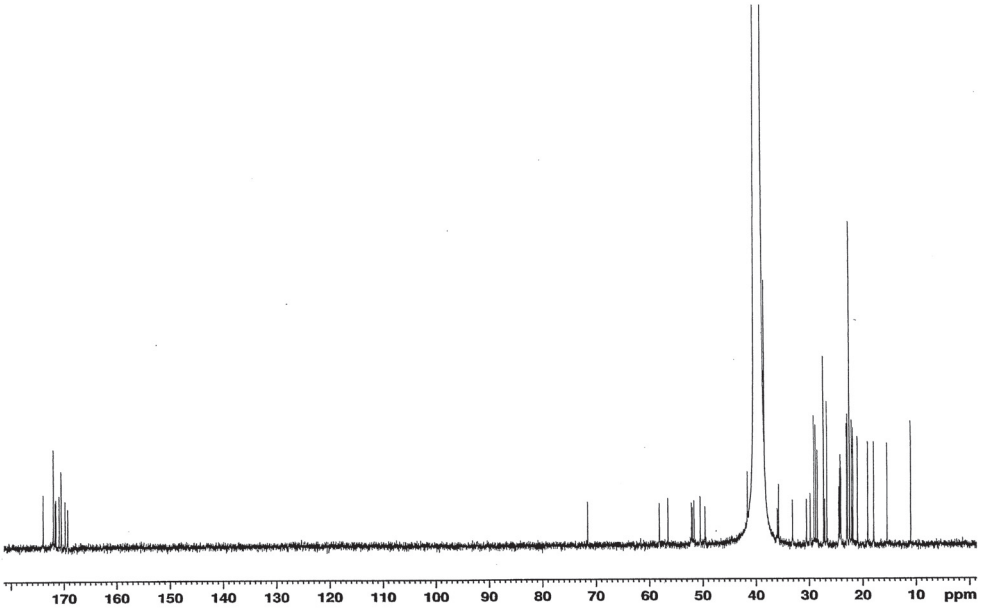

Figure S30. ^{13}C NMR spectrum of *iso*-C_{13} [Ile^{7}]surfactin (**6**) in DMSO-d_6.

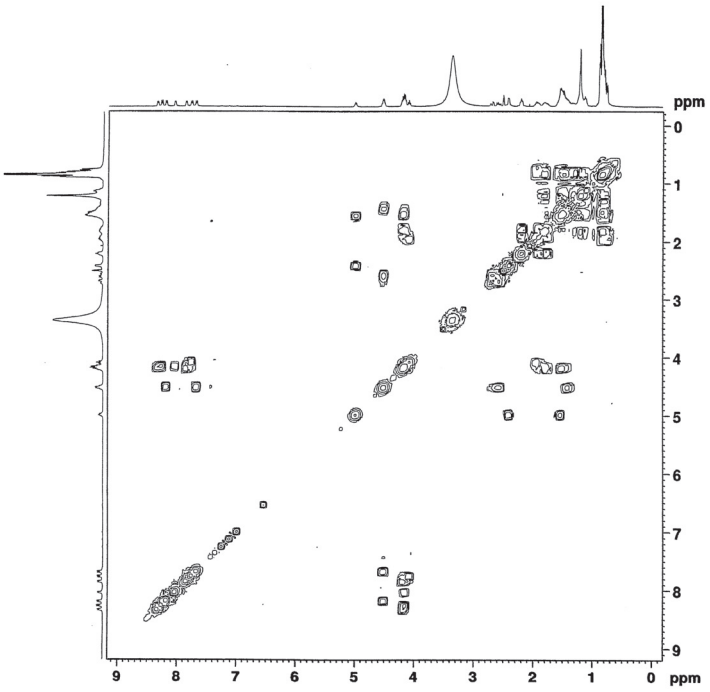

Figure S31. COSY spectrum of *iso*-C_{13} [Ile^7]surfactin (**6**) in DMSO-d_6.

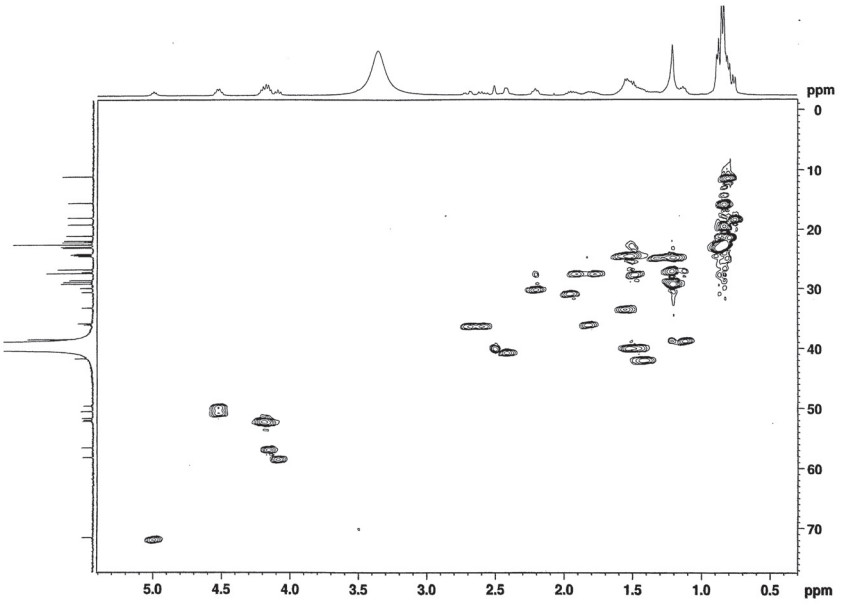

Figure S32. HSQC spectrum of *iso*-C_{13} [Ile^7]surfactin (**6**) in DMSO-d_6.

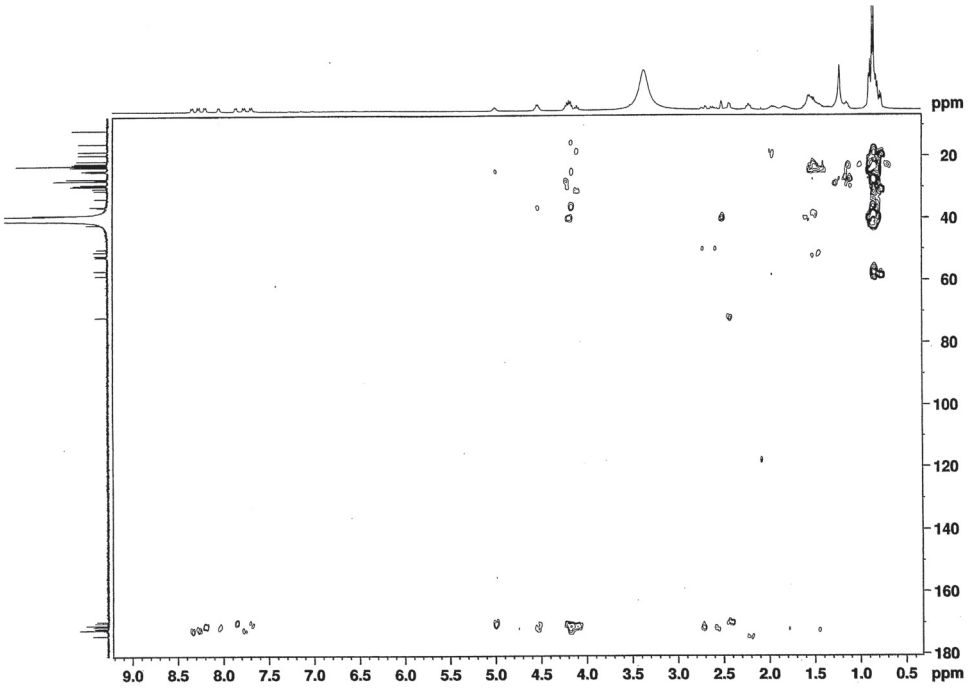

Figure S33. HMBC spectrum of *iso*-C_{13} [Ile^7]surfactin (**6**) in DMSO-d_6.

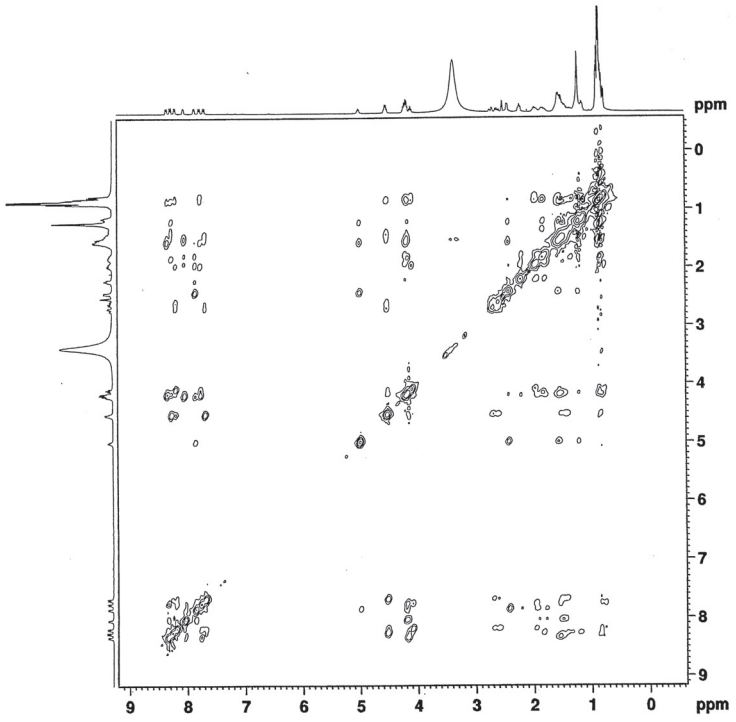

Figure S34. NOESY spectrum of *iso*-C_{13} [Ile^7]surfactin (**6**) in DMSO-d_6.

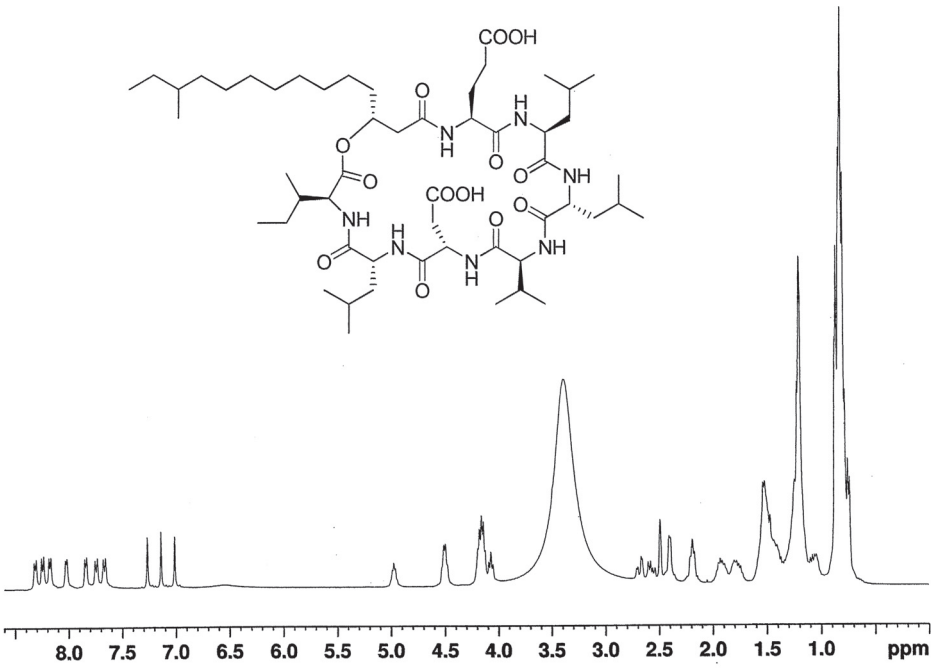

Figure S35. ^{1}H NMR spectrum of *anteiso*-C_{15} [Ile^{7}]surfactin (**8**) in DMSO-d_6.

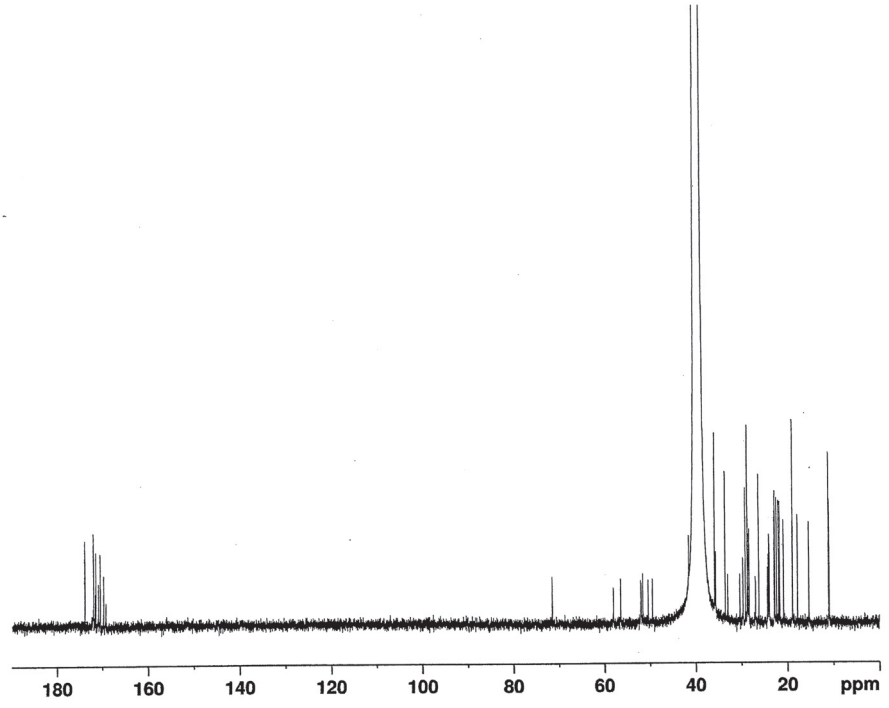

Figure S36. ^{13}C NMR spectrum of *anteiso*-C_{15} [Ile^{7}]surfactin (**8**) in DMSO-d_6.

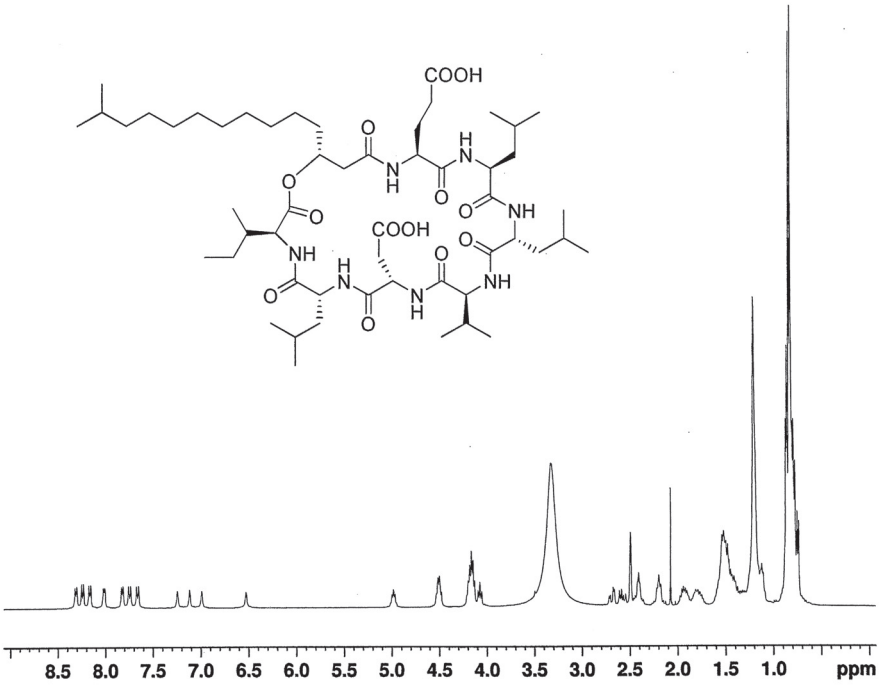

Figure S37. ^{1}H NMR spectrum of *iso*-C_{15} [Ile^{7}]surfactin (**9**) in DMSO-d_6.

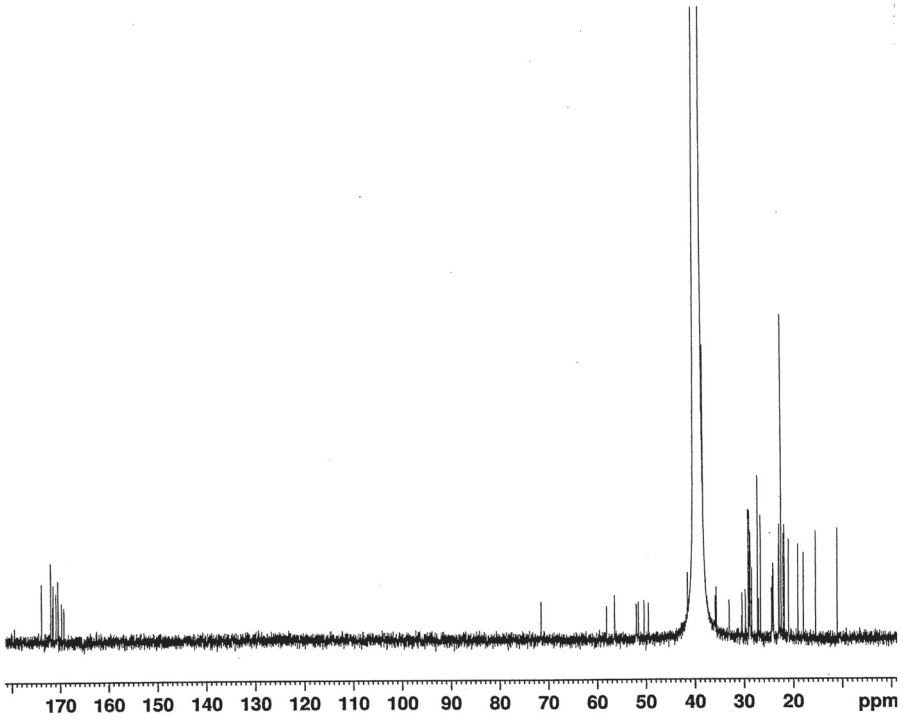

Figure S38. ^{13}C NMR spectrum of *iso*-C_{15} [Ile^{7}]surfactin (**9**) in DMSO-d_6.